A STUDY OF D. .EL ACTION IN REINFORCED CONCRETE CONNECTIONS

Michael Graham Cross

A Dissertation Submitted to the Faculty of Engineering, University of the Witwatersrand, Johannesburg, in partial fulfilment of the requirements for the degree of Master of Science in Engineering

Johannesburg 1975

DECLARATION BY CANDIDATE

I, Michael Graham Cross, hereby declare that the work presented in this dissertation is my own and that it has not been submitted for a degree of another university.

....

December 1975

ACKNOWLEDGEMENTS

I gratefully acknowledge the help of the following people concerned with the preparation of this work:

Professor A.J. Ockleston, who supervised the work, and Mr. A. Hofmeyr, for their guidance and assistance.

The technical and laboratory staff of the Department of Civil Engineering of the University of the Witwatersrand, for their help in the preparation of apparatus used in the experimental program.

The Council for Scientific and Industrial Research and the University of the Witwatersrand, for financial backing of the work.

Mrs. B. Muller, for assistance in the typing of the manuscript.

My father, for continued help and encouragement.

ABSTRACT

This dissertation describes an investigation into the structural characteristics of a dowelled joint in reinforced concrete construction, special attention being paid to the load which such a connection could safely transmit in shear. Concrete construction joints, dowelled joints in highway pavements, connections in precast concrete structures and the attachment of additional elements to slip-formed structures, such as a slab cast onto a slid-wall in the post-slide stage of construction, are typical of the practical issues concerning the designer in this regard.

While certain aspects of dowel action have been fairly extensively studied by various authors, no recognized design guide or recommendation exists as regards the safe load such a dowelled joint can carry, considering all the variables involved. The work described in this dissertation aims at establishing such a design procedure for dowels.

A series of tests was conducted on suitable reinforced concrete models, considering as many of the large number of parameters involved as possible. Experimental results were generally plotted as load-deflection curves, and a suitable theory was developed to fit the experimental data thus obtained. Certain applications of the "beam on elastic foundation" theory were found to correlate well with

experimental data, and this theory has thus been studied in some detail.

The combined experimental and theoretical results were finally used in the establishment of suitable design criteria and safe loads for dowelled connections in reinforced concrete structures.

CONTENTS PAGE

CHAPTER 1

INTRODUCTION : THE DOWEL AS AN ELEMENT OF REINFORCED CONCRETE CONSTRUCTION AND THE PARAMETERS INVOLVED IN ITS ANALYSIS 1

1.1 *THE DOWEL IN REINFORCED CONCRETE CONSTRUCTION* 1

1.2 *THE PARAMETERS INVOLVED IN THE ANALYSIS OF DOWEL ACTION IN REINFORCED CONCRETE CONSTRUCTION*

CHAPTER 2

A STUDY OF THE VARIOUS APPROACHES ADOPTED IN THE ANALYSIS OF THE DOWEL IN REINFORCED CONCRETE CONSTRUCTION 10

2.1 *A STUDY OF DOWEL ACTION IN RELATION TO SHEAR STRENGTH OF REINFORCED CONCRETE BEAMS* 11

2.2 *A STUDY OF DOWEL ACTION WITH SPECIFIC REFERENCE TO CONNECTIONS BETWEEN REINFORCED CONCRETE ELEMENTS* 25

CHAPTER 3 PAGE

THE APPLICATION OF A THEORY FOR DOWELS CROSSING JOINTS IN REINFORCED CONCRETE - AN ANALYSIS OF BEAMS ON FLEXIBLE FOUNDATIONS 35

3.1 *INTRODUCTION* 35

3.2 *THE WINKLER FOUNDATION MODEL* 36

3.3 *COMPLETE AND PARTIAL CONTINUITY* 41

3.4 *THE PASTERNAK FOUNDATION MODEL* 43

3.5 *THE FILONENKO-BORODICH FOUNDATION MODEL* 45

3.6 *THE FOUNDATION MODEL USED IN THIS DISSERTATION FOR THE ANALYSIS OF DOWEL ACTION IN REINFORCED CONCRETE JOINTS AND CONNECTIONS* 46

3.7 *SIMULATION OF ELASTIC FOUNDATIONS USING NUMERICAL TECHNIQUES* 49

CHAPTER 4

THE LABORATORY TEST PROGRAM AND THE COMPARISON OF EXPERIMENTAL AND THEORETICAL RESULTS 51

4.1 *THE ESTABLISHMENT OF A SUBGRADE MODULUS VALUE FOR CONCRETE* 51

4.2 *TESTS ON THE CRACKED-BEAM SPECIMENS : AN INTRODUCTION* 64

4.3 *THE ELASTIC MODULUS AND THE YIELD STRESS OF THE DOWELS USED IN THE CRACKED-BEAM TESTS* 71

4.4 SERIES 1 : *TESTS ON SPECIMENS HAVING A 6,35 mm MILD STEEL DOWEL ON THE BEAM AXIS* 77

		PAGE
4.5	SERIES 2 : *TESTS ON SPECIMENS HAVING A 6,35 mm MILD STEEL DOWEL WITH SMALL COVER*	84
4.6	SERIES 3 : *TESTS ON SPECIMENS HAVING TWO 6,35 mm MILD STEEL DOWELS*	89
4.7	SERIES 4 : *TESTS ON SPECIMENS HAVING A 10,0 mm MILD STEEL DOWEL ON THE BEAM AXIS*	94
4.8	SERIES 5 : *TESTS ON SPECIMENS HAVING A SINGLE, CENTRAL 6,35 mm MILD STEEL DOWEL, AND VARIABLE CRACK WIDTH*	99
4.9	SERIES 6 : *TESTS ON SPECIMENS HAVING A SINGLE, CENTRAL 10,0 mm MILD STEEL DOWEL, AND VARIABLE CRACK WIDTH*	106
4.10	SERIES 7 : *TESTS ON SPECIMENS HAVING A SINGLE 6,35 mm MILD STEEL DOWEL, AND VARIABLE CONCRETE STRENGTH*	111
4.11	SERIES 8 : *TESTS ON SPECIMENS HAVING A SINGLE, CENTRAL 10,0 mm MILD STEEL DOWEL, AND VARIABLE CONCRETE STRENGTH*	115
4.12	SERIES 9 : *TEST ON SPECIMEN HAVING TWO 6,35 mm MILD STEEL DOWELS AND STIRRUPS IN THE REGION OF THE CRACK FACES*	119
4.13	SERIES 10 : *TESTS ON SPECIMENS HAVING A SINGLE 6,35 mm ANGLED DOWEL*	123
4.14	SERIES 11 : *TESTS ON SPECIMENS HAVING A SINGLE 6,35 mm DOWEL BENT INITIALLY TO SIMULATE SLAB-[illegible]TO-WALL CONNECTIONS*	127

PAGE

4.15 SERIES 12 : *TESTS ON SPECIMENS HAVING A SINGLE 6,35 mm HIGH TENSILE STEEL DOWEL ON THE BEAM AXIS* 130

4.16 SERIES 13 : *TESTS ON SPECIMENS HAVING A SINGLE, CENTRAL 6,35 mm MILD STEEL DOWEL, AND A CENTRAL POINT LOAD* 135

<u>CHAPTER 5</u>

<u>THE CORRELATION OF TEST RESULTS AND AN EVALUATION OF SAFE LOADS THAT CAN BE TRANSMITTED BY DOWELLED CONCRETE CONNECTIONS</u> 137

5.1 *THE CONCRETE COVER TO THE DOWELS* 137

5.2 *THE APPLICATION OF THE IFB FOUNDATION MODEL* 142

5.3 *THE ESTABLISHMENT OF AN APPROXIMATE RELATIONSHIP FOR THE DOWELLED CONNECTION YIELD LOAD* 151

5.4 *THE EFFECT OF DOWEL LENGTH* 155

5.5 *A GENERAL EVALUATION OF THE PARAMETERS INVOLVED IN THE ANALYSIS OF DOWEL ACTION* 156

<u>CHAPTER 6</u>

<u>CONCLUDING SUMMARY OF THE STUDY OF DOWEL ACTION</u> 161

<u>LIST OF REFERENCES</u> 163

APPENDIX A | PAGE

A.1 *THE WINKLER FOUNDATION MODEL AND ITS MATHEMATICAL SOLUTION* 167

A.2 *THE EQUATIONS USED BY TERZAGHI FOR DEFORMATIONS UNDER UNIFORMLY LOADED BASES* 169

APPENDIX B

B.1 *THE COMPUTER PROGRAM MODEL, INCORPORATING THE FULL SOLUTION TO THE PFB FOUNDATION MODEL* 170

B.2 *LARGE FRAME COMPUTER PROGRAM SIMULATION OF THE BEAM ON ELASTIC FOUNDATION* 174

APPENDIX C

MIX DESIGN OF THE CONCRETE USED IN THE CRACKED-BEAM AND CUBE SPECIMENS 177

APPENDIX E

DETAILS OF APPARATUS USED IN THE LABORATORY TEST PROGRAM 179

CHAPTER 1
INTRODUCTION: THE DOWEL AS AN ELEMENT OF REINFORCED CONCRETE CONSTRUCTION AND THE PARAMETERS INVOLVED IN ITS ANALYSIS

1.1 *THE DOWEL IN REINFORCED CONCRETE CONSTRUCTION*

The dowelled joint is an essential and integral part of a great number of civil engineering structures, and the subject of the work is essentially a study of the behaviour of such joints in reinforced concrete elements. The joints and connections encountered in concrete construction are varied and some of the typical examples are discussed briefly.

Transverse joints in concrete pavements are necessary to make longitudinal movements of the pavement possible, and to relieve shrinkage and thermal stresses. In most highway designs round steel dowels are placed across the transverse joints. Typical dowels would be round plain bars, 20 mm to 25 mm in diameter, 600 mm in length and placed at about 300 mm to 500 mm centres. One end of the dowel is capped and painted or greased to present the least possible resistance to movement of the pavement. The dowels are most frequently in direct contact with the surrounding concrete. In some designs, however, they project into closely fitting heavy sleeves, which in turn bear in the concrete. Practical construction considerations, observation of performance and experimental data, rather than design analysis, have led to the construction practices in common use. The dowels are required to keep the wearing surfaces on each side of the joint in alignment even if subgrade support is lacking. They are also required to relieve the concrete stresses due to wheel loads in the immediate vicinity of the joints by transforming a part of these wheel loads to the adjacent pavement. To perform these functions the dowels themselves must be strong enough to carry a reasonable part of the load across the joint and, further, they must be dimensioned so that the bearing pressures between the dowel and the surrounding concrete do not exceed permissible values, which would lead to brittle failure of the concrete. They must transfer their portion of the wheel loads with a sufficiently small deflection to offer a measure of side support to the loaded side of the joint even if the pavement rests on a relatively non-yielding subgrade. Analyses carried out in this field by Friberg[7], making use of a mathematical solution presented by Timoshenko and Lessels[24], are fairly comprehensive, but not entirely satisfactory, since it was necessary to use material constants in these analyses which had not been determined experimentally with sufficient accuracy.

In precast concrete construction, various prefabricated structural elements have to be assembled in order to complete the required structure. These connections are very often in the form of bolted or dowelled joints where the steel connector is grouted into the precast concrete unit. A transfer of shear through this connector would again relate to the problem of the solution of dowel action in reinforced concrete, and various authors[24,17] have given some consideration to the problem. The same structural design technique would be applied to the case of the attachment of brackets to existing concrete columns or walls, where the means of connection is a grouted dowel or an expansion type bolt, set into holes drilled into the existing concrete structure.

A common construction practice in this regard applies particularly to slip-formed structures. In the sliding of a reinforced concrete structure, such as a silo, requiring some type of diaphragm slab, for example a roof or floor slab, the following technique is often applied. Bars are bent in the slid-wall, into some material such as polystyrene foam or soft-board, as shown in Fig. 1.1.1. In the post-slide construction phase, these bars are then bent out in some manner and the slab cast onto them (See Fig. 1.1.2). Although some shear is transferred through the ledge in the wall and through the concrete shear interface, the value of shear transferred in this manner cannot always be considered to be reliable, and it is to the designer's advantage to know the safe shear which could be carried by the dowels in this event.

In general reinforced concrete construction, various stages in the concrete pouring program are determined structurally by the inclusion of construction joints. If a transference of shear is required at the joint then this shear must be carried by the concrete at the joint and the steel reinforcement crossing the joint. If the concrete interface at the joint does not carry any shear, owing for example to post construction shrinkage, bad preparation of the joint concrete surfaces, or a deliberate gap for shrinkage or thermal movement reasons, then all the shear must be transmitted by the steel reinforcement crossing the joint, and the action of this reinforcement is then referred to as dowel action. In water retaining structures of modest dimensions, or where there are scouring actions from mechanical stirrers or rotating paddles, practical advantages result from the use of rigid joints throughout the structure. Specifications usually demand preparation of the first-cast concrete, so that good bond is obtained between the first- and second-cast concrete. In larger structures such as reservoirs, however, where the effects of shrinkage and temperature-change become more significant, rigid joints are no longer satisfactory. It then becomes necessary to provide flexible joints, and if shear must be transmitted across such a joint, or in the case of a rigid joint whose concrete surfaces do not provide a reliable shear value, it is the dowel action of the reinforcement passing through the joint which must transmit this shear.

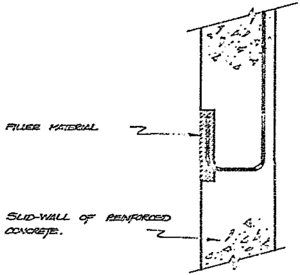

FIG. 1.1.1

EXAMPLE OF POSSIBLE REINFORCEMENT ARRANGEMENT DURING SLIDING.

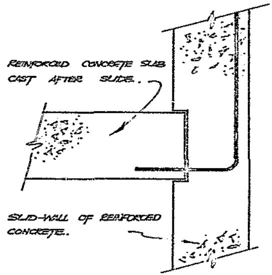

FIG. 1.1.2

EXAMPLE OF REINFORCEMENT DOWELLING SLAB TO SLID-WALL.

Researchers in the fiel. of the shear strength of reinforced concrete beams,[1,3,9,12,13,14,16] recognize the existence of a dowel shear, resulting from the post-cracking action of the main tensile reinforcement. The Joint ASCE-ACI Task Committee ar and Diagonal Tension of the Committee on Masonry an ced Concrete of the Structural Division[26] refer to t as a "dowel shear' and it is recognized as an integral part of the total shear resistance of a reinforced concrete beam. If reinforcing bars cross a crack, shearing displacements along the crack will be resisted, in part, by their dowelling force in the bar. The dowel force gives rise to tensions in the surrounding concrete and these, in combination with the wedging action of the bar deformations, produce splitting cracks along the reinforcement[3], resulting in a decrease in dowel force, which nevertheless remains significant. Although this dowel action has been studied, the large number of variables involved has generally meant that only a few practical cases have been considered. Dowel action of this nature is credited with up to 30% of the interface shear transfer in certain cases[26].

1.2 *THE PARAMETERS INVOLVED IN THE ANALYSIS OF DOWEL ACTION IN REINFORCED CONCRETE CONSTRUCTION*

In the consideration of a typical dowel passing through a construction joint as shown in Fig. 1.2.1 it can be seen immediately that a number of variables are involved in its analysis. The parameters concerning the designer in this regard are as follows:

1.2(a) *Crack Width*

The crack width of the construction joint must be considered. In most practical construction cases this would be zero and in many cases good concrete bond would in fact be obtained between the concrete interfaces (as is already often specified in construction documents). However, the existence of a

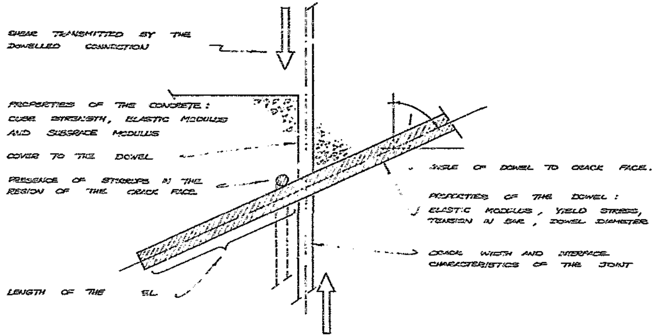

FIG. 1.2.1

SECTION THROUGH A HYPOTHETICAL DOWELLED CONNECTION SHOWING THE PARAMETERS INVOLVED IN THE ANALYSIS OF SUCH A CONNECTION crack width, even if very small, must be considered. This would apply in the case of smooth, oily concrete faces in contact with one another, where the concrete itself transmits no shear across the interface. On the other hand, quite significant crack widths could be considered in highway pavement joints, for example.

1.2(b) *The transfer of shear by the concrete*

If the crack width is zero, then the two alternatives are that either the concrete transmits no shear itself or alternatively, transmits some load owing to friction at the concrete interface. The latter would be the case in shrinkage cracks or shear cracks across a reinforced concrete member, and has been investigated by a method analogous to the analysis of cohesionless soils[17].

1.2(c) *Dowel diameter*

The diameter of the dowel must be considered, especially in relation to the overall dimensions of the particular concrete element under consideration, since this will determine whether the failure mode is controlled by yielding of the dowel or brittle fracture of the concrete mass.

1.2(d) *Yield stress of dowel material*

In addition to the effect of (c) above, the failure mode will further be influenced by the yield stress of the dowel material in relation to other parameters. In particular high tensile steel dowels might induce a brittle fracture type failure of the concrete mass.

1.2(e) *Tensile force in dowel*

The existence of a tensile force in the dowel, due to overall bending of a concrete member, for example, not only affects permissible stresses that might be set up in the dowel due to dowel action, but can in addition influence the deformation pattern of the dowel structure.

1.2(f) *Dowel elastic modulus*

The elastic modulus of the steel dowel will have considerable influence on dowel deformations in the concrete mass, and this in turn will affect the overall joint stiffness and failure patterns.

1.2(g) *Concrete crushing strength*

Not only will the crushing strength of the concrete greatly affect the failure mode of the joint by allowing greater sub-dowel bearing pressures, but the elastic modulus and subgrade modulus of concrete are both dependent on the concrete crushing strength, and these parameters in turn will affect the elastic and elasto-plastic properties of the dowelled joint.

1.2(h) *Cover to dowels*

The concrete cover to the dowels crossing a joint will affect the permissible sub-dowel concrete pressures, since the ultimate load of the joint will be reduced in correspondence with the reduction in the dimension of the fracture line of the concrete. This form of failure will manifest itself to a greater extent in joints in slabs than in the case of walls, where cover may be considered to approach an infinitely large value. Failure modes in the latter case will depend on local crushing of concrete due to sub-dowel concrete pressures.

1.2(i) *The number of dowels crossing the crack face*

This must be considered in conjunction with concrete covers to dowels and overall steel to concrete area ratios for a particular dowelled joint, and will relate to the advantages of a multi-bar joint over a joint of fewer, larger dowels.

1.2(j) *Angle of dowels*

The angle of inclination of the dowel to the crack face must be taken into consideration in the evaluation of stiffness and failure criterion for the dowelled joint, in relation to the expected improvement of shear transfer of judiciously angled dowels.

1.2(k) *Length of dowel*

The length, within certain limits, of a dowel crossing a joint in concrete construction will affect both the overall stiffness characteristics and safety of the joint when considering yield and failure modes.

1.2(l) *Effect of stirrups*

Stirrups in the immediate vicinity of the crack face in a dowelled joint will affect both the elastic deformation properties of the dowel and the failure characteristics of the dowelled joint. This will especially be the case where the failure mechanism relates to the shedding of the concrete cover to the dowels.

1.2(m) *Type of loading*

The principal load to be considered in the case of a dowelled joint is the shear to be transferred across the joint, although this may act in conjunction with other loads, for example overall bending in the concrete member in the region of the joint under consideration.

CHAPTER 2

A STUDY OF THE VARIOUS APPROACHES ADOPTED IN THE ANALYSIS OF THE DOWEL IN REINFORCED CONCRETE CONSTRUCTION

Literature in the field of dowel action in reinforced concrete can be categorized into two distinct approaches:

1) *Dowel action as applied to post cracking analyses of standard reinforced concrete beams.*

2) *Dowel action studied in connection with the transfer of shear by dowels from one mass concrete structural element to another.*

These are fundamentally different concepts and will be dealt with separately. The scope of this dissertation is concerned mainly with the latter concept, although the principles adopted can be referred to both, provided that the necessary adjustments are made. Closely associated with both concepts, but on the other hand making use of an entirely different approach in its analysis, is the case of the cracked section which still transmits a shear across the concrete interface by means of friction. All the above cases have been investigated by various authors and the essence of their findings can be discussed as follows:-

2.1 *A STUDY OF DOWEL ACTION IN RELATION TO SHEAR STRENGTH OF REINFORCED CONCRETE BEAMS*

Dowel action in reinforced concrete beams, although generally not dominant relative to other shear transfer mechanisms, has been studied in numerous instances owing to its role in failure mechanisms in these structural elements. In beams, splitting cracks develop along the tension reinforcement at inclined cracks as a result of dowel effects this allows the crack to open, which in turn reduces the interface shear transfer along the diagonal crack and thus leads to failure.

Following splitting, and the associated loss of stiffness of the concrete surrounding the bar, and hence the decrease in dowel action force, the dowel force has been found to be a function of the stiffness of the concrete under the reinforcement and the distance from the point where the dowel shear is applied to the first stirrups supporting the dowel[3]. Sub-dowel compression failure has also been found to affect this behaviour, but this applies particularly to the cases of slabs or mass concrete and is not as significant in beams. This is important as regards the dowelling of diaphragm slabs to existing walls or the attachment of brackets to concrete structures by means of bolts or grouted or epoxied dowels. Dowel action contributing to the overall shear strength of reinforced concrete beams has been studied by a number of investigators, but as these tests have been characterised by the large number of variables that have to be considered to cover all likely failure mechanisms, reliable results have been obtained for only a few practical cases.

Krefeld and Thurston[16] conducted tests to ascertain the value of dowel shear in reinforced concrete beams. In a study of shear mechanisms they established that the propagation of an inclined crack into the compression zone, leading to ultimate failure, is the direct result of displacements occurring at the point of crack initiation, when the vertical forces acting on the reinforcing bars produce horizontal cracks at the level of the bars. These horizontal cracks, always directed towards the support, signify tensile stresses produced by a combination of bond, horizontal shear and a vertical *(dowel)* shear force, resisted by the reinforcing bars and the concrete below the bars.

The existence of these vertical forces and displacements is made evident by the reversed curvature of the bars and the discontinuity in their deflection increments. The continued abnormal differences in top and bottom bar strains indicate increases in curvature which can be interpreted to mean that shear forces acting on the bars do not disappear after splitting, but continue acting up to ultimate load. The magnitude of this dowel shear force on longitudinal tensile reinforcement has been disregarded by many investigators owing to its relative insignificance when compared to other shear resistance mechanisms in reinforced concrete beams. In addition, the introduction of the dowel shear makes the analysis of the internal forces of the beam statically indeterminate. Hence it is usually assumed that the shear carried by the bars by dowel action is inappreciable, and is, in any case, lost to a large extent after the formation of splitting cracks.

In their test set up (see Fig. 2.1.1), Krefeld and Thurston[16] simulated the above-mentioned diagonal cracks in their beam specimens. A transverse opening permitted the insertion of a steel plate with projecting ends to which the test load was applied, and hence dowel forces could be measured directly at the simulated cracked section.

A constant cylinder strength of 2 500 psi (17,2 MPa) was used for the concrete, and the principal variables considered by the authors were *beam width, bar diameter* and *concrete cover*. During loading, mechanical dial recorders measured deflections at both simulated cracks, giving load-deflection curves as shown in Fig. 2.1.2. (See also Table 2.1.1).

In most cases the load increased to first cracking, after which splitting extended to the support. Any increase of load beyond this condition would be due to suspension action of the tensile reinforcement. Although the number of tests was insufficient to completely evaluate the large number of variables involved, the following important conclusions were drawn:

1) The shear force resisted by the longitudinal tensile reinforcement decreased with increasing distance from the support. It was not known

(BEAMS ARE IDENTIFIED IN TABLE 2.1.1)

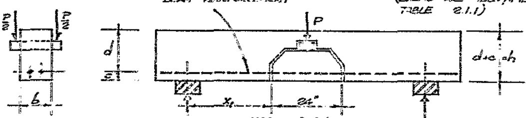

FIG. 2.1.1

BEAM SPECIMENS USED FOR DOWEL TESTS BY KREFELD AND THURSTON.

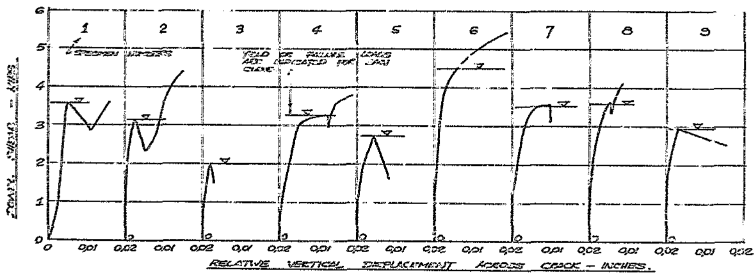

FIG. 2.1.2

LOAD-DEFLECTION CURVES FOR ABOVE TESTS:

(BEAMS ARE IDENTIFIED IN TABLE 2.1.1)

TABLE 2.1.1

RESULTS OF BEAM SPECIMEN TESTS CONDUCTED BY
KREFELD AND THURSTON GIVING F-δ CURVES IN FIG. 2.1.2

Specimen Number	b x h (in)	Bar Diameter (in)	d (in)	c (in)	x_1 (in)	f'cy (in)	(V_1) test (lb)
1	6x12	⅞"	10,06	1,94	12	2650	3575
2	6,12x12	⅞"	10,06	1,94	18	2650	3150
3	6x12	⅞"	10,06	1,94	24	2290	2000
4	8x12	⅞"	10,06	1,94	12	2620	3250
5	8,12x12	⅞"	10,06	1,94	30	2600	2750
6	6x15	⅞"	10,06	4,94	12	2390	4500
7	6x15	⅞"	10,06	4,94	24	2390	3500
8	6,25x12	1⅛"	9,94	2,06	12	2770	3600
9	6x12	1⅛"	9,94	2,06	12	2770	2950

to what extent this was the result of the variation in tensile force existing in the reinforcing bars. From a theory set up later by Johnston and Zia[13], it wo would appear that this certainly could have been the case. (See Fig. 2.1.4)

2) Bar shear resistance increased with larger concrete cover below the bars. This is significant only in the particular case of the shear resistance of longitudinal tensile reinforcement in beams, since the *structure resisting the dowel force* in this case is in fact a combination of the tensile reinforcement and the concrete cover below the bars, as shown in Fig. 2.1.3. (This is verified later by Johnston and Zia[13]).

3) In general it was found that approximately two thirds of the shear resistance was carried by the concrete above the crack, and about one third by the *dowel structure* shown in Fig. 2.1.3. Jones [14], in an earlier investigation, concluded that the longitudinal steel functions as a dowel and that it "contributes a substantial part of the shear resistance at failure". (It must be emphasised that this dowel action is *fundamentally different* to that studied in connection with the load transferred by dowel

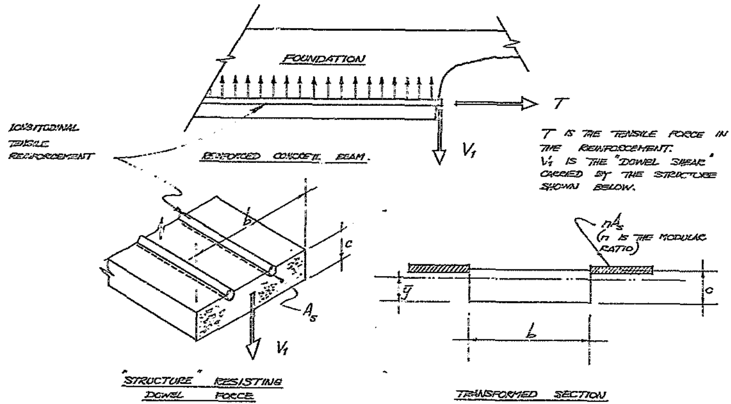

FIG. 2.1.3

THE "DOWEL STRUCTURE" IN REINFORCED CONCRETE BEAMS.

across a structural connection).

4) Initially, and based on empirical data obtained from tests. the authors formulated the following expression for the ultimate shear which could be carried by the above *dowel structure* (See Fig. 2.1.2).

$$V_1 = C_1 \,.\, \sqrt{f'_{cy\ell}}\ (dIb^3)^{\frac{1}{4}} \qquad 2.1.1$$

where C_1 is a factor involving *unknown effects of combined stresses* (See Chapter 5:2), I is the second moment of area of the *dowel structure* (from the *transformed section* given in Fig. 2.1.3), $f'_{cy\ell}$ is the concrete cylinder strength and b and d are obtained from Fig. 2.1.1. Equation 2.1.1 was modified empirically to take into account the variation of V_1 with crack distance from the support, to give:

$$V_1 = b\ \sqrt{f'_{cy\ell}} \left[1{,}3\ \left(1+\frac{180p}{\sqrt{f'_{cy\ell}}}\right)c+d\right]\frac{1}{\sqrt{x_1/d}} \qquad 2.1.2$$

(p is an experimentally determined factor)

Where all symbols may be obtained from Fig. 2.1.1. It is most important to note that these equations are empirical, and since test data was all in Imperial units, like units must be considered when evaluating these equations.

The authors conclude that diagonal cracks in beams alter the normal stress distribution and that the longitudinal reinforcement participates in resisting an appreciable amount of the external shear. This shear resistance, acting in conjunction with the embedding concrete, depends on the size of bars, spacing, depth of cover below bars and the strength of the concrete. The normal trajectory of the diagonal tension cracks in beams (reflecting the direction of the principal tensile stresses) is *interrupted* with a change in direction when the cracks have propagated into the compressive zone. This modification of crack propagation is directly related to *horizontal cracking* along the bars when maximum "dowel" resistance is developed. The forces acting on the bars produce bending of the bars and stresses in the surrounding concrete, accompanied by deformations.

The above approach was extended to quite an extent by the work of Johnston and Zia[13] in their study of the dowel action of longitudinal reinforcement in reinforced concrete beams. In contrast to the purely empirical relationships established by Krefeld and Thurston[15], the authors based their study on the concept of a beam on elastic foundation, but on the other hand did not have extensive test results to substantiate their theory. However, their analysis was more comprehensive than that of any previous researchers in that they considered the additional effects of bar tension and the action of stirrups. Their analysis, as in the case of earlier researchers, is principally a study of dowel action in the post-cracking stage of the shear failure of reinforced concrete beams.

For the particular case of the shear failure in reinforced concrete beams, five failure modes relating to post-cracking dowel action can be considered. The longitudinal tensile reinforcement, *acting in conjunction with the concrete cover below the bars* as shown in Fig. 2.1.3, is treated as an axially loaded composite beam on elastic (Winkler) foundation. The stirrups are assumed to be elastic supports to the bar, provided that the bar deflects downwards at these points of support. Material failure is characterized by the yielding of the dowel under combined tension and shear or under combined tension and bending. Support failure results from horizontal cracking of the concrete at reinforcement level or yielding of the stirrup. These failure modes and failure criteria are best indicated in summarized form as in Table 2.1.2.

In their formulation of these failure modes the authors make use of the various solutions to the following differential equation, which is derived from the consideration of a composite beam on Winkler foundation, subjected to a constant tensile force (see Chapter 3):

$$E_c I_c \cdot \frac{d^4y}{dx^4} - T \cdot \frac{d^2y}{dx^2} + ky = 0 \qquad 2.1.3$$

where y is the deflection of the (composite) bar, x is the horizontal distance measured along the bar, E_c is the modulus of elasticity of concrete, I_c is the second moment of area of the transformed composite beam(see Fig. 2.1.3), k is the foundation modulus for the composite beam of width b, (it must be noted here that this value will be considerably different '' the subgrade modulus to be applied to the case of dowels crossing preformed cracks or joints in reinforced concrete structures - see Chapter 4.2 on the experimental determination of subgrade modulus) and T is the axial force in the bar. The solution to equation 2.1.3 for the case of $0 < T < 2\sqrt{kE_cI_c}$, which includes realistic values of T encountered in practice, is

$$y = (G_1e^{\alpha x}+G_2e^{-\alpha x})\cos\beta x + (G_3e^{\alpha x}+G_4e^{-\alpha x})\sin\beta x \qquad 2.1.4$$

in which

$$\alpha = (\lambda^2 + \frac{T}{E_cI_c})^{\frac{1}{2}} \qquad 2.1.5$$

$$\beta = (\lambda^2 - \frac{T}{E_cI_c})^{\frac{1}{2}} \qquad 2.1.6$$

$$\lambda^2 = (\frac{k}{4E_cI_c})^{\frac{1}{2}} \qquad 2.1.7$$

and G_1, G_2, G_3 and G_4 are constant coefficients to be determined from boundary conditions. These boundary conditions vary depending on the failure mode encountered and an extensive list of stiffness coefficients and mode solutions has been established by the authors[13]. The value of k, the subgrade modulus for concrete for the beam width, is given by the authors as:

$$k = \frac{E_cb'}{d} \qquad 2.1.8$$

where $b' = b - mD_s$
and b is the beam width, d is the effective depth of the beam, m is the number of bars and D_s is the bar diameter.

It may be noted that equation 2.1.8 indicates a linear relationship between subgrade modulus and Young's Modulus of concrete and that k has units N/mm², and is thus not the true concrete subgrade modulus (see Chapters 3 and 4.2 on concrete subgrade modulus). In order to obtain the full series of stiffness coefficients, four distinct failure modes were considered by the authors:

1) Cracking of concrete cover, which is primarily a function of the tensile strength of the concrete, and is related to the critical deflection, y_c, of the composite bar (a disadvantage of the theory established by the authors is that a value for y_c must be assumed before proceeding with the analysis).

2) Yielding of the dowel under combined tension and shear.

3) Yielding of the dowel under combined tension and bending.

4) Yielding of the stirrup (only the first stirrup is considered to give support to the dowel).

TABLE 2.1.2: FAILURE MODES AND CRITERIA FOR REINFORCED CONCRETE BEAMS GIVEN BY JOHNSTON AND ZIA [2]

FAILURE MODES	FAILURE CRITERIA: DOWEL CONCRETE FAILURES	FAILURE CRITERIA: DOWEL MAIN BAR FAILURES
 $0 < r \leq a$ (a = STIRRUP SPACING)	HORIZONTAL CRACKING OF COVER.	SHEAR AND TENSION YIELDING OF BAR.
 $0 < r \leq a$	HORIZONTAL CRACKING OF COVER AT FIRST STIRRUP.	SHEAR + TENSION OR BENDING + TENSION YIELDING OF BAR.
 $0 < r \leq a$	YIELDING OF FIRST STIRRUP	SHEAR + TENSION OR BENDING + TENSION YIELDING OF BAR.
 $r = 0$	HORIZONTAL CRACKING OF COVER.	SHEAR + TENSION YIELDING OF BAR.
 $r = 0$	YIELDING OF FIRST STIRRUP	SHEAR + TENSION OR BENDING + TENSION YIELDING OF BAR.

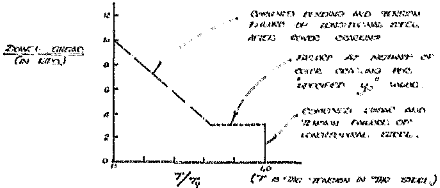

FIG. 2.1.4

[illegible]

Interaction curves were plotted for various failure modes as shown by a typical interaction curve in Fig. 2.1.4.

The authors' theory correlated fairly well with tests conducted by Gergely[9], the predicted values generally falling within 25% of the experimental results. However, the all important value, y_c, the critical deflection of the dowel causing cracking of the concrete cover, was not satisfactorily established. In addition, the value of subgrade reaction used by the authors relates particularly to the *dowel structure in reinforced concrete beams*, and is not applicable to the case of a dowelled connection in reinforced concrete construction.

2.2 *A STUDY OF DOWEL ACTION WITH SPECIFIC REFERENCE TO CONNECTIONS BETWEEN REINFORCED CONCRETE ELEMENTS.*

The term "connection" has many applications in this regard but principally this differentiates between shear resistance by dowel action in reinforced concrete beams and shear transfer across some intentionally preformed crack or joint in a concrete structure. Specific cases of cracking do occur in some structural elements which result in a situation very similar to the latter type of shear transfer referred to above, those being cases where a *shear plane* exists at some point in the structure. This type of shear transfer has been studied fairly extensively by Mast[17] and later by Hofbeck et al[18]. The concept of the dowel as a beam on elastic foundation is not used in these cases. The design philosophy followed in general is that joints should have ductility and should therefore have some amount of reinforcing steel passing through them, so that the design should not rely entirely on the tensile strength of the concrete. The *shear friction* theory advanced by Mast considers the shear force to be resisted by friction along a hypothetical crack. The relationship between steel area required across such a crack, or shear interface, and the shear force to be transmitted by the crack is given by

$$V_u = A_s f_y \tan \phi \qquad 2.2.1$$

where V_u is the shear force acting at the shear interface at ultimate load, A_s is the area of steel crossing the crack normal to the shear interface, f_y is the yield strength of the reinforcing steel and ϕ is the angle of internal friction of the concrete shear interface. It is important to note that this theory predicts that no load can be transmitted in the case of a smooth crack - this is fundamentally different to the concept that will be developed later in this dissertation (See Chapters 3 and 4). Push-off tests conducted by Anderson[2] and the Portland Cement Association resulted in the envelope shown in Fig. 2.2.1. The value for tan ϕ of 1,4 refers particularly to the case of a rough concrete to concrete interface. Mast foun this envelope to have good application in the design of steel for a corbel, for example, such as shown in Fig. 2.2.2.

Hofbeck et al[12] developed the above theory to some extent and found that Mast's shear friction theory actually made use of an "apparent" friction angle and can only be applied to low stress level cases. They conducted push-off tests using concrete models shown in Fig. 2.2.3 (which were later developed by Dulacska[5] when conducting further dowel tests). The authors concluded that:

1) A pre-existing crack definitely reduces the ultimate shear transfer strength.

2) Dowel action of reinforcing bars crossing the shear plane is insignificant in initially uncracked concrete, but is *substantial in concrete with a pre-existing crack along the shear plane.*

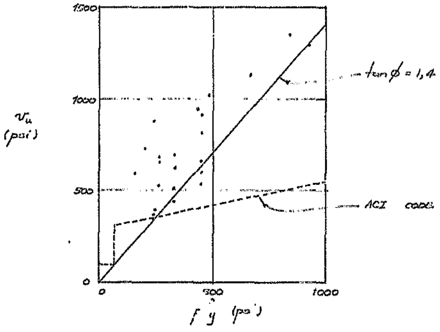

<u>RESULTS OF SHEAR TESTS CONDUCTED BY ANDERSON AND THE PCA</u>

<u>NOTE:</u> FOR A SHEAR INTERFACE OF DEPTH d AND WIDTH b, EQUATION 2.2.1 CAN BE REWRITTEN AS:

$$v_u = p f_y \cdot \tan \phi$$

WHERE: $v_u = V_u / bd$

AND p = STEEL RATIO = A_s / bd.

<u>FIG. 2.2.1</u>

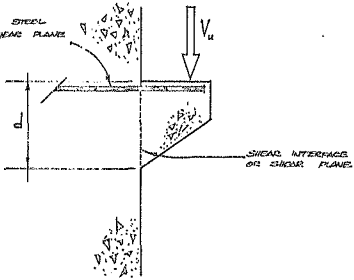

FIG. 2.2.2

APPLICATION OF MAST'S THEORY TO A CORBEL.

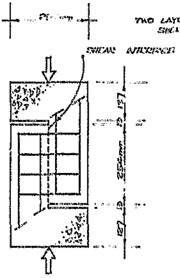

FIG. 2.2.3

DETAILS OF PUSH-OFF SPECIMENS USED IN SHEAR TESTS CONDUCTED BY HOFBECK ET AL.[12]

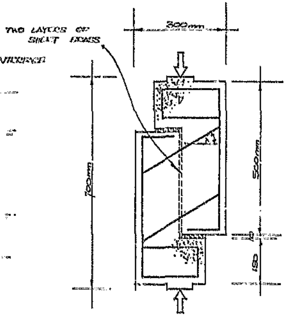

FIG. 2.2.4

DETAILS OF TEST SPECIMENS USED BY [illegible]

3) The shear friction theory gives a reasonably conservative estimate of shear transfer strength in normal weight concrete with a pre-existing crack along the shear plane and reinforced with intermediate grade reinforcement if tan ϕ is assumed to be 1,4, provided that pf_y is less than $0{,}15f'_c$ or 600 psi (42 kgf/cm^2 or 4,14 MPa), whichever is the lesser value.

This concept of the initially cracked shear plane was further developed by the work of Dulacska[5], who considered the dowel action of steel bars crossing artificial cracks in concrete. These artificial cracks were intended to simulate the effect of a crack which opens slightly, thereby losing the friction described by Mast and Hofbeck et al. Bars crossing this type of intentional crack may be said to counterac. shear deflection by "pure" dowel action.

The test specimens used by Dulacska were essentially a development of those used by Hofbeck et al as can be seen in Fig. 2.2.4.

Loads and shear deflections were measured during tests on fifteen such specimens, and test results led to the establishment of an empirical formula for the shear force which could be carried by such a joint at ultimate load:

$$T_f = \rho b^2 \gamma \sigma_y . n \sin\delta \left[\sqrt{1 + \frac{\sigma_c}{3\rho\gamma^2\sigma_y \sin^2\delta}} - 1 \right] \qquad 2.2.2$$

In equation 2.2.2, T_f is the failure force, b is the bar diameter, δ is the angle of the dowels, σ_y is the yield stress of the steel dowels, σ_c is the cube strength of concrete, n is the coefficient of local compression of concrete, γ is a constant and ρ is given by the expression:

$$\rho = 1 - N^2/N_y^2 \qquad 2.2.3$$

where N is the tensile force in the bar crossing the crack and N_y is the tensile force including yield in pure tension in the bar.

The coefficient of local compression of concrete (see Chapter 5 for a more detailed discussion) is *assumed* by Dulacska to be 4. Test results give γ as 0,05 and ρ was approximately unity for all tests. The substitution of these values into equation 2.2.2 gave fairly good correlation between theoretical and test results and the main conclusions drawn from the test series were that:

1) The bar crossing the artificial crack is deformed by the action of the shear force. In addition the bar breaks the sharp concrete edge at the crack face, causing load crushing of the concrete.

2) The failure shear force of the dowel action was determined by test for the parameters considered.

3) The dowel behaviour is almost ideally elasto-plastic.

For the parameters considered in the test series the equations derived appear to have good application. However, being empirical, and relying on an assumed value for n, rather than a value developed on a rational basis, the equations cannot readily be extended to include other parameters. They are nevertheless a valuable guide-line to the ultimate load that can be expected from a dowelled connection having properties similar to the specimens tests. Cracking of concrete cover was precluded however, owing to the design of the test specimens.

A theoretical investigation into dowel action of bars crossing cracks in highway pavements was undertaken by Friberg[7], making use of a general mathematical solution to the Winkler foundation model presented by Timoshenko and Lessels[24]. The dowel is considered to be an infinitely long structure supported by an elastic mass from its boundary surface. A simple, discontinuous foundation support is used, expressing the stiffness of the structure and the elastic mass by the following constant:

$$m = \sqrt[4]{\frac{k_o b}{4EI}} \qquad 2.2.4$$

in which k_o is a *modulus of support* for the elastic mass (and has dimension force per length cubed), b is the width of the structure, E is the modulus of elasticity of the structure and I is the moment of inertia of the structure.

Friberg develops Timoshenko's solution to the differential equation for an elastic structure supported by an elastic mass, considering particular loading conditions associated with a dowel in a highway pavement. Considering the loading to be the form shown in Fig. 2.2.5, the author shows that the maximum bending moment in the dowel can be expressed by the relationship

$$M_{max} = \frac{-Pe^{-mx_m}}{2m} \sqrt{1+(1+ma)^2} \qquad 2.2.5$$

In equation 2.2.5, P is the shear force applied at the joint centre line, a is the crack width, m is the constant described in equation 2.2.4, and x_m is the point along the structure where the maximum moment occurs, given by the solution of $\frac{dM}{dx} = 0$, the relationship for moment being established from Timoshenko's solution[324].

The elastic deflection of the crack faces can be shown to be given by the relationship:

$$\Delta = \frac{P}{2EI} \left(\frac{1+(1+ma)^2}{m^3} + \frac{a^3}{6}\right) \qquad 2.2.6$$

Equations 2.2.4 through 2.2.6 are all based on an elastic analysis and it is clear that they are dependent on the value k_o, the *modulus of support* of the "elastic" concrete mass. This is unfortunate, since the author was unable to give a reliable value for k_o in the case of mass concrete, so that although this elastic approach appears to have a good rational basis, the final equations are not fully reliable, owing to the assumptions involved in evaluating the material constants. Values for k_o varying from

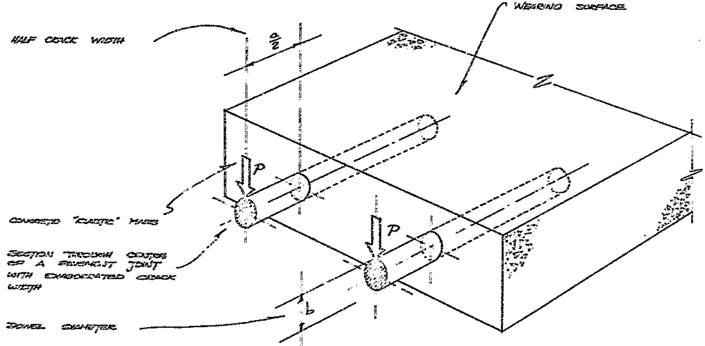

FIG. 2.2.5

SHEAR LOADING AT CENTRE OF PAVEMENT JOINT GIVING STRESSES IN DOWELS AND CONCRETE SUB-DOWEL [illegible] AS IN [illegible] [illegible].

30 000 lb/in^3 (8,2N/mm^3) to close to 2 million lb/in^3 (543 N/mm^3) were considered in the discussion of Friberg's paper. It must be noted that these values are not related to concrete strengths in any way, but the author's values probably refer to 20 MPa (3 000 psi) concrete. Despite this large discrepancy, the concept of treating the "pure dowel" as a beam on a discontinuous elastic foundation is a very valuable one, especially if a reasonably accurate experimental evaluation of the subgrade modulus of concrete is obtained.

Technical literature in the field of dowel action in reinforced concrete can thus be seen to rely on both empirical and rational approaches. The rational approach makes use of variations of the theory of the beam on elastic foundation. Studies of the dowel action also comprise the following two major fields: firstly dowel action as applied to shear failures of reinforced concrete beams and secondly as applied to joints or connections in reinforced concrete structures. In the former the rational approach considers the structure resisting shear failure by dowel action to be the *composite reinforcing bar and concrete cover structure*. In the latter case, which can be referred to as *pure dowel action*, the dowel resists shear forces across the joint as an *independent* structure and not as a *composite* dowel structure. It is this latter concept that is the principal concern of this dissertation, although both concepts have been drawn from in further developing a suitable theory to be applied to the dowel crossing connections in concrete structures.

CHAPTER 3

THE APPLICATION OF A THEORY FOR DOWELS CROSSING JOINTS IN REINFORCED CONCRETE - AN ANALYSIS OF BEAMS ON FLEXIBLE FOUNDATIONS

3.1 *INTRODUCTION*

The concept of a beam on elastic foundation appears to have good application as regards the study of a steel dowel embedded in concrete, provided that a reliable value for the concrete subgrade modulus can be established (see Chapter 4.1). The specific model used by the authors who have considered this analogy[4,13] is based on the Winkler assumption. In order to establish the relative merits of the various models which can be used, a brief study of the various concepts is undertaken.

Beams and plates supported over a large part or over the whole of their dimensions on deformable media are found in a large variety of technical problems. In some of these problems the identity of the beam or plate and of the foundation is clearly established, whereas in others, the concept is of a more abstract nature, the similarities being of a purely mathematical form. In the case of the dowel crossing an open joint, the dowel can be considered to be the beam, and the concrete of the slab or wall its elastic foundation. This of course surmises small elastic deflections of the joint structure. Many different types of foundation model have been developed through the years, the most well-known being the Winkler type of foundation. Each type of foundation model has special application to a particular type of practical engineering problem, and in some cases a number of different models might have to be considered to obtain the most representative results. Judgement is necessary in determining the best use of a foundation model application to a practical problem and in addition in assessing whether a structural element is in fact a beam on elastic foundation or not, using guide lines given by various authors on the subject[10,23]. Mathematical models can be established for both beams and plates on elastic foundation, the plate being the more general concept in mathematical terms. However, consideration is given only to the beam on elastic foundation in this case, since this more closely simulates to steel dowel embedded in a concrete mass.

3.2 *THE WINKLER FOUNDATION MODEL*

The simplest representation of an elastic foundation was provided by E. Winkler as early as 1867[11]. It was Zimmerman who took up the Winkler assumption and developed it into a comprehensive analytical system. The Winkler foundation assumes that the deflection at every point is proportional to the pressure applied at that point. A model of their type of foundation would be best represented by an infinite row of closely spaced springs, each deforming only under the pressure it directly receives, implying a discontinuity of response. This leads to a mathematically simple, but nevertheless very significant solution.

In a system of orthogonal axes, the x axis being parallel to the axis of the foundation surface, Winkler's assumption can be written mathematically as:

$$p = k_o y \qquad 3.2.1$$

If units of newtons (force) and millimetres (length) are adopted in equation 3.2.1, then p is the pressure applied to the foundation (in N/mm²) and y is the corresponding deformation that the foundation undergoes (in mm).

The constant, k_o has units N/mm³ and is known as the *foundation modulus* or the *modulus of support* or the *coefficient of subgrade reaction*. As discussed in Chapter 2.2, the actual value of the constant is subject to question in many applications, and a part of this dissertation is devoted to the establishment of a subgrade modulus for concrete subjected to a sub-dowel pressure. An apparent advantage of the Winkler-Zimmerman solution in this regard is that k_o only enters into the mathematical relationships under a fourth root and thus errors introduced in estimating values for k_o will be reduced substantially in the final solutions for stresses in the foundation. This is true to a certain extent, but it can be shown that it is not the case for all stress solutions, and thus it must be accepted that the ultimate utility of the mathematical relationships established in this manner is vitally dependent on a realistic value of k_o (referred to as the *subgrade modulus* in this dissertation).

The differential equation for the Winkler beam on elastic foundation can be derived by considering vertical equilibrium in Fig. 3.2.1, from which

$$\frac{dQ}{dx} = ky - q \qquad 3.2.2$$

and since the shear, Q, is given by the differentiation of the moment, it can be substituted into the following equation:

$$-EI.\frac{d^2y}{dx^2} = M \qquad 3.2.3$$

This substitution leads to the Winkler differential equation, given by:

$$\frac{d^4y}{dx^4} + \frac{k}{EI} \cdot y = \frac{q}{EI} \qquad 3.2.4$$

where y is t deflection of the beam or dowel, x is the point along the axis of the beam where deflection is considered, k is related to the subgrade modulus of the concrete by $k = k_o.b$, wh is the width of the beam (or the diameter of the dowel). Thus k can be seen to have units of pressure. EI is the flexural rigidity of the beam and q is the load on the beam, where q is a function of x. The solution to equation 3.2.4 can be shown to be:

$$y = Ae^{-mx} \sin(mx+\alpha) + Be^{+mx} \sin(mx+\beta) + \frac{q}{k} \qquad 3.2.5$$

where m is given by the relationship:

$$m = \sqrt[4]{\frac{k}{4EI}} \qquad 3.2.6$$

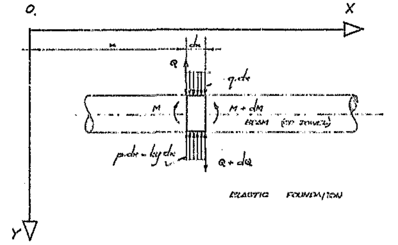

FIG. 3.2.1

ELEMENT OF BEAM CONSIDERED IN THE FORMULATION OF THE WINKLER FOUNDATION MODEL DIFFERENTIAL EQUATION.

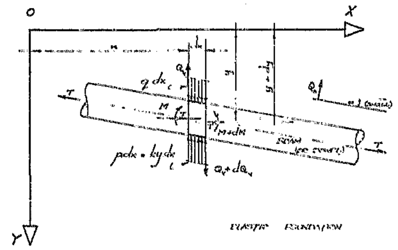

FIG. 3.5.1

ELEMENT OF BEAM CONSIDERED IN THE FORMULATION OF THE FILONENKO-BORODICH FOUNDATION MODEL DIFFERENTIAL EQN.

Four arbitrary constants (A, B, α and β) must be solved for in equation 3.2.5 before obtaining the final solution to a particular problem. These are obtained from known end conditions of deflection, slope, bending moment and shear and by the successive differentiation of equation 3.2.5 as shown in Appendix A[18]. In the general solution of equation 3.2.4, the expression $e^{-mx} \sin (mx + \alpha)$ represents a sine wave with enormous damping. If the beam can be considered to be infinite, which can be shown to be the case for dowels, the general solution simplifies to:

$$y = Ae^{-mx} \sin (mx + \alpha) \qquad 3.2.7$$

This is a result of $y \to 0$ as $x \to \infty$. It can thus be seen that deflections, shears and moments disappear very rapidly along the axis of the beam from the point of loading. The two arbitrary constants, A and α, of equation 3.2.7 are solved for from conditions at the origin of the semi-infinite beam, and this would correspond to the loading at the crack face in the case of dowels. Elastically supported beams may be subdivided into short, medium or long beams. The limiting values for this classification are given by Hetényi[10] as:

Short beams	$m\ell < \frac{\pi}{4}$
Medium beams	$\frac{\pi}{4} < m\ell < \pi$
Long beams	$m\ell > \pi$

where ℓ is the length of the beam, (or the length of the dowel from the crack face) and m is given by equation 3.2.6.

Short beams are considered to be rigid with respect to the foundation. Reactions are calculated by the familiar footing method with trapesoidal pressure distributions. Beams of intermediate length are considered to be finite beams on elastic foundation and in this case both ends must be considered in solving for the four arbitrary constants. Long beams may be idealised to semi infinite or infinitely long beams and thus only two arbitrary constants need be solved for. All practical dowels can be shown to belong to the *long beam* category by evaluating Hetenyi's classification limits, and consequently this analysis will be adhered to for Winkler and other foundation models.

Although the Winkler foundation does not model the practical dowel exactly, it does provide exact and rigorous solutions to some engineering problems, such as the case of a thin-walled cylindrical tube subjected to axisymmetric loading, for example. Since the Winkler assumption of no interconnection between adjacent springs can result in the model not yielding entirely satisfactory solutions in some instances, however, other foundation models are considered, particularly relating to the study of the steel dowel embedded in concrete.

3.3 *COMPLETE AND PARTIAL CONTINUITY*

The problem of the Winkler model, of total discontinuity of foundation response, is overcome mathematically in a number of ways. Complete continuity is obtained if the deflection line is considered to be a continuous function ψ of the absolute difference of the coordinates of the point of application of the load, ζ, and the position, x, where the deflection is produced. This is represented mathematically by:

$$y = \psi(| x - \zeta |) \qquad 3.3.1$$

This relationship leads to an involved partial differential equation and the mathematical difficulties in finding practical solutions are greatly increased for this type of foundation model. In addition to this, researchers have discovered that most materials exhibit properties different to those predicted by the theory of elastic isotropic solids. It thus becomes necessary to formulate mathematical models for cases between the simple Winkler and the complex elastic continuum types.

In the formulation of a mould representing a partially continuous foundation, Hetenyi found that embedding a second continuous beam in the foundation material gave partial shear interconnection. This model leads to an eighth order differential equation, the eight arbitrary constants being solved for from the end conditions of the two beams. This type of foundation model has good application in beam grillages but is not suited to the problem of the steel dowel embedded in concrete. The form of partial continuity sought here is well represented by the Pasternak foundation model.

3.4 *THE PASTERNAK FOUNDATION MODEL*

Pasternak assumes the existence of shear interactions between the spring elements of the Winkler model[11]. This is accomplished by connecting the ends of the springs to a beam consisting of incompressible vertical elements, which deform only under transverse shear. For the derivation, the vertical equilibrium of a unit *shear layer* element is considered (See Fig. 3.4.1). Assuming the material of the foundation to be homogeneous and isotropic, and if the shear modulus of the material is given by G, then the relationship between shear stress and deflection is given by:

$$\tau = G.\frac{dy}{dx} \qquad 3.4.1$$

Since unit length of shear layer is considered, the shear force can be written as:

$$S = G.\frac{dy}{dx} \qquad 3.4.2$$

Considering equilibrium of Figure 3.4.1,

$$\frac{dS}{dx} + p - q = 0 \qquad 3.4.3$$

and hence the relationship between pressure and deflection for the Pasternak foundation model is given by:

$$p = ky - G.\frac{d^2y}{dx^2} \qquad 3.4.4$$

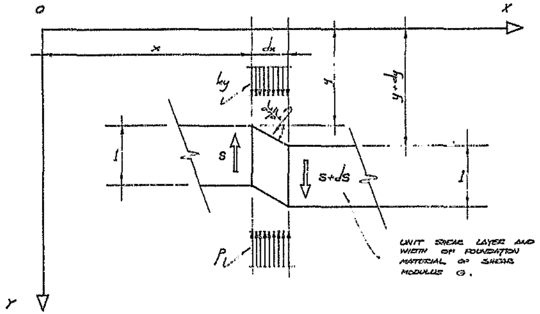

FIG. 3.4.1

ELEMENTARY UNIT SHEAR LAYER OF FOUNDATION MATERIAL CONSIDERED IN THE FORMULATION OF THE PASTERNAK DIFFERENTIAL EQUATION.

(Compare with equation 3.2.1, the mathematical relationship for the Winkler model). Equation 3.4.4 results in the differential equation shown below, derived in a manner similar to that of the Winkler model.

$$EI.\frac{d^4y}{dx^4} - G.\frac{d^2y}{dx^2} + k.y = q \qquad 3.4.5$$

The advantage of this relationship is that the parameter G is easily obtained for the foundation material considered.

3.5 *THE FILONENKO-BORODICH FOUNDATION MODEL*

This model is also intended to achieve some degree of interaction between spring elements[11], and in this case the top ends are considered to be connected to a constant tension field T. Although this would be a difficult parameter to evaluate in terms of the foundation material, it has good application in the form used by Johnston and Zia[13], where T was used to represent the tension in the longitudinal tensi[illegible] [illegible]forcement. The differential equation for this fou[illegible] [illegible]del is obtained by considering equilibrium of Fig. [illegible].1, where

$$\frac{dM}{dx} + T.\frac{dy}{dx} - Q_v = 0 \qquad 3.5.1$$

and

$$\frac{dQ_v}{dx} = ky - q \qquad 3.5.2$$

From these two equations, the differential equation can be derived as follows:

$$EI.\frac{d^4y}{dx^4} - T.\frac{d^2y}{dx^2} + ky = q \qquad 3.5.3$$

Equation 3.5.3 can be considered to be an extension of the Winkler model, taking into account tension in the beam structure, or in the *dowel* for the particular case of a dowel embedded in concrete.

3.6 *THE FOUNDATION MODEL USED IN THIS DISSERTATION FOR THE ANALYSIS OF DOWEL ACTION IN REINFORCED CONCRETE JOINTS AND CONNECTIONS*

After a study of available foundation models it was decided that the shear interactions of the Pasternak model best describe the foundation material of concrete. In addition, any tensions existing in the dowel can be taken into account using the Filonenko-Borodich foundation model. The overall differential equation describing the elastic behaviour of the dowels tested is thus considered to be as follows, provided consistent dimensions are used throughout.

$$\frac{d^4y}{dx^4} - \left[\frac{G + T}{EI}\right].\frac{d^2y}{dx^2} + \frac{k_ob}{EI}.y = \frac{q}{EI} \qquad 3.6.1$$

Equation 3.6.1 is a combination of equations 3.4.5 and 3.5.3 and in this dissertation is referred to as the Pasternak-Filonenko-Borodich (PFB) foundation model. In equation 3.6.1, considering the use of units N and mm throughout, y is the dowel deflection (a function of x), in mm, x is the distance measured along the dowel in mm, G is the shear modulus of the concrete mass foundation in N/mm^2, T is the tension which exists in the steel dowel in the region of the crack face in N, E is the elastic modulus of the steel dowel in N/mm^2, k_o is the subgrade modulus of the concrete foundation in N/mm^3, b is the diameter of the steel dowel in mm and q is the loading on the dowel (in N/mm if uniform, although q may also be zero or a function of x).

In the case of the steel dowel embedded in concrete and crossing a crack of width a, the loading on the dowel can be considered to be a shear force P at the centre of the crack (see Fig. 2.2.5) and q thus becomes zero. If the dowel under consideration crosses the crack face at an angle δ, the loads at the crack face on the dowel will be given by:

$$\text{Shear} = P.\sin\delta \qquad 3.6.2$$

$$\text{Moment} = \frac{Pa}{2}.\sin\delta \qquad 3.6.3$$

Equation 3.6.1 can be integrated and solved as a semi-infinite beam on elastic foundation, the arbitrary constants being obtained from conditions of shear and moment described by equations 3.6.2 and 3.6.3. The solution to the PFB differential equation yields the following expression for deflection:

$$y = \frac{P\sin\delta \cdot e^{-\alpha x}}{(3\alpha^2-\beta^2)\beta}\left[\frac{4\alpha\lambda^2}{k}\cdot\cos\beta x + \frac{2\lambda^2}{k}(\alpha^2-\beta^2).\sin\beta x + \frac{a\beta}{2EI}.\cos\beta x - \frac{a\alpha}{2EI}\cdot\sin\beta x\right] \qquad 3.6.4$$

In equation 3.6.4,

$$k = k_o b$$

$$\lambda = \sqrt[4]{\frac{k}{4EI}}$$

$$\alpha = \sqrt{\lambda^2 + \frac{(G+T)}{EI}}$$

$$\beta = \sqrt{\lambda^2 - \frac{(G+T)}{EI}}$$

Having solved the differential equation for the deflection y, equations for rotation, moment and shear can also be obtained for the embedded dowel. These equations appear in the computer program "DOWEL" (in Appendix B) and are used for the stress analysis of dowels crossing joints in reinforced concrete construction. In addition, deflections at the crack face for a shear, P, can be calculated using the solutions given above and these are compared with the experimentally obtained load-deflection curves.

It can be seen that this elastic solution deals with a number of the parameters mentioned in Chapter 1.2, these being:

- Concrete cube strength, in relation to subgrade modulus and shear modulus of the concrete
- Dowel diameter
- Dowel tension
- Dowel angle

- Dowel elastic modulus
- Crack width of construction joint.

In addition, limit analysis and ultimate loads on dowelled connections can be investigated using these solutions, if the dowel yield stress is known and the subgrade modulus is assumed to be constant to failure (this is shown in Chapter 4 to be a close approximation).

3.7 *SIMULATION OF ELASTIC FOUND. TONS USING NUMERICAL TECHNIQUES*

Large frame computer programs can be used to simulate the beam on elastic foundation concept. The Winkler concept in particular can be closely modelled by treating the foundation as a number of discrete members of particular stiffness in uniaxial tension or compression. The method was used to verify certain of the calculations of the analytical methods used in this dissertation, but an inherent disadvantage is that a knowledge of the subgrade modulus is still necessary in order to establish with certainty a suitable stiffness for the foundation members used. Nevertheless selected output shown in Appendix B.2 compares favourably with results of the PFB foundation model in Fig. 4.4.2 as regards deflections for approximately similar loads, the elastic modulus for concrete being used very satisfactorily in this case for the foundation members.

It can be seen that the discontinuity of the foundation members implies that only the Winkler model can be simulated in this manner. Methods of shear interaction were attempted but generally proved unsatisfactory, since they could not be related to the properties of the foundation material as readily as the Pasternak foundation model, for example, which incorporated the shear modulus of the foundation material. The advantages are the simplicity of the data programming (see Appendix B.2) if the large frame program is readily available, and in addition, discontinuities in the stiffness of the foundation material, such as would be caused by stirrups, are easily dealt with. However, the PFB foundation model gave more satisfactory results generally, and was thus used to a greater extent in the analysis of the experimental data.

It can be seen that the discontinuity of the foundation members implies that only the Winkler model can be simulated in this manner. Methods of shear interaction were attempted but generally proved unsatisfactory, since they could not be related to the properties of the foundation material as readily as the Pasternak foundation model, for example, which incorporated the shear modulus of the foundation material. The advantages are the simplicity of the data programming (see Appendix B.2) if the large frame program is readily available, and in addition, discontinuities in the stiffness of the foundation material, such as would be caused by stirrups, are easily dealt with. However, the PFB foundation model gave more satisfactory results generally and was thus used to a greater extent in the analysis of the experimental data.

CHAPTER 4

THE LABORATORY TEST PROGRAM AND THE COMPARISON OF EXPERIMENTAL AND THEORETICAL RESULTS

4.1 *THE ESTABLISHMENT OF A SUBGRADE MODULUS VALUE FOR CONCRETE*

Although the testing program commenced with tests on the cracked-beam specimens shown in Fig. 4.2.1, it was interrupted by a series of tests on cubes to establish a concrete subgrade modulus and by so doing to prove that the theory developed in Chapter 3 could be used in the analysis of dowelled connections in reinforced concrete. It was felt that variations in subgrade modulus given by Friberg[7], for example, were so large as to make it impossible to apply the theory to the test results. In addition, the value given by Johnston and Zia[12] was applicable only to the dowel structure of reinforced concrete beams and not to the dowelled joint under study.

The subgrade modulus results from a very local sub-dowel pressure-deflection phenomenon and for this reason it was assumed that the main variable affecting it would be the crushing strength of the concrete used. The bar diameter, b, is taken into account in the analysis by the introduction of the adjusted subgrade modulus k, where $k = k_o b$, k_o being the true subgrade modulus. The variation of sub-dowel cover depth was expected to have little effect on most practically dimensioned joints. This was in fact found to be the case for the specimens considered and was also verified by the theoretical determination of the subgrade modulus using equations advanced by Terzaghi[22]. The implication is that for the specimens considered in the test program, and also for the range of dowel diameter to concrete cover ratios likely to be encountered in practice, the subgrade modulus will be a function of the single variable, the cube strength of the concrete.

In order to establish a relationship between subgrade modulus and cube strength of concrete, tests were conducted on specially prepared cube specimens using the Amsler hydraulic testing machine. At the time of the casting of the cubes, short, straight lengths of mild steel reinforcing rod were set into the upper surface of some of the cubes, others being crushed as normal for control purposes. On average the bars were about 80 mm in length and they were cast into the concrete of the cube as shown in Fig. 4.1.1, the concrete being of the mix design described in Appendix C. Since the subgrade modulus is essentially a *sub*-dowel phenomenon it was felt that the value obtained from these specimens could be applied directly to the fully embedded dowel of the cracked-beam specimens. Six and ten millimetre diameter steel rods were used, but the true bearing widths were usually between half and two-thirds of the rod diameters, resulting in bearing areas of the magnitude given in Table 4.1.1. Pressure was applied to the sub-dowel concrete through the short dowels by

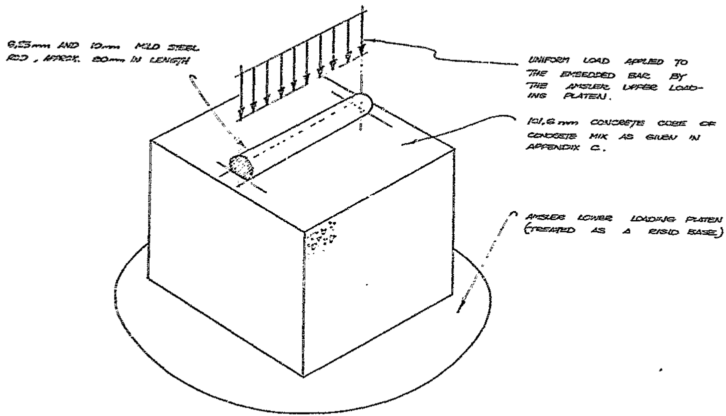

FIG. 4.1.1

TYPICAL TEST SPECIMEN USED FOR THE EXPERIMENTAL DETERMINATION OF A SUBGRADE MODULUS FOR CONCRETE.

means of the loading platens of the Amsler machine. An advantage of this particular testing machine is that the upper loading platen is sprung and able to tilt, ensuring an even distribution of pressure over the full length of the mild steel bars embedded in the concrete cubes.

For each cube tested in this manner, load-deflection curves (F-δ curves) were plotted and resulting subgrade moduli were recorded against cube strengths obtained from standard cube tests being run concurrently (see Table 4.1.1). The load was measured directly from the Amsler dial and the deflection was obtained from the readings of two Mitutoyo mechanical deflection gauges, placed diametrically opposite one another on the Amsler loading platens. Characteristic curves for the tests conducted in this manner for concrete cube strengths 12 MPa and 34 MPa are shown in Figs. 4.1.2 and 4.1.3 respectively and a summary of all tests is given in Table 4.1.1. In order to obtain a realistic value for the sub-dowel pressure experienced by the concrete of the cube, the steel bar bearing area was measured accurately on completion of the test program. The value of the subgrade modulus was obtained from the elastic zone of the load deflection curves established by test. For the PFB foundation model the pressure-deflection relationship is:

$$p = k_o y - (G+T)\frac{d^2y}{dx^2} \qquad 4.1.1$$

If curvature is considered to be negligible for these uniformly loaded short dowels, then the equation can be written as:

$$p = k_o y \qquad 4.1.2$$

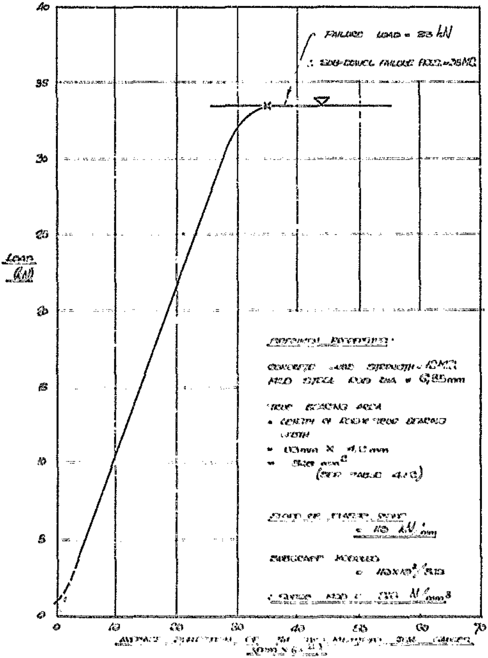

FIG. 4.12

(SPECIMEN NO. 3)

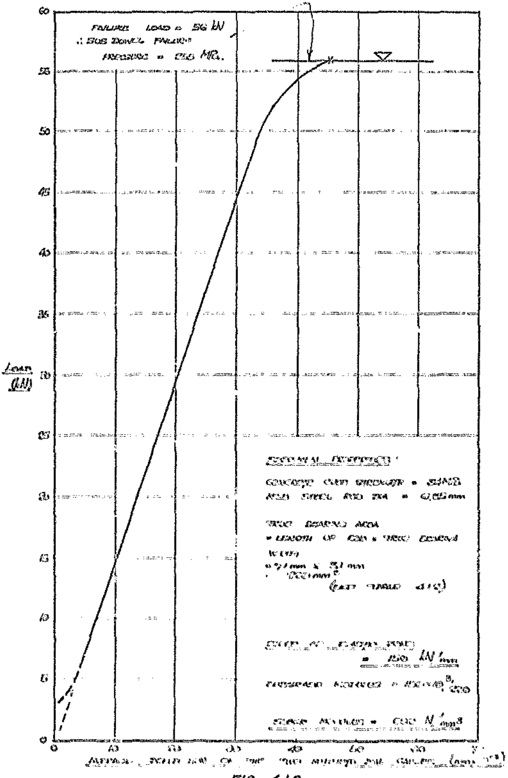

FIG. 4.1.3

TABLE 4.1.1

SUMMARY OF CUBE TEST RESULTS ESTABLISHING A VALUE FOR k_o, THE CONCRETE SUBGRADE MODULUS

Specimen Number	Concrete Cube Strength (MPa)	Cube Sub-dowel Depth (mm)	Dowel Diameter (mm)	Slope of F-δ Curve ($N/mm \times 10^5$)	Bearing Area of Bar (mm^2)	Concrete Subgrade Modulus (Mpa/mm)	Sub-dowel Pressure at Failure (MPa)
1	12	50	6,35	0,6	234	256	94
2	12	50	10,0	1,1	375	293	80
3	12	100	6,35	1,1	348	316	95
4	12	100	10,0	1,7	498	341	82
5	28	100	6,35	1,6	273	586	200
6	28	100	10,0	2,2	389	566	170
7	34	100	6,35	1,5	220	682	255
8	34	100	10,0	4,2	563	746	135
9	36	100	6,35	2,6	336	773	180
10	36	100	10,0	3,0	424	708	153
11	36	100	10,0	2,5	467	750	150
12	40	100	10,0	2,7	350	772	230

For the tests considered, if the load recorded is given by F, the length of the steel rod by L and the actual bearing width by B (where B<b), then the value for the subgrade modulus can be given as:

$$k_o = \left(\frac{F}{\delta}\right) \cdot \frac{1}{LB} \qquad 4.1.3$$

In equation 4.1.3, $\frac{F}{\delta}$ is the slope of the load-deflection curves obtained from tests.

The ultimate loads taken by these short dowels are a good indication of the magnitude of the sub-dowel pressures to be expected at failure in actual structures, although more representative values are obtained in the cracked-beam tests. Nevertheless, it is evident that sub-dowel pressures at failure can be expected to be somewhat higher than the cube strength of the concrete used (see Chapter 5 for a more detailed study).

Before presenting a statistical evaluation of the experimental data, consideration is given to a theoretical value for subgrade modulus that could be expected for the specimens considered, in order to obtain an idea of the validity of the cube test program and the likely structure of the mathematical function relating subgrade modulus and cube strength of concrete. Terzaghi[22] considers the case of settlement on the surface of a semi-infinite solid due to a vertical point load on a finite area. Assuming the solid to be perfectly elastic, the law of superposition of stress and strain is valid and hence the settlement due to a load on a finite area can be computed by integration (as first performed by

Newmark in 1935) of the basic Boussinesq equations for stresses under a point load. This integration yields the elastic settlement Δ_ρ under the centre of a uniformly loaded area of width B and length L to be:

$$\Delta_\rho = 2qB \cdot \frac{(1-\mu^2)}{E} \; I_\rho \qquad 4.1.4$$

In equation 4.1.4, q is the pressure on the loaded area, μ and E are Poisson's ratio and the elastic modulus respectively of the foundation material and I_ρ is a function of the non-dimensional number ℓ, where $\ell = \frac{L}{B}$ (see Appendix A.2) For the steel bars considered ℓ was in the region of 20 and B was about 4 to 5 mm. A small increase in B results in a corresponding decrease in I_ρ and since the deflection is dependent on the product BI_ρ, results obtained from equation 4.1.4 are not very sensitive to small changes in B. For typical test specimens, I_ρ was calculated to have a value of about 1,5. Poisson's ratio was assumed to be 0,2 and constant for the elastic loading considered. Equation 4.1.4 could thus be rewritten as:

$$\frac{q}{\Delta_\rho} = \frac{1}{2} \left(\frac{E}{0{,}96BI_\rho}\right) \qquad 4.1.5$$

Since $\frac{q}{\Delta_\rho}$ represents the subgrade modulus k_0, the following approximate relationship was established from equation 4.1.5, using typical values for the specimens considered.

$$k_0 \doteq \frac{E}{15} \qquad 4.1.6$$

It would thus appear that the subgrade modulus is related directly to the elastic modulus of the foundation material (see equation 2.1.8). It must be noted, however, that equation 4.1.6 refers particularly to the semi-infinite foundation, which is not the case for the cube specimens considered, where the lower loading platen could be treated as a rigid base.

Terzaghi considers the case of settlements on the surface of an elastic layer resting on a rigid base in a method similar to that described for the semi-infinite foundation case. For this case the settlement under the centre of the loaded area is given by:

$$\Delta_{\rho D} = \frac{2qB}{E}\left[(1-\mu^2)F_1 + (1-\mu-2\mu^2)F_2\right] \qquad 4.1.7$$

where the symbols are identical to those in equation 4.1.4 and in addition F_1 and F_2 are functions of the two dimensionless numbers ℓ and d, where $\ell = \frac{L}{B}$ and $d = \frac{2D}{B}$.

D, the depth of the elastic layer considered, varied from 50 mm to 100 mm. For D = 50 mm, and based on steel rod sizes used in the semi-infinite foundation case, the F functions were calculated to be approximately

$$F_1 \doteq 1{,}0$$

$$\text{and} \quad F_2 \doteq 5{,}0$$

(see Appendix A.2)

For the case of D = 100 mm, these functions were approximately:

$$F_1 \doteq 1{,}4$$

$$\text{and} \quad F_2 \doteq 3{,}4$$

Using a technique similar to that described for the semi-infinite foundation, the values for subgrade modulus were calculated to be:

$$k_o \doteq \frac{E}{37} \qquad 4.1.8$$

$$k_o \doteq \frac{E}{33} \qquad 4.1.9$$

It is apparent from equations 4.1.8 and 4.1.9 that even fairly large differences in elastic layer depth have only a small effect on the value for subgrade modulus. This was substantiated by tests and since in most practical dowelled joints concrete surfaces will not be constrained by rigid supports, the variation will become even less significant. An average of these two equations would thus appear to give a reasonable value from the test program, and the relationship is thus best given by:

$$k_o \doteq \frac{E}{35} \qquad 4.1.10$$

CP 110[27] gives an approximate relationship between short term static modulus of elasticity for normal weight concrete and its cube crushing strength as shown in Table 4.1.2. Since the range is given as being ± 4 to 6 GPa, it can be assumed that the elastic modulus is related to the cube strength by a quadratic exponential, using a least squares fit, without the introduction of significant errors. From the information presented in CP 110, if the general mathematical relationship is assumed to be

TABLE 4.1.2

RELATIONSHIP BETWEEN CUBE STRENGTH AND ELASTIC MODULUS FOR NORMAL WEIGHT CONCRETE GIVEN IN CP 110

Cube Crushing Strength of Concrete (MPa)	Modulus of Elasticity (GPa)
20	25
25	26
30	28
40	31
50	34
60	36

$$E = c_1 \sqrt{f'_c}$$

where c_1 is given by $c_1 = \sqrt{\frac{\Sigma E_i^2}{\Sigma (f'_c)_i}}$, then the following approximate relationship holds (both properties being measured in MPa):

$$E = 4900 \sqrt{f'_c} \qquad 4.1.11$$

From equations 4.1.10 and 4.1.11, the mathematical relationship between subgrade modulus and cube strength of concrete can be written as:

$$k_o = 140 \sqrt{f'_c} \qquad 4.1.12$$

In equation 4.1.12, k_o will have units N/mm^3 or MPa/mm and f'_c will have units MPa.

From the results of the cube tests (shown in Figs. 4.1.2 and 4.1.3, and summarized in Table 4.1.1), it is apparent that a relationship similar to equation 4.1.12 can be established, also using the least squares method. In a manner similar to that used above, the relationship established from the data given in Table 4.1.1 can be given as:

$$k_o = 120 \sqrt{f'_c} \qquad 4.1.13$$

which appears to have fairly good correlation with equation 4.1.12, (the same units being used). Although the number of tests performed was insufficient to give a conclusive relationship, and in spite of the fact that parameters such as bar diameter and subgrade depth do have a slight effect on the value for k_o, an average of equations 4.1.12 and 4.1.13, giving

$$k_o = 130 \sqrt{f'_c} \qquad 4.1.14$$

is found to have very good correlation with results obtained from the cracked-beam tests, when applying the PFB theory to the results. It is thus equation 4.1.14 that is ultimately used for the detailed analysis and evaluation of the dowelled connection test series, and which is recommended as a reasonably realistic value for practice (Fig. 4.1.4 shows this curve superimposed on test results). It may also be noted from the shape of the load-deflection curves for subgrade modulus (see Figs. 4.1.2 and 4.1.3) that the value may be assumed to be almost constant up to the failure pressure, which will invariably be somewhat higher than the cube crushing strength of the concrete.

Following the establishment of a realistic subgrade modulus for concrete, a theoretical evaluation of the cracked-beam specimen tests becomes possible. The various parameters considered in these tests are grouped as far as possible but the number of variables involved complicated this procedure to a large extent. The cracked beam specimen tests (or tests on true dowelled connections) are thus as follows:

4.2 *TESTS ON THE CRACKED-BEAM SPECIMENS: AN INTRODUCTION*

A basic prerequisite of the *dowelled connection* test program was that the apparatus developed had to be designed in such a way that the effects of all the parameters dis-

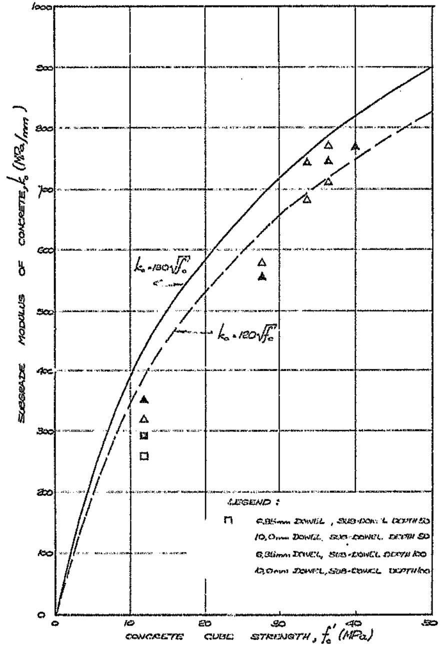

FIG. 4.1.4

RELATIONSHIP BETWEEN SUBGRADE MODULUS AND CUBE STRENGTH FOR NORMAL WEIGHT CONCRETE cussed in Chapter 1.2 could be investigated. In addition, it was considered important that an attempt be made to simulate slab-onto-wall connections as encountered in silo construction, for example, since spalling of concrete cover could be an important factor in the design of this type of joint. This would also be true in the case of a pavement joint (see Fig. 2.2.5). Test specimens of the type used by Hofbeck et al and later by Dulascka (see Figs. 2.2.3 and 2.2.4) were eliminated on these grounds. The specimen type eventually considered to be most suitable was a beam of 101 mm by 101 mm cross-section and spanning 250 mm between preformed artificial cracks, provided that the outer portions of the beam adjacent to the cracks could be held encastre by suitably designed clamps to simulate the effect of end-fixity of a wall, for example. The specimens used for the tests on dowels crossing reinforced concrete joints were thus of the form shown in Fig. 4.2.1. Approximately fifty such specimens were tested, varying the parameters discussed in Chapter 1.2. Control cube tests were run concurrently with these tests, since cube strength was a major parameter affecting the performance of the dowelled joint. The concrete used for all tests was designed to have a cube crushing strength of 30 MPa at 7 days, which was generally the time of testing unless the parameter being investigated was the concrete strength itself. Rapid Hardening Portland Cement was used in the mix design to obtain quick strength and thus speed up the testing program. Details of the concrete mix appear in Appendix C. Six and ten millimetre diameter mild steel dowels were

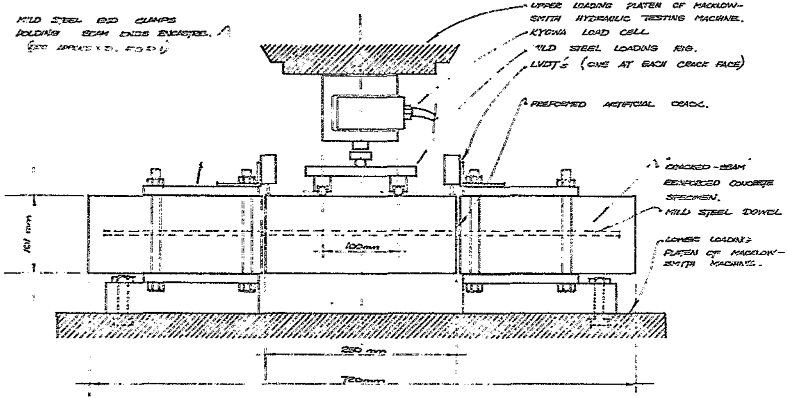

FIG. 4.2.1

TYPICAL "CRACKED-BEAM" REINFORCED CONCRETE SPECIMEN USED TO DETERMINE A LOAD-DEFLECTION RELATIONSHIP FOR A DOWELLED-CONNECTION generally used in the cracked-beams, although later tests included the use of high tensile steel round dowels. The artificial crack formers were made of three materials. For crack widths of 6 to 8 mm, polystyrene foam was used and for crack widths of 3 mm to 0 mm, mild steel formers were used (as shown in Fig. 4.2.2), these being used in conjunction with well oiled stiff paper for zero crack widths. Dowels were held in position by the crack formers at the time of casting, the Vee-Bee machine being used for good compaction. The crack formers were removed when the moulds were stripped, usually 24 hours after casting and specimens were cured in a water bath until the time of testing.

The loading system on the beams, indicated in Figs. 4.2.1 and 4.2.6, was decided upon to give as pure shear across the crack face as possible without causing local compression in the concrete in the vicinity of the joint or interfering with the operation of the LVDT's(Linear Variable Differential Transformers). Loading was applied at a fixed rate for all tests, using the Macklow-Smith hydraulic testing machine of 340 kN capacity, shown in Figs. 4.2.3 and 4.2.4. The output from each cracked-beam test was in the form of a load-deflection curve, plotted autographically on the Watanabe X-Y Recorder, shown in Fig. 4.2.5. For this purpose, use was made of a 20 kN capacity Kyowa load cell and two LVDT's, one situated at each crack face, the mean deflection being recorded. A check was kept on autographic plots by mechanical Mitutoyo gauges (see Fig. 4.2.6). These were also used to measure deflections which

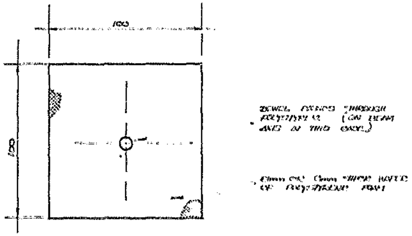

[illegible] FOAM [illegible] [illegible] [illegible] [illegible]
AND [illegible] [illegible] [illegible]

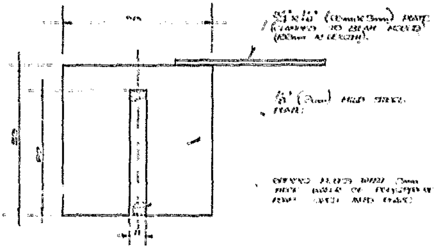

[illegible] [illegible] [illegible] [illegible] [illegible] [illegible]
[illegible] OF [illegible] AND [illegible]

FIG. 4.2.2

[illegible]

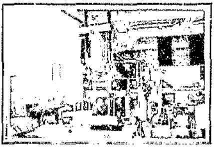

FIG. 423

[illegible]

FIG. 426

[illegible]

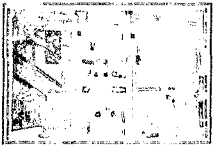

FIG. 424

[illegible]

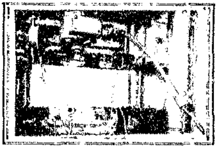

FIG. 427

[illegible]

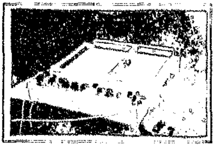

FIG. 425

[illegible]

FIG. 428

[illegible]

were greater than the linear range of the LVDT's (this being approximately ± 1 mm - see Appendix D).

The large number of parameters was tested by 13 test series, a summary of these series being given in Table 4.2.1.

4.3 *THE ELASTIC MODULUS AND THE YIELD STRESS OF THE DOWELS USED IN THE CRACKED-BEAM TESTS*

In addition to the requirement of a realistic value for concrete subgrade modulus for the concrete of the cracked-beam specimen, values for the elastic modulus and yield stress had to be established with reasonable accuracy for the steel dowels used, in order that the theory established in Chapter 3 could be used effectively. For this reason a number of 6,35 mm and 10 mm mild steel rod specimens were subjected to uniaxial tensile tests, using the Macklow-Smith hydraulic testing machine.

The characteristic curve obtained from the mild steel bar test series is given in Fig. 4.3.1 and from this curve the following values were used for the elastic modulus and yield stress of these mild steel 6,35 mm and 10 mm diameter dowels:

Elastic Modulus	210 GPa
Yield Stress	250 MPa

High tensile steel round bars of 6,35 mm diameter were used in later tests and the characteristic curve for these dowels is shown in Fig. 4.3.2. From this curve the

TABLE 4.2.1

SUMMARY OF TESTS CONDUCTED ON
DOWELLED CRACKED-BEAM SPECIMENS:

	1	2	3	4	5	6	7
Test Series Number	Concrete Cube Strength (MPa)	Dowel Diameter (mm)	Dowel Material	[illegible]	Concrete Cover (mm)	Crack Width (mm)	Loading Type
1	30	6,35	Mild Steel	Single Central	47	8	Two Point
2	30	6,35	Mild Steel	Single, Top of Beam	Variable	8	Two Point
3	30	6,35	Mild Steel	Double, Top and Bottom	Variable	8	Two Point
4	30	10,0	Mild Steel	Single, Central	45	8	Two Point
5	30	6,35	Mild Steel	Single, Central	47	Variable	Two Point
6	30	10,0	Mild Steel	Single, Central	45	Variable	Two Point

<u>TABLE 4.2.1 CONTINUED</u>

	1	2	3	4	5	6	7
7	Variable	6,35	Mild Steel	Single, Central	47	8	Two Point
8	Variable	10,0	Mild Steel	Single, Central	45	8	Two Point
9	30	6,35	Mild Steel	Double, Top and Bottom + Stirrups	15	8	Two Point
10	30	6,35	Mild Steel	Single, 40° at face	47	6	Two Point
11	30	6,35	Mild Steel	Single, central, bars bent initially	47	8	Two Point
12	30	6,35	High Tensile Steel	Single, Central	47	8	Two Point
13	30	6,35	Mild Steel	Single, Central	47	8	Central Point Load

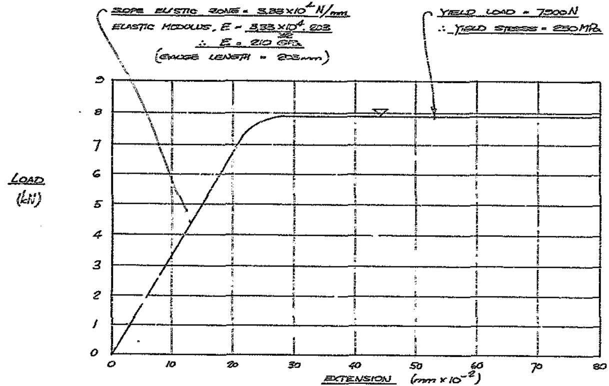

FIG. 4.3.1

CHARACTERISTIC LOAD - EXTENSION CURVE FOR 6.35mm MILD STEEL DOWELS SUBJECTED TO UNIAXIAL TENSION.

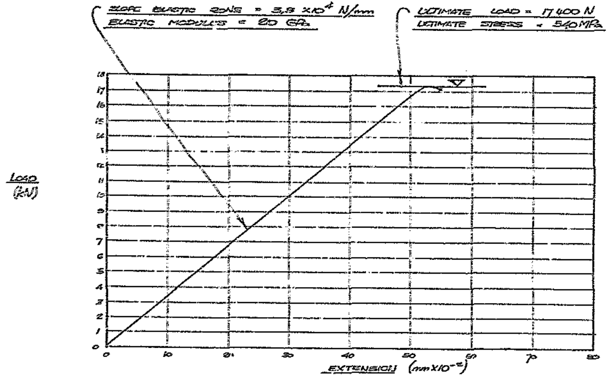

FIG. 4.3.2

CHARACTERISTIC LOAD - EXTENSION CURVE FOR 6,35 mm HIGH TENSILE STEEL DOWELS SUBJECTED TO UNIAXIAL TENSION following properties were established for high tensile steel dowels of 6,35 mm diameter:

Elastic Modulus	210 GPa
Failure Stress	540 MPa

The values given above were then used in the application of the PFB foundation model to the cracked-beam test results.

following properties were established for high tensile steel dowels of 6,35 mm diameter:

Elastic Modulus	210 GPa
Failure Stress	540 MPa

The values given above were then used in the application of the PFB foundation model to the cracked-beam test results.

4.4 SERIES 1 : *TESTS ON SPECIMENS HAVING A 6,35 mm MILD STEEL DOWEL ON THE BEAM AXIS*

The implication of large concrete cover is that the expected mode of failure would be yielding of the mild steel dowel (probably in conjunction with local crushing or plasticity of the sub-dowel concrete) before cracking and fracture of the concrete cover occurs (see Figs. 4.2.7 and 4.2.8). The 6,35 mm diameter dowel was situated on the beam axis for this test series and the load applied through bright steel rod loading platens, using the Macklow-Smith hydraulic testing machine. The crack formers of polystyrene foam were chipped out at the time of stripping of the moulds and the beams were then tested at 7 days. The cracked-beam specimens were loaded to failure (or yield) and the following parameters were all constant for this test series:

Concrete cube strength at approximately 30 MPa
Dowel diameter 6,35 mm
Dowel angle 90^0 (normal to crack face)
Crack width 8 mm
Concrete cover 47 mm (From this it follows that the ratio between cover and dowel diameter, d_c, is 7,4).

Very consistent results were obtained for the series of beams tested in this manner and the characteristic load-deflection curve, for a concrete cube strength of 30 MPa, is given in Fig. 4.4.1. Details of individual tests are tabulated in Table 4.4.1, together with those of the final

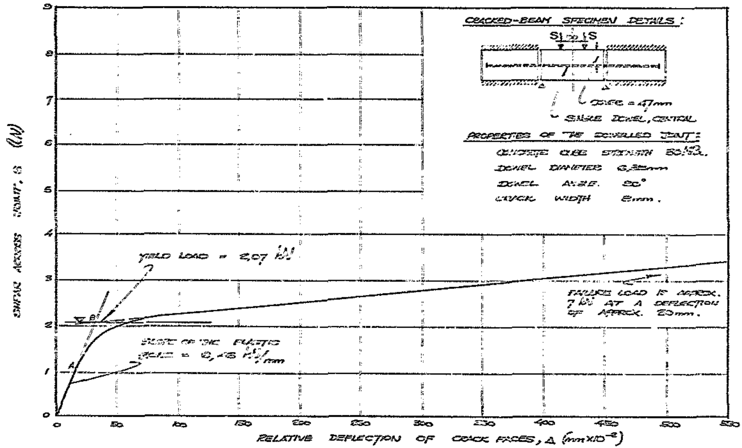

FIG. 4.4.1

CHARACTERISTIC LOAD-DEFLECTION CURVE FOR SERIES 1 : SINGLE 6.35mm MILD STEEL DOWEL ON THE BEAM AXIS

TABLE 4.4.1

SUMMARY OF TEST RESULTS FOR SERIES 1 :
SPECIMENS WITH 6,35 mm DIAMETER DOWEL ON BEAM AXIS

	Specimen Number	Concrete Cube Strength (MPa)	Slope of Elastic Zone of S-Δ curve (kN/mm)	Load at Elastic Limit (kN)	Load at "Yield" (kN)	At Failure Load (kN)	At Failure Crack face deflections (mm)
Experimental Results	1	29,6	6,35	1,00	2,00	Approximately 7 kN	Approximately 20 mm
	2	27,8	6,40	1,10	2,15		
	3	27,8	6,40	1,05	1,90		
	4	30,0	6,25	1,05	2,20		
	Average	29,0	6,35	1,05	2,10		
	Characteristic Results	30,0	6,46	1,07	2,07		
	PFB predicted results	30,0	6,49	1,03	1,80	Theory no longer applicable.	

characteristic curve for 30 MPa concrete. A theoretical evaluation of these test results was obtained using the PFB foundation model in the computer program "DOWEL" (see Appendix B.1). The value for concrete subgrade reaction used in the analysis is that established in Chapter 4.1. Typical printouts for data corresponding to that of the characteristic curve are included in Figs. 4.4.2 and 4.4.3, and the corresponding values for moment, shear and concrete sub-dowel pressure along the dowel axis are plotted in Fig. 4.4.4.

The experimentally obtained characteristic load-deflection curve comprises the following main portions:
The curve is perfectly elastic up to point A and the value for slope obtained from the program "DOWEL" has extremely good correlation with the experimentally observed value as is evident from Table 4.4.1. At A, the limit of elasticity, the PFB theory still holds and the predicted shear load causing the extreme fibre stress in the mild steel dowel to approach 250 MPa compares well with the observed limit of elasticity. From point A, increasing the load causes yielding of the dowel outer fibres until at the idealized point of yield B, it is assumed that the mild steel dowel has yielded completely, and the fully plastic moment of resistance of the dowel has been developed. Associated with this yielding of the steel is some local crushing or elasticity of the sub-dowel concrete. If this phenomenon is assumed to have a small effect on the overall shape of the sub-dowel pressure diagram, then k_o remains approximately constant up to the yield load at B, and the PFB founda-

PROPERTIES OF THE DOWELLED JOINT
****

CONCRETE PROPERTIES

CUBE STRENGTH= 30.0 MPa
ELASTIC MODULUS= 25.5 GPa
SUBGRADE MODULUS= 712.0 MPa/m

DOWEL PROPERTIES

DOWEL DIAMETER= 6.4 mm
DOWEL TENSION= 0.0 N
DOWEL ANGLE= 90.0 Degrees
ELASTIC MODULUS= 213.0 GPa
YIELD STRESS= 250.0 MPa
FULLY PLASTIC MOM OF RES= 10922.7 N mm

CRACK WIDTH= 0.0 mm
SHEAR FORCE ACROSS JOINT= 1030.0 N

PFD FOUNDATION RESULTS
****

STRESSES IN DOWEL

X (mm)	Y ORD (mm)	THETA (rad)	MOMENT (N mm)	SHEAR (N)	BRG STRS (MPa)	SH STRESS (MPa) (surface)	CONC STR (MPa)	TENS+BDG STR (MPa)
0.0	.05367	-.03919	-4130.0	-933.1	-160.1	-29.0	40.0	160.1
5.0	.02703	-.00066	-6459.9	-69.6	-251.0	-1.0	23.4	251.0
10.0	.00731	-.00269	-5737.3	376.3	-222.9	9.5	10.3	222.9
15.0	-.00022	-.00134	-3967.9	375.1	-154.2	11.7	2.4	154.2

FOR A SHEAR FORCE OF 1030.0 N, THE RELATIVE DEFLECTION OF THE CRACK FACES IS .159 mm

THE SLOPE OF THE ELASTIC ZONE OF THE LOAD/DEFL CURVE IS 6.49 kN/mm

FIG. 4.4.2

PROPERTIES OF THE DOWELLED JOINT
****

CONCRETE PROPERTIES

CUBE STRENGTH= 30.0 MPa
ELASTIC MODULUS= 25.5 GPa
SUBGRADE MODULUS= 712.0 MPa/m

DOWEL PROPERTIES

DOWEL DIAMETER= 6.4 mm
DOWEL TENSION= 0.0 N
DOWEL ANGLE= 90.0 Degrees
ELASTIC MODULUS= 213.0 GPa
YIELD STRESS= 250.0 MPa
FULLY PLASTIC MOM OF RES= 10922.7 N mm

CRACK WIDTH= 3.0 mm
SHEAR FORCE ACROSS JOINT= 1030.0 N

PFD FOUNDATION RESULTS
****

STRESSES IN DOWEL

X (mm)	Y ORD (mm)	THETA (rad)	MOMENT (N mm)	SHEAR (N)	BRG STRS (MPa)	SH STRESS (MPa) (surface)	CONC STR (MPa)	TENS+BDG STR (MPa)
0.0	.09329	-.01146	-7031.9	-1639.2	-279.9	-50.2	71.4	279.9
5.0	.05210	-.00799	-11270.9	-136.9	-639.2	-1.3	43.9	639.2
10.0	.03505	-.00464	[illegible]	535.1	-361.6	16.6	10.1	361.6
15.0	-.00035	-.00217	-3904.2	606.5	-239.4	20.4	4.2	239.4

FOR A SHEAR FORCE OF 1030.0 N, THE RELATIVE DEFLECTION OF THE CRACK FACES IS .277 mm

THE SLOPE OF THE ELASTIC ZONE OF THE LOAD/DEFL CURVE IS 6.49 kN/mm

FIG. 4.4.3

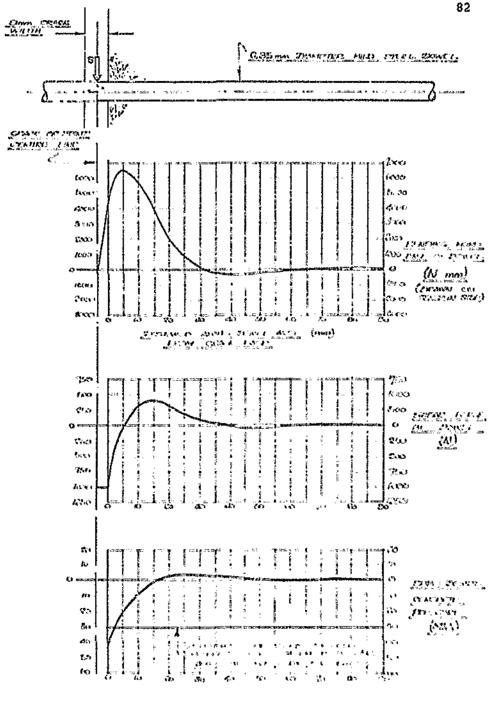

FIG. 4.4.4

tion model predicts the yield load which will give the dowel fully plastic moment of resistance to within 15% of the experimentally observed value*. From point B there appears to be a further increase in load-carrying capability of the dowelled joint. This is almost certainly a result of the suspension effect of the mild steel dowels, which now carry load in a catenary fashion. Extreme yielding of the steel dowel occurs before the concrete cover finally cracks, the load carried by the joint at this stage being in the region of 7 kN and the relative deflection of the crack faces about 20 mm (see Fig. 4.2.8).

The ultimate mode was thus a yielding of the mild steel dowel prior to brittle fracture of the concrete cover. If the subgrade modulus curves are idealized as in Figs. 4.1.2 and 4.1.3 then theory predicts sub-dowel pressures of approximately 2,4 times the concrete cube strength for the load causing full yielding of the mild steel dowels.

The general shape of the load-deflection curve (up to a crack deflection of about 1 mm) compares very well with results of tests on reinforced concrete beams by Krefeld and Thurston (see Fig. 2.1.2, specimen number 6 in particular). In addition the yield load obtained experimentally is fairly close to the value measured by Dulacska, who used specimens of a considerably different type, as shown in Fig. 2.2.4.

* (See Chapter 5.2 for a more detailed account).

4.5 SERIES 2 : *TESTS ON SPECIMENS HAVING A 6,35 mm MILD STEEL D..EL WITH SMALL COVER*

The expected mode of failure for this test series is fracture of the concrete cover prior to the fully plastic moment of resistance of the mild steel dowel being attained. Two typical specimens, each having a single dowel, but one having 17 mm of concrete and the other 12 mm cover, were tested in this series. The load-deflection curves for these two cases are given in Fig. 4.5.1, and are plotted on the same system of axes to give an indication of the development of the curve with increasing cover. The crack width was kept constant at 8 mm and consequently the crack formers were again polystyrene foam wafers. The principal parameters kept constant for this test series were:

Concrete cube strength at 27,8 MPa
Dowel diameter 6,35 mm
Dowel angle 90^0
Crack width 8 mm.

The experimentally obtained load-deflection curves comprised a number of basic sections:
As in Series 1, the curve is elastic up to point A and although the sub-dowel depth is substantially less than that for the specimens used in Series 1, the slope is practically identical, verifying the assumption that the concrete subgrade modulus is not sensitive to sub-dowel foundation depths and is thus approximately a function of the single variable, cube strength of the concrete, in the

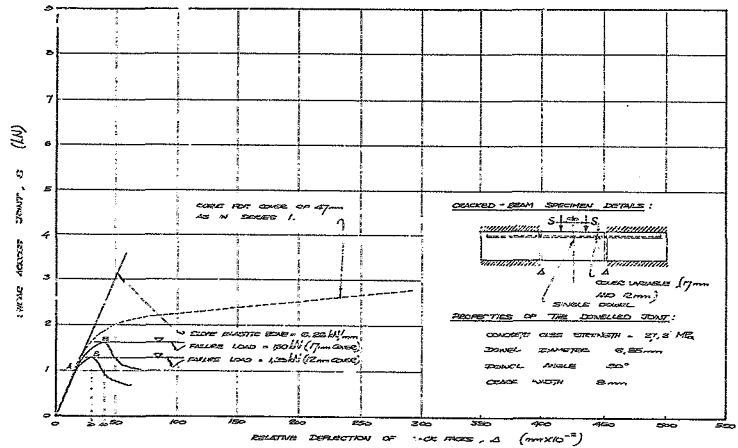

FIG. 4.5.1

LOAD - DEFLECTION CURVES FOR SERIES 2 : SINGLE 6,35mm MILD STEEL DOWEL - CONCRETE COVER VARIABLE.

TABLE 4.5.1

SUMMARY OF RESULTS FOR SERIES 2 :
SPECIMENS WITH 6,35 mm DIAMETER DOWELS –
COVER VARIABLE

	Specimen Number	Concrete Cube Strength (MPa)	Cover to dowel (mm)	Slope of S-Δ Curve Elastic Zone (kN/mm)	Load at Elastic Limit (kN)	At Failure	
						Exp'tal Load (kN)	PFB predicted sub-dowel pressure (MPa)
Exp'tal results	1	27,8	17	6,26	1,00	1,60	
	2	27,8	12	6,26	1,00	1,35	
Predicted results	1	27,8	17	6,25	0,99		61,6
	2	27,8	12	6,25	0,99		51,9

elastic range. As can be seen from Table 4.5.1, which gives a comparison between experimental and PFB predicted results, the correlation is good in the elastic zone. The predicted load at A, the limit of elasticity, also compares very well with the experimentally obtained value. With further increase in load from point A, the curve changes as a result of the combined effects of yielding of the dowel extreme fibres and local crushing of the sub-dowel concrete. Failure occurs at B *before the fully plastic moment of resistance of the dowel has been attained.* This is verified by theory, which predicts moments in the dowel less than the fully plastic moment for the experimentally obtained failure loads. For the case of the specimen with 17 mm cover, the moment in the dowel approaches the full yield value (for the load of 1,6 kN), and it would thus appear that a "critical cover" can be obtained.

For given constant parameters of concrete cube strength, crack width, dowel geometry and dowel material, there exists a cover to dowel diameter ratio, $(d_c)_{crit}$, such that the failure load for the dowelled connection coincides with the yield load. For the parameters considered in Series 1 and 2 it would appear that a value of $(d_c)_{crit}$ of approximately 4 can be applied and a design criterion would thus be that the cover provided to the dowel should be such that d_c exceeds the value of 4. (this concept will be dealt with more thoroughly in Chapter 5). The failure modes for the specimens of Series 2 were thus brittle fracture of the concrete cover, and the ratios, d_c, of 2,7 and 1,9 respectively indicate this mode of failure (both being less than

4). The sub-dowel concrete pressures at failure are 61,6 MPa and 51,6 MPa for the 17 mm and 12 mm cover specimens respectively, and are still in excess of the cube strength of the concrete used, in spite of the fact that the cover was small. The failure loads recorded are substantially lower than those of Series 1, and consequently lower than ultimate loads predicted by Dulacska, whose specimens specifically recorded "yield type" failures.

4.6. SERIES 3 : *TESTS ON SPECIMENS HAVING TWO 6,35 mm MILD STEEL DOWELS*

In order to establish changes in elastic behaviour of a dowelled joint with increasing number of dowels crossing the crack face, a test series having 2 dowels was undertaken. In addition, load-carrying capability of the joint after first cracking of the cover to the top dowels was also studied, in order to establish the overall increase in safety of this type of joint over the type tested in Series 2. Two 6,35 mm diameter mild steel dowels were used in each specimen, one at the top and the other at the bottom of the beam section. The two specimens tested in this series had covers to the top dowels of 17 mm and 12 mm respectively, giving a similar configuration to Series 2 specimens. The schematic elevation of the specimen is shown inset in Fig. 4.6.1. Crack widths were again 8 mm and the crack formers were thus polystyrene foam. The load-deflection curves for these joints are given in Fig. 4.6.1 and the parameters kept constant were:

Concrete cub strength at	27,8 MPa
Dowel diameters	6,35 mm
Dowel angles	90^0
Crack width	8 mm

The load-deflection curves obtained experimentally were found to comprise the following sections:

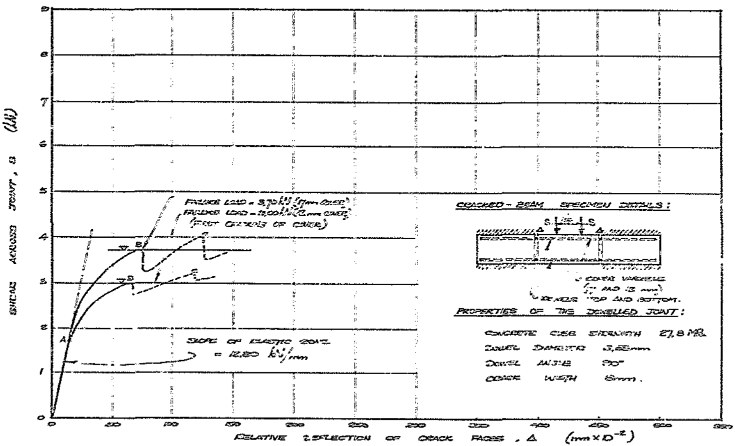

FIG. 4.6.1

LOAD – DEFLECTION CURVES FOR SERIES B : TWO 6.35 mm MILD STEEL DOWELS – COVER TO TOP DOWEL VARIABLE.

TABLE 4.6.1

SUMMARY OF TEST RESULTS FOR SERIES 3:
SPECIMENS HAVING TWO 6,35 mm DIAMETER DOWELS

	Specimen Number	Concrete Cube Strength (MPa)	Cover to top dowel (mm)	Slope of S-Δ Curve Elastic Zone (kN/mm)	Load at Elastic Limit (kN)	At Failure: Exp'tal Load (kN)	At Failure: PFB predicted sub-dowel pressure (MPa)
Exp'tal results	1	27,8	17	12,80	1,75	3,70	
	2	27,8	12	12,80	1,70	3,00	
Predicted results	1	27,8	17	12,50	1,98		71,2
	2	27,8	12	12,50	1,98		57,8

The part up to point A is linearly elastic and it can be seen from Table 4.6.1 that the slope is very close to twice that of the curves in Series 3. This implies that for a multi-dowel joint subjected to a shear force only, each dowel can be assumed to carry an equal portion of the total shear and consequently each can be analysed using the PFB foundation model by substituting the relevant shear force. This would probably still be the case for a joint subjected to a substantial bending moment in addition to the shear, which would cause tensions and compressions in different dowels, since these forces can be considered in the analysis if they can be evaluated. At A, the limit of elasticity, the PFB foundation model predicts loads slightly higher than those recorded experimentally, the error only being in the region of 10% however. From A, a further increase in load results in the yielding of the extreme fibres of both dowels, again probably associated with a small amount of local crushing of the sub-dowel concrete. At point B, first shedding of the concrete cover occurs (at one of the crack faces, that is), but it can be seen that a recovery in load-carrying capability occurs, so that there is eventually a further increase in load to the point of cracking of concrete cover at the other crack face (at C). The reason for this increase in load is that the lower dowels are carrying load in a manner similar to the specimens in Series 1 and thus the failure mode is not catastrophic as is the case for Series 2. For the same reason sub-dowel pressures at first failure of top cover are slightly higher than those for Series 2, as can be seen from a comparison of Tables 4.5.1 and 4.6.1. These differences of pressure are not significant and the principal advantage can be seen to be in the post-cracking stage. An extrapolation of these curves (had failure of the cover not occurred) gives the predicted load at yield approximately twice that for Series 1, and it can thus be seen that both stiffness and yield load are doubled when the number of dowels is doubled, provided both dowels have d_c larger than the critical value - taken to be approximately 4 (the cube strength of the concrete is not significantly different, and the crack geometry is identical, to Series 1).

4.7 SERIES 4 : *TESTS ON SPECIMENS HAVING A 10,0 mm MILD STEEL DOWEL ON THE BEAM AXIS*

This series of tests was undertaken to compare performance of dowels of varying diameter, and to verify that the PFB foundation model was still applicable. In addition to the necessary comparison of the results in the elastic zone, relationships between d_c ratios and pressures on the sub-dowel concrete at failure could also be compared as a check on the validity of the concept of the critical value for d_c. The 10,0 mm diameter dowel was situated on the beam axis for each specimen and the ratio, d_c, was thus in the order of 4,5. If the critical value of 4, established in Chapter 4.5, is considered to be correct, it would appear that full yielding of the dowel occurs just before cracking of the cover for these specimens. This is in fact substantiated by this test series - the results being summarized in Table 4.7.1 and the characteristic curve being given in Fig. 4.7.1. Crack formers were again polystyrene foam, and the parameters kept constant for this series were:

Concrete cube strength at about 30 MPa	
Dowel diameter	10,0 mm
Dowel angle	90°
Crack width	8 mm

The characteristic load-deflection curve can be described as follows:

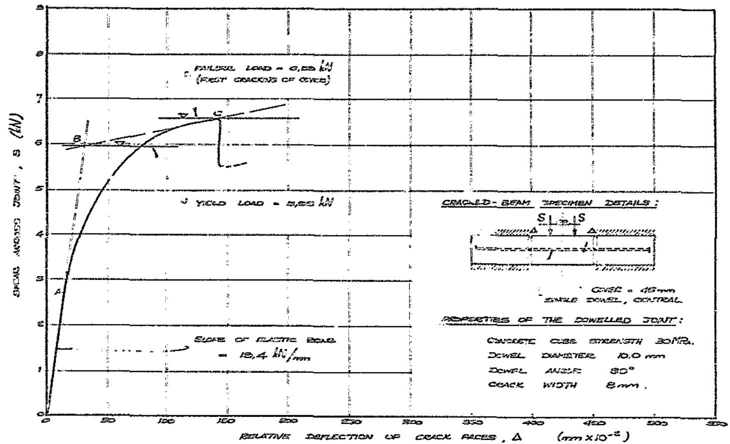

FIG. 4.7.1

CHARACTERISTIC LOAD-DEFLECTION CURVE FOR SERIES 4 : SINGLE 10,0mm MILD STEEL DOWEL ON THE BEAM AXIS .

TABLE 4.7.1

SUMMARY OF TEST RESULTS FOR SERIES 4 :
SPECIMENS WITH 10 mm DIAMETER DOWEL ON BEAM AXIS

	Specimen Number	Concrete Cube Strength (MPa)	Slope of Plastic [illegible]e of Curve (kN/mm)	Load at Elastic Limit (kN)	Load at "Yield" (kN)	At Failure: Load (kN)	At Failure: Crack face Deflection (mm)
Experimental results	1	30,0	20,0	2,60	6,00	6,50	1,30
	2	27,1	18,5	2,55	5,55	6,50	1,50
	3	28,3	18,4	2,65	5,85	6,25	1,10
	Mean Values	28,5	18,97	2,60	5,80	6,42	1,30
	Characteristic Results	30,0	19,40	2,67	5,95	6,59	1,30
PFB results for 30 MPa concrete		30,0	16,90	3,00	5,55		

Up to point A the curve is elastic, and the PFB predicts the slope to be slightly lower than the experimentally observed value as can be seen from Table 4.7.1. The effect could possibly be a result of a slight increase in subgrade modulus value as discussed in Chapter 4.1 (see equation 4.1.4), but as the results fall within 15% of the experimental values the theory is still considered to be applicable. The load at the elastic limit determined experimentally is slightly lower than the PFB foundation model predicted value, indicating that there is not a general trend for the theory to underestimate results for bars of larger diameter. After point A, the curve again becomes non-linear owing to the effects of dowel yield and local foundation crushing and the yield load at B is well predicted by the PFB model. With only a small increase of load from B, shedding of the concrete cover to the 10,0 mm dowel occurs. The failure load of 6,59 kN, only slightly higher than the yield load of 5,95 kN, indicates that the concept of critical cover to dowel diameter ratio, d_c, could have general application (at this stage for constant crack width of 8 mm and concrete cube strength of 30 MPa). If the cover to the 10,0 mm dowel were increased, it can be seen from the extrapolation of the straight line BC in Fig. 4.7.1 that the curve would have the same general shape as that of Series 1. The actual shape of the experimentally determined load-deflection curve compares well with the shape of the curve obtained by Krefeld and Thurston for Specimen 7 in particular in their test series.

It may be noted from both Table 4.4.1 and Table 4.7.1 that the predicted yield load using the PFB foundation model falls *slightly below* that recorded experimentally (although predicted values using this model compare very well with those given by equation 2.2.2 - Dulacska's equation). This is the result of the use of the elastic modulus of steel in the post-yield stage. The substitution of a reduced modulus would be more correct owing to yield of extreme fibres and this does in fact give results closer to the experimental values. Since the PFB results are not sensitive to changes in elastic modulus of the dowel, however, the analysis using the elastic modulus at least gave approximate guide lines (see Chapter 5.2).

4.8 SERIES 5 : *TESTS ON SPECIMENS HAVING A SINGLE CENTRAL 6,35 mm MILD STEEL DOWEL, AND VARIABLE CRACK WIDTH*

The principal reason for this test series was the verification of the PFB foundation theory as the crack width proceeded from 8 mm to zero, the crack width likely to be encountered most often in practice. Tests on specimens of zero crack width were not as reliable as other tests, since it proved difficult to eliminate friction completely from the crack faces of the beam specimens. On the other hand, an extrapolation of results from tests on specimens with crack width greater than zero, to give expected results for zero crack width, gives a good indication of friction effects for the specimens used, when compared with actual experimental results. The 6,35 mm diameter dowels were situated on the beam axis for this test series and in addition to using polystyrene crack formers, mild steel crack formers (as shown in Fig. 4.2.2) were used for the 3 mm and zero crack width specimens.

The procedure was that the openings in the mild steel crack formers were filled with a wafer of polystyrene foam, taped to the steel, and the dowel then passed through this polystyrene making removal of the crack formers possible at the time of stripping of the moulds for the 3 mm crack width specimens. For the specimens with zero crack width, the beam centre portion was cast first, using the crack formers as mould-ends. After 24 hours the mild steel formers were removed, and thin, stiff, well oiled paper was placed over the exposed concrete surface containing the protruding dowel.

The beam ends were then cast around this protruding dowel against the oiled surface, using a slightly compensated mix so that the beam had an approximately uniform concrete cube strength at the time of testing of 7 days. The average cube strength of 6 cubes (3 from each mix) was used in the analysis of these specimens.

The specimens were loaded to yield using a two-point loading system as before and the parameters kept constant for the test series were:

Concrete cube strength at about 30 MPa
Dowel diameter 6,35 mm
Dowel angle 20°
Concrete cover 47 mm

The variation in the load-deflection curves is shown in Fig. 4.8.1, where the results for 8 mm, 6 mm and 3 mm crack width specimens are compared, by plotting the results on the same axes. The variations in slope, elastic limit and yield load with changes in crack width are compared with predicted PFB results in Table 4.8.1. The correlation obtained is generally good (although the experimentally observed slope of Specimen 3 seemed somewhat lower than expected) and the variation in joint characteristics of stiffness and ultimate load capabilities with variation of crack width appear to be well modelled by the PFB foundation.

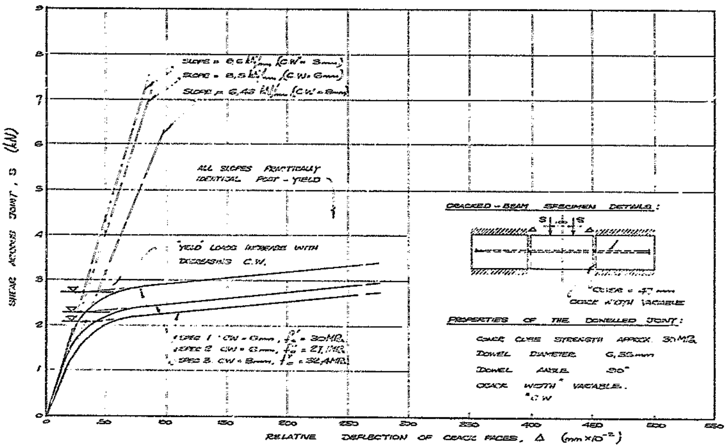

FIG. 4.8.1

LOAD - DEFLECTION CURVES FOR SERIES S : SINGLE 6,35 mm MILD STEEL DOWEL - CRACK WIDTH VARIABLE.

TABLE 4.8.1

SUMMARY OF TEST RESULTS FOR SERIES 5 :
SPECIMENS WITH 6,35 mm DOWEL ON BEAM AXIS –
CRACK WIDTH VARIABLE

	Specimen Number	Concrete Cube Strength (MPa)	Crack Width (mm)	Slope of Elastic Zone of S-Δ Curve (kN/mm)	Load at Elastic Limit (kN)	Load at "Yield" (kN)	At Failure
Experimental Results	1	30,0	8	6,46	1,07	2,07	Failure Values approximate only (See Table 4.4.1)
	2	27,1	6	8,50	1,17	2,10	
	3	32,4	3	8,60	1,41	2,81	
Predicted Results	1	30,0	8	6,49	1,03	1,80	
	2	27,1	6	7,50	1,18	2,00	
	3	32,4	3	10,20	1,53	2,62	

Having established that the PFB foundation model applies to all these curves, the mathematical model is used to extrapolate the expected values of slope, elastic limit and load at yield for a specimen of zero crack width and these values are compared with the experimentally obtained values in Table 4.8.2. The graphical comparison is shown in Fig. 4.8.2. It can be seen from this comparison that even though the concrete surfaces were well oiled and care was taken to ensure that they were straight and did not bear on one another, a significant contribution from friction is present (PFB predicted results are generally 65 to 75% of the experimental values). This implies that construction joints designed on the basis of zero crack width and no friction will be conservative, provided no shrinkage (thermal or otherwise) occurs that might cause separation of the concrete surfaces. On the other hand, the attachment of brackets to precast concrete elements could be designed using the zero crack width principle, neglecting friction effects. [illegible]sign of bolted or riveted steel connections follows [illegible] principle in this regard - the friction of the steel plates generally being neglected and all shear considered to be transferred from plate to plate by the shear action of the bolt or rivet cluster (except in the case of "friction-grip" bolts). The fundamental difference would be that whereas the shear stress in the bolt generally controls in the case of the bolted steel connection, shear stresses are generally insignificant in dowels crossing reinforced concrete joints - the controlling stresses being bending in the dowel or sub-dowel concrete pressures.

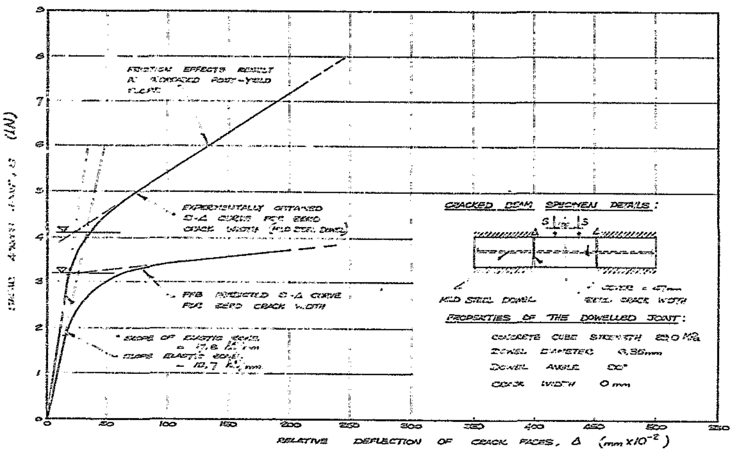

FIG. 4.8.2

GRAPHICAL COMPARISON OF EXPERIMENTAL AND PREDICTED RESULTS FOR SPECIMENS OF ZERO CRACK WIDTH. (SERIES 5)

TABLE 4.3.2

SERIES [illegible] : COMPARISON OF EXPERIMENTAL AND PREDICTED RESULTS FOR SPECIMENS WITH A CENTRAL 6,35 mm DIAMETER DOWEL AND ZERO CRACK WIDTH

	Specimen Number	Concrete Cube Strength (MPa)	Crack Width (mm)	Slope of S-Δ Curve Elastic Zone (kN/mm)	Load at Elastic Limit (kN)	Load at "Yield" (kN)	At Failure
Experimental Results	1	26,9	0	16,9	3,43	4,40	Failure Values Approximate only (See Table 4.4.1)
	2	28,3	0	18,7	2,82	3,75	
	Average	29,0	0	17,8	3,12	4,08	
PFB predicted results		29,0	0	12,7	1,88	3,21	

4.9 SERIES 6 : *TESTS ON SPECIMENS HAVING A SINGLE CENTRAL 10,0 mm MILD STEEL DOWEL AND VARIABLE CRACK WIDTH*

As for Series 5, this test series established the validity of the PFB foundation results with variation of crack width, but in this case investigated consistency with increasing dowel diameter as well. In addition, failure modes(cracking and spalling of concrete cover) could be investigated in this series, since a d_c ratio approximately equal to the critical value meant that the failure of the cover would occur at about the yield load and could thus be recorded easily. It was noted in this test series that beam specimens of zero crack width again exhibited increased stiffness and yield loads, owing to friction effects of the concrete surfaces. Crack formers were used in an identical manner to Series 5 and again care was taken to ensure that there was minimum friction on the shear interface.

The specimens were loaded to failure of the cover and the parameters kept constant for this test series were:

Concrete cube strength approximately 30 MPa	
Dowel diameter	10,0 mm
Dowel angle	90^0
Concrete cover	45 mm

The variation in load-deflection curves with varying crack width is shown in Fig. 4.9.1, where results for specimens with 8 mm, 3 mm and zero crack width specimens are compared. A summary of test results in Table 4.9.1 indicates the

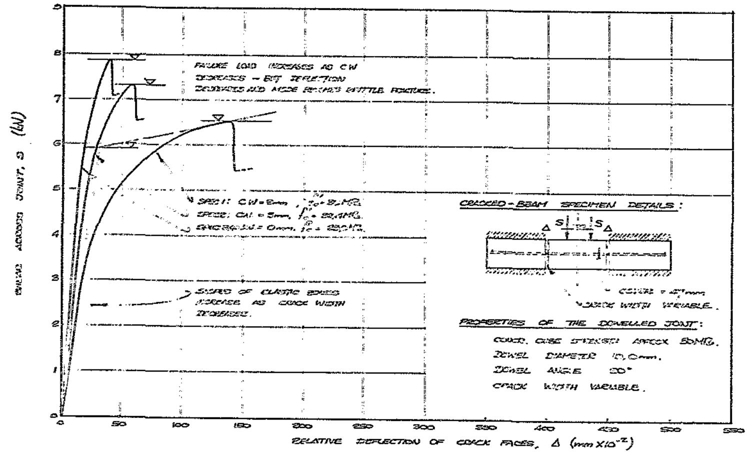

FIG. 4.9.1

LOAD-DEFLECTION CURVES FOR SERIES 6: SINGLE 10.0mm MILD STEEL DOWEL — CRACK WIDTH VARIABLE.

TABLE 4.9.1

SUMMARY OF TEST RESULTS FOR SERIES 6 :
SPECIMENS WITH 10,0 mm DIAMETER DOWEL,
CENTRAL-CRACK WIDTH VARIABLE

	Specimen Number	Concrete Cube Strength (MPa)	Crack Width (mm)	Slope of S-Δ Curve Elastic Zone (kN/mm)	Load at Elastic Limit (kN)	Load at "Yield" (kN)	At Failure: Load (kN)	At Failure: Predicted Sub-Dowel Pressure (MPa)
Experimental Results	1	30,0	8	19,4	2,67	5,95	6,59	
	2	32,4	3	26,5	3,45		7,30	
	3	29,6	0	31,4	4,89		7,94	
	4	28,3	0	37,5	4,50		7,90	
	Ave 3,4	29,0	0	34,5	4,70		7,92	
Predicted Results	1	30,0	8	16,9	3,00	5,55		
	2	32,4	3	23,6	4,10	7,08		103
	3,4	29,0	0	27,4	5,02	8,52		100

correlation between experimental and theoretical results, and this is generally good for the specimens having a crack width greater than zero, but the PFB foundation again predicts slope of the elastic zone and yield load less than the values obtained experimentally for zero crack width specimens (an exception is that the elastic limit appears to be well predicted). It is interesting to note, however, that although the failure load increases overall with decreasing crack width, the yield load exceeds the failure load slightly for the zero crack width specimen, whereas the reverse is true for the 8 mm crack width specimens. This is reflected in the general change in shape of the load-deflection curve as the crack width decreases (see Fig. 4.9.1). In addition, the relative deflection of the crack faces at failure becomes smaller. This effect is not considered to be significant in establishing a general relationship for $(d_c)_{crit}$, however. If the maximum crack width for a joint is considered to be approximately 8 mm, then the value of $(d_c)_{crit}$ of 4 will be a conservative estimate for all other joints, since failure of the concrete cover, which depends on the deflection and curvature of the dowel at the crack face, occurs at a higher load as the crack width decreases, although the ultimate mode changes. This increase in expected failure load is well modelled by the PFB foundation if sub-dowels concrete pressures are considered to be critical for spalling of the concrete cover.

It can be seen that the PFe foundation model predicts values closer to experimental values for this series than for Series 5 for specimens of zero crack width. Thus the value of the friction present is difficult to evaluate quantitatively and would appear to rely on casting techniques when moulding the specimens.

4.10 SERIES 7 : *TESTS ON SPECIMENS HAVING A SINGLE, CENTRAL 6,35 mm MILD STEEL DOWEL, AND VARIABLE CONCRETE STRENGTH*

Having established the validity of the PFB foundation model for a variety of configurations of specimen geometry, the correlation with cube strength was then tested in Series 7 and 8. These tests were conducted specifically to verify the application of the assumed function relating concrete subgrade modulus to cube strength (see Equation 4.1.14). Constant crack widths of 8 mm were used for this series and consequently crack formers were again of polystyrene foam. The same concrete mix was used as for previous specimens, but testing occurred at different intervals, thus varying the concrete strength. Ultimate modes were generally yield types failures (a combination of dowel yield and sub-dowel concrete plasticity) and the principal parameters kept constant for this test series were:

Dowel diameter	6,35 mm
Crack width	8 mm
Dowel angle	90^{0}
Concrete cover	47 mm

The overall improvement of the load-deflection curve characteristics for these specimens with increasing cube strength of concrete is clearly indicated in Fig. 4.10.1. A summary of test results, compared with predicted results, given in Table 4.10.1, indicates that the assumed function for concrete subgrade modulus gives reasonable correlation

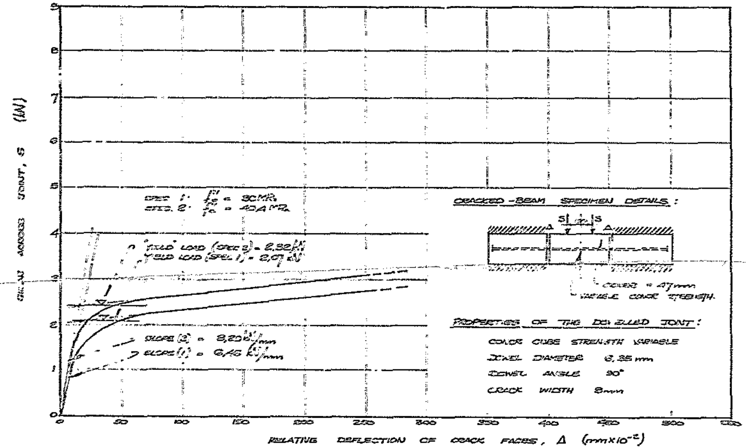

FIG. 4.10.1

LOAD - DEFLECTION CURVES FOR SERIES 7: SINGLE 6.35 mm MILD STEEL DOWEL - CONCRETE STRENGTH VARIABLE.

TABLE 4.10.1

SUMMARY OF TEST RESULTS FOR SERIES 7 :
SPECIMENS WITH 6,35 mm DIAMETER DOWEL,
CENTRAL-CONCRETE STRENGTH VARIABLE

	Specimen Number	Concrete Cube Strength (MPa)	Crack Width (mm)	Slope of S-Δ Curve Elastic Zone (kN/mm)	Load at Elastic Limit (kN)	Load at "Yield" (kN)	At Failure
Exp'tal Results	1	30,0	8	6,46	1,07	2,07	Failure Values Approx. only (See Table 4.4.1).
	2	40,4	8	8,20	1,42	2,32	
Predicted Results	1	30,0	8	6,49	1,03	1,80	
	2	40,4	8	7,10	1,06	1,90	

between experiment and theory, and this is supported by the results of Series 8. The indication is certainly that the relationship is not linear, and the quadratic function chosen not only compares fairly well with the cube and crack-beam specimen test results, but in addition compares well with elastic modulus type variations with concrete strength as given in CP 110. The relationship given in Equation 4.1.14 thus appears to give good overall results.

4.11 SERIES 8 : *TESTS ON SPECIMENS HAVING A SINGLE, CENTRAL 10,0 mm MILD STEEL DOWEL AND VARIABLE CONCRETE STRENGTH*

This test series was conducted for the same reasons as Series 7, but was slightly more comprehensive since the use of the larger diameter dowel made possible the study of the transition from brittle failure to yield type ultimate modes with increase in cube strength of the concrete. Tests were conducted on specimens having 8 mm crack width and thus crack formers were again polystyrene. The 10,0 mm dowel was situated on the beam axis and the specimens were all loaded to failure or yield (whichever occurred first). The principal parameters kept constant for the test series were:

Dowel diameter	10,0 mm
Crack width	8 mm
Dowel angle	20^0
Concrete cover	45 mm

The test results are given in Fig. 4.11.1 and a summary of test results together with theoretically predicted results is given in Table 4.11.1. It is evident from the results that the load-deflection curve parameters of elasticity, load at elastic limit and load at yield(or failure) all increase with increasing concrete strength. In addition, the trend of these increases is well modelled by the PFB foundation, using the quadratic relationship for subgrade modulus. An interesting feature of the trend in ultimate conditions is that the ultimate mode undergoes a transition as the cube strength of the concrete used increases.

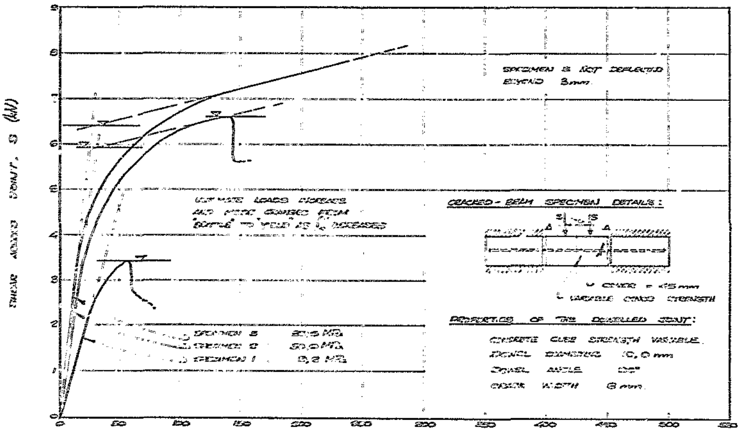

FIG. 4.II.1

LOAD - DEFLECTION CURVES FOR SERIES B : SINGLE 10,0 mm MILD STEEL DOWEL - CONCRETE STRENGTH VARIABLE.

TABLE 4.11.1

SUMMARY OF TEST RESULTS FOR SERIES 8 :
SPECIMENS WITH 10,00 mm DIAMETER DOWEL,
CENTRAL-CONCRETE STRENGTH VARIABLE

	Specimen Number	Concrete Cube Strength (MPa)	Slope of S-Δ Curve Elastic Zone (kN/mm)	Load at Elastic Limit (kN)	Load at "Yield" (kN)	At Failure: Load (kN)	At Failure: PFB predicted Sub-dowel Pressure (MPa)
Experimental Results	1	9,2	9,40	2,35		3,40	
	2	30,0	19,4	2,67	5,95	6,59	
	3	39,5	23,4	2,68	6,40	7,84	
Predicted Results	1	9,2	11,0	2,88	4,89		47
	2	30,0	16,9	3,00	5,55		Theory not Applicable
	3	39,5	18,5	3,26	5,67		

It is apparent that the failure mode for the 9,2 MPa concrete is catastrophic, whereas the mode for the 39,5 MPa concrete is of the yield type, similar to the characteristic curve for Series 1.

This phenomenon will reflect on $(d_c)_{crit}$ values, since although a d_c ratio of 4 is adequate for 30 MPa concrete, it would have to be substantially larger for 9,2 MPa concrete, all other joint parameters being equal. An approximate relationship for safe d_c ratios is established on this basis in Chapter 5. It is thus evident that the overall safety of a construction joint increases and there is a tendency for the failure mode to become a yield (plastic) type, as the strength of the concrete used in the joint increases, all other joint parameters being equal.

4.12 SERIES 9 : *TEST ON SPECIMEN HAVING TWO 6,35 mm MILD STEEL DOWELS AND STIRRUPS IN THE REGION OF THE CRACK FACES*

The specimen geometry for this test was identical to that of the specimens of Series 3, the cover in this case being 15 mm (the average value of the two specimens tested in Series 3). In addition, 6,35 mm diameter mild steel stirrups were fixed in position in the vicinity of the crack face, about 10 mm cover being left between the stirrups and the crack face. The principal reason for this test was to evaluate the effect the addition of stirrups had on load-deflection curve parameters, especially at ultimate load. The specimen crack width was 8 mm, and polystyrene crack formers maintained the position of the reinforcement during casting. The principal parameters kept constant for this test series were:

Concrete cube strength at	32,4 MPa
Dowel diameters	6,35 mm
Dowel angle	90°
Concrete cover to top dowel	15 mm
Crack width	8 mm

Clearly, the curve expected had the stirrups not been present would have been an average of the two curves given in Fig. 4.6.1. However, the actual curve is shown in Fig. 4.12.1 and the advantages to be gained by the inclusion of stirrups are clearly indicated, especially as regards ultimate loads and post-cracking behaviour.

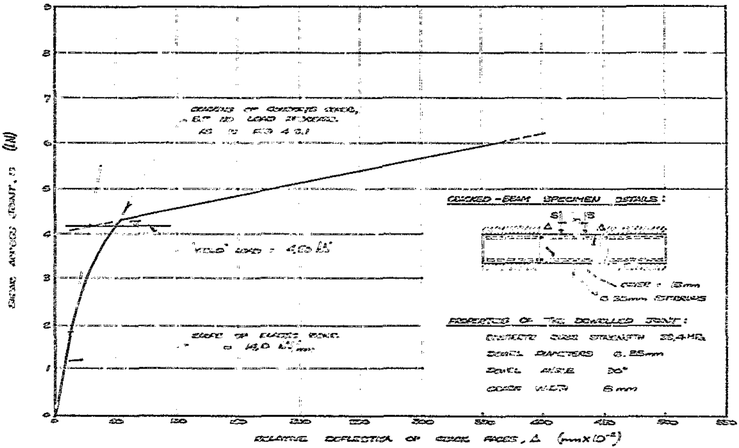

FIG. 4.12.1

LOAD - DEFLECTION CURVE FOR SERIES C : SPECIMEN HAS 2 6.25mm DOWELS AND STIRRUPS AT THE CRACK FACE.

TABLE 4.12.1

COMPARISON BETWEEN EXPERIMENTAL AND THEORETICAL RESULTS FOR SERIES 9 : SPECIMEN WITH TWO 6,35 mm DIAMETER DOWELS AND STIRRUPS AT THE CRACK FACE

	Specimen Number	Concrete Cube Strength (MPa)	Cover to Top Dowel (mm)	Slope of S-Δ Curve Elastic Zone (kN/mm)	Load at Elastic Limit (kN)	Load at "Yield" (kN)
Exp'tal Results	1	32,4	15	14,8	1,90	4,20
Predicted Results	1	32,4	15	13,4	2,06	3,60

Table 4.12.1 gives the comparison between experimentally obtained results and the PFB predicted values for the specimen geometry neglecting the stirrups. It is interesting to note that the stirrups do not affect the joint stiffness significantly. The load at yield, although substantially larger than the failure values obtained in Series 3, is still reasonably well predicted by the PFB foundation model. It would thus appear that the principal advantage to be gained by the addition of stirrups is that the ratio, d_c, can be brought below the critical value, and thus the joint can still be designed using the "yield" ultimate conditions. In the event of the reinforcement geometry being such that the criterion (of minimum cover to the bars subjected to dowel shear) cannot be met, the inclusion of stirrups in the vicinity of the crack face would increase the safety of the joint. This would have general application to dowels where spalling of the concrete is likely to occur. Fixing the dowel in position by means of a suitably placed stirrup greatly reduces the risk of spalling of the surrounding concrete. Thus, although stirrups in the region of the crack face do not significantly affect the elastic properties of the joint or even the ultimate load, if the dowel has infinite cover and spalling is not a problem, they have a significant effect on the safety of a joint whose dowels have insufficient cover.

4.13 SERIES 10 : *TESTS ON SPECIMENS HAVING A SINGLE 6,35 mm ANGLED DOWEL*

This dowel configuration, shown inset in Fig. 4.13.1, was tested to establish the effect that dowel angle to crack face (or shear interface) had on the joint as regards over-all joint stiffness and ultimate modes. In addition the validity of the PFB foundation model with increasing dowel angle was investigated.

In the process of casting of these specimens it was found that 6 mm crack formers were best suited for use in conjunction with the bent-up bars of these specimens. Thus the crack formers were made of polystyrene and they maintained the position of the reinforcement during the casting program. The principal parameters kept constant for this test series were:

Concrete cube strength at approximately 30 MPa	
Dowel diameter	6,35 mm
Dowel angle	40°
Concrete cover	47 mm
Crack width	6 mm

The average load-deflection curve is shown in Fig. 4.13.1 and a summary of experimental results and theoretically predicted values is given in Table 4.13.1. The general shape of the load-deflection curve is very similar to that obtained for Series 1, there being a general trend toward increase of both stiffness and ultimate loads with the angled dowels, however. The load deflection curve comprises

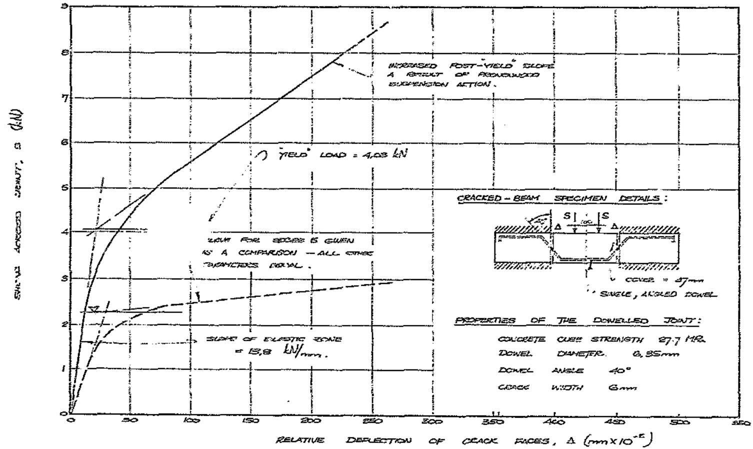

FIG. 4.13.1

CHARACTERISTIC LOAD - DEFLECTION CURVE FOR SERIES 10 : SINGLE 6,35mm MILD STEEL, ANGLED DOWEL.

TABLE 4.13.1

SUMMARY OF TEST RESULTS FOR SERIES 10 : SPECIMENS WITH A 6,35 mm DIAMETER DOWEL CROSSING THE CRACK FACE AT 40°

	Specimen Number	Concrete Cube Strength (MPa)	Dowel Angle (approx)	Crack Width (mm)	Slope of S-Δ Curve Elastic Zone (kN/mm)	Load at Elastic Limit (kN)	Load at "Yield" (kN)
Experimental Results	1	27,1	40°	6	19,9	2,10	4,10
	2	28,3	40°	6	17,6	2,24	3,95
	Average	27,7	40°	6	18,8	2,17	4,03
Predicted Results		27,7	40°	6	18,2	1,60	3,20

same basic parts as that shown in Fig. 4.4.1, and it can be seen that the slope of the curve in the post-yield stage is significantly steeper than that for the curve of Series 1. This supports the assumption that this increase in load-carrying capability of the joint is caused by suspension effects. The PFB foundation model predicts the slope in the elastic zone well but underestimates both the load at the elastic limit and the yield load. This is probably a result of the use of the incorrect modulus for the steel in predicting yield conditions, and in addition the effect of local compression and plasticity of the sub-dowel concrete in the region of the crack face appear to be less significant for the angled dowels, resulting in higher yield loads. (Predicted sub-dowel concrete pressures are also generally low compared with results of previous series, indicating that the sub-dowel concrete might remain elastic to a higher load). Nevertheless, the trend is fairly well modelled by the PFB foundation, the results generally tending to be conservative.

A comparison of curves for identical specimens, except for the dowel angle, indicates the significant advantages to be gained by a judicious choice of the angle of the dowel. The direction of the angle to the crack face is important and must be such that part of the shear is transferred by tension in the dowel. If the dowel were angled incorrectly, it would affect the performance of the joint *adversely* (see Series 11).

4.14 SERIES 11 : *TESTS ON SPECIMENS HAVING A SINGLE 6,35 mm DOWEL, BENT INITIALLY TO SIMULATE SLAB-ONTO-WALL CONNECTIONS*

In order to compare the performance between dowelled specimens such as those of Series 1 (where it was known that the dowels passed through the joint normal to the crack face) and those bent out after casting of the beam ends, as would probably be encountered in practice (see Fig. 1.1.1 and 1.1.2), this test series was conducted. During the casting program the dowels were cast into the beam end portions initially. The dowel lengths were about 400 mm each for each specimen (see sketch inset in Fig. 4.14.1). After 24 hours the bars were bent into position and the central portion of the beam specimen was cast, using an adjusted concrete mix so that the cube strength would be approximately constant at the time of testing of 7 days. The cube strength of the concrete was determined from the average of six cube tests, three being taken from each mix. Crack formers were again polystrene foam and the basic parameters kept constant for this test series were:

Concrete cube strength at 29,9 MPa
Dowel diameter 6,35 mm
Dowel angle approximately 90°
Concrete cover approximately 47 mm
Crack width 8 mm

The experimentally determined load-deflection curves are given in Fig. 4.14.1 and it is evident from a comparison

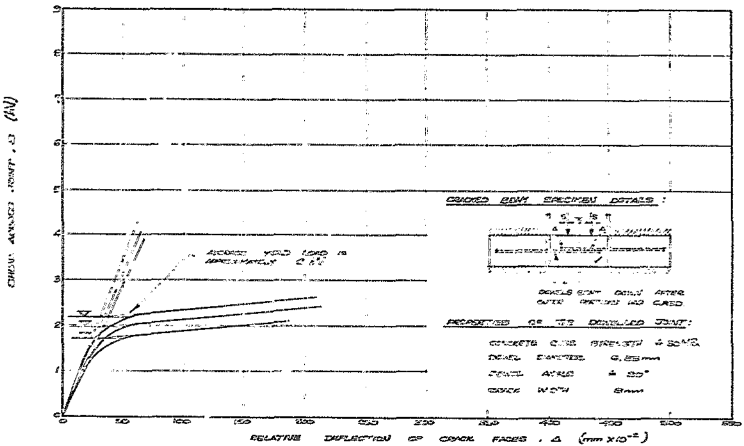

FIG. 4.14.1

LOAD - DEFLECTION CURVES FOR SERIES 'F' DOWELS BENT INITIALLY TO SIMULATE SLAB-ONTO-WALL TYPE CONNECTIONS.

between these curves and the curve shown in Fig. 4.4.1 that there is no significant difference in the results. The only disadvantage of the practice adopted in this series is that the angle of the dowel in the immediate vicinity of the dowel may be such that it affects the performance of the joint adversely (this would increase the experimental scatter slightly). The scatter of experimental results in general, however, is such that the load factors used for the yield loads, or the choice of permissible dowel loading stresses or sub-dowel concrete pressures, would take into account these discrepancies. The design criteria applied to these joints would thus be identical to those for Series 1.

4.15 SERIES 12 : *TESTS ON SPECIMENS HAVING A SINGLE 6,35 mm HIGH TENSILE STEEL DOWEL ON THE BEAM AXIS*

Three specimens were tested in this series, two having 8 mm crack width and one of zero crack width. The results of these tests can thus be compared with those of Series 1 and 5, since the specimen geometries are identical in every respect except the yield stress of the dowel materials. The casting and crack-forming techniques were identical to those of previous specimens and the principal parameters kept constant for this test series were:

Concrete cube strength at	28,9 MPa
Dowel diameter	6,35 mm
Dowel angle	90^{0}
Crack widths	8 mm and zero
Concrete cover	47 mm

The average load-deflection curve for the 8 mm crack width specimens and the curve for the zero crack width specimen are shown in Fig. 4.15.1 and the curves can be compared with those in Figs. 4.4.1 and 4.8.2 respectively, as shown in Table 4.15.1. There is good correlation between the slopes of the elastic zones of these test curves and tests on mild steel dowels. This is to be expected since the elastic modulus of the dowel material is unchanged and the sub-dowel concrete is still elastic. The PFL model also gives good agreement in this zone, the predicted slope being 6,42 kN/mm for the 8 mm crack width specimens.

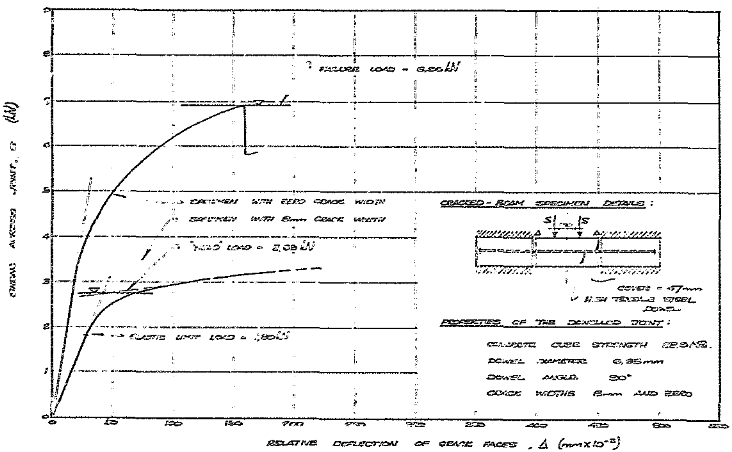

FIG. 4.15.1

LOAD - DEFLECTION CURVES FOR SERIES 12 : SPECIMENS WITH A SINGLE 6.35mm DIAMETER HIGH TENSILE STEEL DOWEL

TABLE 4.15.1

SERIES 12 : COMPARISON BETWEEN TEST ON HIGH TENSILE AND MILD STEEL 6,35 mm DIAMETER DOWELS

	Specimen Number	Concrete Cube Strength (MPa)	Dowel Material	Crack Width (mm)	Slope of S-δ Curve Elastic Zone (kN/mm)	Load at Elastic Limit (kN)	Load at "Yield" (kN)	Load at Failure (kN)
Experimental Results	1	28,9	High Tensile Steel	8	6,40	1,80	2,69	
	2	30,0	Mild Steel	8	6,46	1,07	2,07	
	3	28,9	High Tensile Steel	0	16,8	3,40		6,95
	4	29,0	Mild Steel	0	17,8	3,12	4,08	> 7

It is interesting to note that although extreme fibres are not near yield (or ultimate) stress, the curves become non-linear well before yield or fracture occurs. This confirms that the non-linearity of the load-deflection curves is the result of two phenomena:

1. Yielding of the dowel extreme fibres
2. "Plastic" deformation of the sub-dowel concrete.

In the case of the specimens with mild steel dowels, yielding of the dowel material was the dominant effect and probably occurred just before the sub-dowel concrete began to deform plastically. For the high tensile steel specimens, however, the plastic yield of the subgrade in the region of the crack face is dominant and occurs before yielding of the dowel material. The PFB foundation model predicts sub-dowel concrete pressures in the order of 2,4 times the cube strength at the experimentally determined elastic limit. This implies that two limiting criteria, the lower of which will control the design, must be applied when considered working loads for dowelled connections in general:

1. A permissible bending stress in the dowel
2. A permissible concrete sub-dowel pressure.

It is evident from a comparison of test results that these limits will result in very similar working loads in the case of mild steel dowels, whereas the concrete pressure will control a design using high tensile dowels. The implication is that mild steel appears to be a more satisfactory dowel material for medium strength concretes.

In addition, the use of high tensile steel dowels results in a transition of the mode of failure of the dowelled connection (evident in the comparison of test results for the specimens of zero crack width). Because the high tensile steel dowels remain elastic after the load-deflection curve elastic limit, and therefore do not deform as readily as the mild steel dowels in this range, the tendency for the concrete to fracture and spall is increased. The post "yield" phenomenon of the 8 mm crack width specimens is again a result of suspension effects, the sub-dowel concrete having yielded sufficiently to allow the dowel (which is still elastic, although near ultimate stress) to carry load in a catenary fashion.

4.16 SERIES 13 : *TESTS ON SPECIMENS HAVING A SINGLE, CENTRAL 6,35 mm MILD STEEL DOWEL, AND A CENTRAL POINT LOAD*

The loading system on the specimens tested in this dissertation could possibly have an effect on the observed load-deflection curves. Owing to the specimen geometry, however, this effect is expected to be small (in addition, the two-point loading system chosen for general tests meant that the loads were as close to the crack face as possible without interfering with the operation of the LVDT's). Nevertheless, this test series was undertaken in order to investigate the possible effect of a change in position of the load on the central beam portion. The basic parameters kept constant for this test series were:

Concrete cube strength at approximately 30 MPa	
Dowel diameter	6,35 mm
Dowel angle	90°
Crack width	8 mm
Concrete cover	47 mm

The experimental results of this test series were very similar to those for Series 1 (specimen geometries and test parameters were identical except for the loading types). Slopes of the elastic zones were practically identical for both test series, although elastic limit and "yield" loads appeared to be slightly lower for this test series. The principal reasons for these phenomena are a slight increase of end rotation of the central beam section coupled with a slight increase in the tension in the dowel. The effect of end rotation will not be significant in practical connections, however, since these will generally have a number of dowels crossing the shear interface. The resulting tensions set up in the dowels can be considered in the analysis using the PFB foundation model. Thus the effects on the load-deflection curves are insignificant in general and the theory used can therefore be applied to a dowelled slab connection, the slab being subject to any loading system.

The position of the point load also affects fracture parameters of the concrete cover, since the tensile cracks originate under these point loads (see Figs. 4.2.7 and 4.2.8). For a practically loaded slab, however, cracks will generally propagate along the length of the dowel for some distance before turning to the beam surface, and thus the recommendations for minimum cover requirements will generally be conservative (although the possibility of point loads inducing tension cracks as in the specimens tested is thus also considered.)

CHAPTER 5

THE CORRELATION OF TEST RESULTS AND AN EVALUATION OF SAFE LOADS THAT CAN BE TRANSMITTED BY DOWELLED CONCRETE CONNECTIONS

5.1 *THE CONCRETE COVER TO THE DOWELS*

Test results indicate that a minimum concrete cover to the dowel is necessary to ensure the safe transfer of shear by the dowelled convection. The two basic ultimate modes of failure evident from Chapter 4 are:

(1) Brittle fracture and spalling of the concrete cover occurs prior to the dowel "yield" load being reached.

(2) The dowel "yield" load (Yield of the dowel material or sub-dowel plasticity or a combination of both) is attained before fracture of the cover occurs.

In the consideration of the overall safety of a dowelled connection, the latter "yield" mode is obviously desirable - in addition the steel dowel is generally more highly stressed in this mode, resulting in a more economical overall joint design. A minimum cover to a steel bar subjected to a dowel shear exists for any dowelled connection and if the cover exceeds this value the joint can be designed using a consistent "yield" procedure. A value for a critical concrete cover to dowel diameter ratio, $(d_c)_{crit}$, giving the concrete cover that would result in points (1) and (2) above being reached at the same load, was introduced in Chapter 4. This critical value was purely an experimental observation and as such relied on experimental technique and specimen geometry. In particular the loading system affected the spalling of the concrete cover since tensile cracks developed under the point loads. However, the crack propagation of approximately 45^0 meant that the point load was probably very close to the critical position in this regard. For a load situated a large distance from the dowelled joint, tensile cracks would develop parallel to the reinforcement before breaking out to the upper surface of the beam or slab (in a manner similar to that described in Table 2.1.2). The fracture energy of such a crack would invariably be greater than that for the specimens tested. The value for the critical d_c ratio is thus conservative for other variations of loading systems. As such, the $(d_c)_{crit}$ ratio can be applied as a general design criterion for all dowelled connections. The principal parameter affecting the value of $(d_c)_{crit}$ will be the cube strength of the concrete used in the dowelled connection. Tests indicated that crack width and dowel material (mild or high tensile steel) also affect the value of $(d_c)_{crit}$. These effects are not as significant as that of the concrete strength, however, since although both parameters tend to change the ultimate mode, the failure load will generally be in excess of the yield load (the value of $(d_c)_{crit}$ of approximately 4 refers to a specimen with a crack width of 8 mm, mild steel dowels and concrete cube strength of 30 MPa). Table 5.1.1 indicates that the

TABLE 5.1.1

ESTABLISHMENT OF A RELATIONSHIP FOR $(d_c)_{crit}$ VALUES FROM VARIOUS TEST SERIES OF CHAPTER 4

Test Series	Approximate Concrete Cube Strength (MPa)	d_c Ratio (cover/ dowel dia)	Yield Load (kN)	Failure Load (kN)	$\left[\frac{\text{Yield load}}{\text{Fail. Load}}\right]^{1,5} \cdot d_c$	Approximate $(d_c)_{crit}$ Value
2	30	1,9	2,07	1,35	3,86	4
2	30	2,7	2,07	1,60	3,97	
4	30	4,5	5,95	6,59	3,61	
8	10	4,5	4,89	3,40	7,76	8
8	40	4,5	6,40	≐ 9	2,70	3

relationship

$$(d_c)_{crit} \doteq d_c \cdot \left(\frac{\text{Yield Load}}{\text{Failure Load}}\right)^{1.5} \qquad 5.1.1$$

has good correlation with experimental data for specimens of 30 MPa cube strength. Although the number of tests performed was insufficient to establish equation 5.1.1 conclusively, it can be applied to specimens of varying cube strength to give values of $(d_c)_{crit}$ of 3 for 40 MPa concrete and 8 for 10 MPa concrete. These results are used in turn to give the following approximate relationship between concrete cube strength and $(d_c)_{crit}$ ratios:

$$\sqrt{f'_c} \cdot (d_c)_{crit} \doteq 22 \qquad 5.1.2$$

Equation 5.1.2 gives the cover that will result in the failure load being equal to the "yield" load. It is desirable, however, that the "yield" load be in excess of the failure load for a safe construction joint. In order to achieve this and also to take account of the experimental scatter, a tentative relationship is:

$$\sqrt{f'_c} \cdot (d_c)_{safe} \doteq 30 \qquad 5.1.3$$

This equation is used to derive a table of safe minimum covers for dowels subjected to shear loadings, if the dowels are to be analysed as having "yield" type ultimate modes (see Table 5.1.2). If the cover is less than the values specified in Table 5.1.2, stirrups must be provided in the region of the crack face and must be positioned such that they restrain the potential deflection of the dowel at the

TABLE 5.1.2

RECOMMENDED SAFE CONCRETE COVERS IN MILLIMETRES TO REINFORCEMENT SUBJECTED TO DOWEL SHEAR LOADINGS

Dowel Diameter (mm) \ Concrete Cube Strength (MPa)	10	20	30	40	50	60
6	60	40	35	30	25	25
8	75	55	45	40	35	30
10	95	65	55	45	40	40
12	115	80	65	55	50	45
16	150	105	90	75	70	60
20	190	135	110	95	85	75
25	240	170	135	120	105	95
32	300	215	175	150	135	125

crack face. The indication from tests is that the diameter and spacing of the stirrups chosen could follow normal reinforced concrete design procedures, although it is important that the end stirrup be placed as close to the crack face of the joint as possible.

5.2 *THE APPLICATION OF THE PFB FOUNDATION MODEL*

Having established that all dowels can be designed as having "yield" type ultimate modes provided that the cover requirements of Chapter 5.1 are met, the PFB foundation model can be used generally to predict safe loads for dowelled joints. It is apparent from test results of Chapter 4 that the PFB foundation model has good overall application, especially in the elastic zone of the experimentally determined load-deflection curves. Even "yield" loads were predicted reasonably well for the mild steel dowels (assuming that dowel material yield was the principal contributing factor to the overall yield of the connection). Being essentially an elastic analysis, however, the PFB model generally underestimated these loads, owing to the development of the stress diagrams shown in Fig. 5.2.1. These stress diagrams develop in the post-"elastic limit" portion of the load-deflection curves and ultimately cause "full yield" of the dowelled connection. Fig. 5.2.1 refers particularly to the mild steel dowelled connection - for the case of the high tensile steel dowel the principal contributing factor is generally plasticity of the sub-dowel concrete. The diagrams of Fig. 5.2.1 indicate

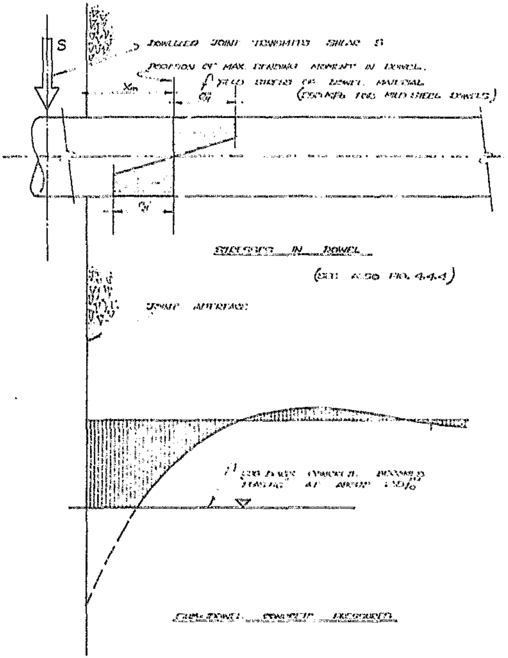

FIG. 5.2.1

that both reduced elastic modulus and concrete subgrade modulus values should be used in the prediction of "yield" loads, and this is chiefly why the PFB model underestimates "yield" loads for mild steel dowelled joints.

Tests on high tensile steel dowels (see Series 12, Chapter 4.15) indicate that the sub-dowel concrete begins to "Yield" under a load of 1,8 kN, corresponding to a sub-dowel concrete pressure of approximately 2,5 times the cube strength (this is the average sub-dowel pressure of the crack face calculated using the PFB model). The implication is that for medium strength concretes, dowelled with mild steel reinforcement, dowel extreme fibres generally yield prior to "plasticity" of the sub-dowel concrete being attained (see Series 1, Chapter 4.4). The value of 2,5 f'_c, the onset of plasticity of the sub-dowel concrete, has good agreement with results of failure theories obtained for concrete subjected to combined stresses given by Newman and Newman[18]. The actual state of stress of the sub-dowel concrete is difficult to establish, but it is certainly not subjected to a uniaxial pressure. Biaxial test results for normal weight concretes with a volume fraction of coarse aggregate of about 0,5 (similar to the concrete of the specimens tested) indicate a strength envelope resulting in an effective concrete strength of 1,5 f'_c. "Triaxial compression" tests give failure surfaces that can be represented mathematically by.

$$\frac{\sigma_1}{f'_c} = 1 + 3,7\left(\frac{\sigma_3}{f'_c}\right)^{0,86} \qquad 5.2.1$$

(for $\sigma_1 > \sigma_2 = \sigma_3$)

In equation 5.2.1, σ_1, σ_2 and σ_3 are principal stresses and f'_c is the concrete cube strength. The effective concrete strength is thus dependent on the constraining triaxial pressures, σ_2 and σ_3. If these are approximately half the cube strength, the effective strength will be 3 times the concrete cube strength. A sub-dowel triaxial state of stress seems likely in dowelled connections and thus "yield" pressures (local crushing of the sub-dowel foundation) in the order of 2,5 f'_c appear to be realistic. The relationship between these values and the assumed coefficient of local compression of 4 by Dulacska is also evident.

First yielding of the mild steel dowelled connection thus occurs when either

(1) The dowel extreme fibres reach a bending (or combined bending and tension) stress of 250 MPa

or

(2) The sub-dowel concrete pressure reaches a value of approximately 2,5 times the concrete cube strength.

If permissible stresses are thus taken to be 150 MPa and 1,5 f'_c respectively for the mild steel dowel and the sub-dowel concrete, the PFB foundation model can be used to predict safe working loads for dowelled connections. These safe working loads are given in Tables 5.2.1 and 5.2.2 for mild steel dowels and in Tables 5.2.3 and 5.2.4 for high tensile steel dowels, where the permissible stress in the

TABLE 5.2.1

TABLE OF SHORT TERM, STATIC, SAFE WORKING LOADS IN KILONEWTONS FOR SINGLE MILD STEEL DOWELS, WELL GROUTED, HAVING ADEQUATE COVER AND LENGTH AND CROSSING THE JOINT NORMAL TO THE CRACK FACE.

	JOINT CRACK WIDTH = 10 mm						JOINT CRACK WIDTH = 5 mm						JOINT CRACK WIDTH = 0 mm (NO CONCRETE FRICTION)					
CONCRETE CUBE STRENGTH (MPa) / DOWEL DIAMETER (mm)	10	20	30	40	50	60	10	20	30	40	50	60	10	20	30	40	50	60
6	0,37	0,45	0,46	0,47	0,48	0,49	0,45	0,63	0,65	0,66	0,68	0,68	0,56	0,94	1,01	1,06	1,10	1,14
8	0,65	0,97	0,99	1,00	1,01	1,02	0,73	1,25	1,31	1,36	1,40	1,43	0,92	1,39	1,83	1,90	1,96	2,01
10	1,03	1,68	1,74	1,79	1,83	1,86	1,16	2,11	2,22	2,26	2,33	2,38	1,34	2,40	3,06	3,15	3,22	3,29
12	1,45	2,62	2,75	2,81	2,86	2,90	1,63	2,96	3,48	3,56	3,63	3,69	1,85	3,57	4,49	4,69	4,84	4,98
16	2,52	4,55	5,72	5,88	6,00	6,07	2,76	5,02	6,87	7,08	7,25	7,40	3,06	5,20	8,04	8,99	9,12	9,32
20	3,84	6,93	9,60	10,17	10,36	10,52	4,13	7,54	10,69	12,17	12,42	12,62	4,55	8,85	11,84	14,56	14,99	15,35
25	5,79	10,53	14,65	[illegible]	18,05	18,38	6,20	11,28	16,01	20,48	20,95	21,34	6,52	12,00	17,3	22,31	24,83	25,42
32	9,15	16,57	25,56	30,15	33,04	33,71	9,68	17,65	25,00	32,03	37,50	38,27	10,00	18,75	26,47	34,48	41,30	44,12

(SHADED AREA INDICATES THAT SUB-DOWEL CONCRETE PRESSURE CONTROLS – OTHERWISE STRESS IN DOWEL CONTROLS.)

BASED ON:

(1) PFB FOUNDATION MODEL SOLUTION
(2) PERMISSIBLE STRESS OF 150 MPa IN DOWEL.
(3) PERMISSIBLE CONCRETE SUB-DOWEL PRESSURE OF $1,5f_c'$.

TABLE 5.22

TABLE OF SHORT TERM, STATIC, SAFE WORKING LOADS IN KILONEWTONS FOR SINGLE MILD STEEL DOWELS, WELL-GROUTED, HAVING ADEQUATE COVER AND LENGTH AND CROSSING THE JOINT AT 45° TO THE CRACK FACE.

Dowel diameter (mm) \ Concrete cube strength (MPa)	Joint crack width = 10 mm						Joint crack width = 5 mm						Joint crack width = 0 mm (no concrete friction)					
	10	20	30	40	50	60	10	20	30	40	50	60	10	20	30	40	50	60
6	0,53	0,57	[illegible]	0,60	0,61	0,61	0,63	0,78	0,80	0,81	0,83	0,84	[illegible]	1,09	1,15	1,20	1,24	1,28
8	0,94	1,22	1,24	1,25	1,26	1,27	1,09	1,52	1,58	1,65	1,67	1,71	[illegible]	2,00	2,08	2,15	2,20	2,25
10	[illegible]	2,08	2,15	2,20	2,24	2,27	1,63	2,56	2,64	2,70	2,75	2,80	[illegible]	3,28	3,43	3,52	3,58	3,63
12	2,06	3,26	3,35	3,41	3,46	3,50	2,20	3,53	4,09	4,17	4,23	4,29	2,62	4,79	5,03	5,15	5,44	5,45
16	3,56	6,44	6,90	6,96	7,08	7,14	3,81	7,80	7,92	8,11	8,27	8,40	4,25	7,83	9,48	9,72	9,90	10,07
20	5,42	9,80	11,61	11,83	12,01	12,17	5,98	10,64	13,31	13,67	13,90	14,07	6,53	11,67	15,31	15,74	16,06	16,30
25	8,20	14,55	19,71	20,13	20,49	20,80	8,77	18,56	22,18	22,65	23,08	23,40	9,29	17,04	21,59	25,66	26,27	26,74
32	12,83	23,44	32,23	36,06	36,67	37,22	13,64	24,79	[illegible]	39,68	40,43	41,10	14,42	25,55	37,86	43,90	45,05	45,73

(SHADED AREA INDICATES THAT SUB-DOWEL CONCRETE PRESSURE CONTROLS — OTHERWISE STRESS IN DOWEL CONTROLS)

BASED ON:

(1) PFB FOUNDATION MODEL SOLUTION

(2) PERMISSIBLE STRESS OF 150 MPa IN DOWEL.

(3) PERMISSIBLE CONCRETE SUB-DOWEL PRESSURE OF $1,5 f'_c$.

TABLE 5.2.3

TABLE OF SHORT TERM, STATIC, SAFE WORKING LOADS IN KILONEWTONS FOR SINGLE HIGH TENSILE STEEL DOWELS, WELL GROUTED HAVING ADEQUATE COVER AND LENGTH AND CROSSING THE JOINT NORMAL TO THE CRACK FACE.

CONCRETE CUBE STRENGTH (MPa) / DOWEL DIAMETER (mm)	JOINT CRACK WIDTH = 10mm						JOINT CRACK WIDTH = 5 mm						JOINT CRACK WIDTH = 0 mm (NO CONCRETE FRICTION)					
	10	20	30	40	50	60	10	20	30	40	50	60	10	20	30	40	50	60
6	[illegible]	[illegible]	0,77	0,78	0,80	0,80	0,45	[illegible]	1,08	1,10	1,13	1,13	[illegible]	[illegible]	[illegible]	1,77	1,88	1,90
8	0,60	[illegible]	1,65	1,67	1,68	1,70	[illegible]	[illegible]	[illegible]	2,27	2,33	2,38	[illegible]	,69	[illegible]	[illegible]	3,27	3,35
10	[illegible]	1,84	2,00	2,98	3,03	3,10	1,16	2,11	2,09	3,80	3,83	3,87	[illegible]	[illegible]	[illegible]	4,55	5,37	5,48
12	1,40	2,30	[illegible]	4,65	4,77	4,85	1,65	2,93	4,19	[illegible]	6,05	6,15	1,25	[illegible]	[illegible]	[illegible]	[illegible]	8,30
16	2,52	4,65	[illegible]	[illegible]	[illegible]	10,12	2,73	[illegible]	7,11	9,10	11,03	12,33	[illegible]	[illegible]	[illegible]	[illegible]	[illegible]	[illegible]
20	[illegible]	[illegible]	9,60	[illegible]	[illegible]	17,58	4,13	7,54	[illegible]	[illegible]	[illegible]	[illegible]	[illegible]	9,55	11,64	15,11	16,25	[illegible]
25	5,79	10,53	14,85	[illegible]	22,01	[illegible]	6,20	11,23	16,01	[illegible]	21,85	[illegible]	6,52	12,00	17,31	22,31	27,17	31,80
32	[illegible]	16,57	[illegible]	30,16	36,14	42,65	9,63	17,65	25,00	32,00	[illegible]	[illegible]	10,00	18,75	[illegible]	34,15	[illegible]	46,91

(SHADED AREA INDICATES THAT SUB-DOWEL CONCRETE PRESSURE CONTROLS -- OTHERWISE STRESS IN DOWEL CONTROLS)

BASED ON:

(1) PFB FOUNDATION MODEL SOLUTION.
(2) PERMISSIBLE STRESS OF 250 MPa IN DOWEL.
(3) PERMISSIBLE CONCRETE SUB-DOWEL PRESSURE OF $1,5f'_c$.

TABLE 5.2.4

TABLE OF SHORT TERM, STATIC, SAFE WORKING LOADS IN KILONEWTONS FOR SINGLE HIGH TENSILE STEEL DOWELS, WELL GROUTED, HAVING ADEQUATE COVER AND LENGTH AND CROSSING THE JOINT AT 45° TO THE CRACK FACE.

CONCRETE CUBE STRENGTH (MPa) / DOWEL DIAMETER (mm)	JOINT CRACK WIDTH = 10 mm						JOINT CRACK WIDTH = 5 mm						JOINT CRACK WIDTH = 0 mm (NO CONCRETE FRICTION)					
	10	20	30	40	50	60	10	20	30	40	50	20	10	20	30	40	50	60
6	[illegible]	[illegible]	0,98	1,00	1,02	1,02	0,93	1,14	1,32	[illegible]	1,38	1,40	[illegible]	[illegible]	1,92	2,00	2,07	2,13
8	[illegible]	[illegible]	2,07	2,08	2,10	2,12	[illegible]	[illegible]	2,63	2,72	[illegible]	2,85	[illegible]	[illegible]	[illegible]	3,58	3,67	3,75
10	[illegible]	[illegible]	3,58	4,67	3,73	3,78	[illegible]	[illegible]	[illegible]	4,50	4,58	4,67	[illegible]	[illegible]	[illegible]	5,87	5,97	6,07
12	[illegible]	[illegible]	[illegible]	5,68	5,77	5,83	[illegible]	[illegible]	[illegible]	6,95	7,05	7,15	[illegible]	[illegible]	[illegible]	8,65	9,07	9,08
16	[illegible]	[illegible]	[illegible]	[illegible]	11,60	11,90	[illegible]	[illegible]	[illegible]	[illegible]	13,78	14,00	[illegible]	[illegible]	[illegible]	[illegible]	16,50	16,78
20	5,42	9,80	[illegible]	[illegible]	20,02	20,28	[illegible]	[illegible]	[illegible]	[illegible]	23,17	23,45	[illegible]	[illegible]	[illegible]	[illegible]	[illegible]	27,32
25	[illegible]	[illegible]	[illegible]	[illegible]	[illegible]	34,67	[illegible]	[illegible]	[illegible]	[illegible]	[illegible]	33,00	[illegible]	[illegible]	[illegible]	[illegible]	[illegible]	44,57
32	[illegible]	[illegible]	[illegible]	[illegible]	[illegible]	[illegible]	[illegible]	[illegible]	[illegible]	[illegible]	[illegible]	[illegible]	[illegible]	[illegible]	[illegible]	[illegible]	[illegible]	[illegible]

(SHADED AREA INDICATES THAT SUB - DOWEL CONCRETE PRESSURE CONTROLS -- OTHERWISE STRESS IN DOWEL CONTROLS)

BASED ON :

(1) PFB FOUNDATION MODEL SOLUTION

(2) PERMISSIBLE STRESS OF 250 MPa IN DOWEL.

(3) PERMISSIBLE CONCRETE SUB-DOWEL PRESSURE OF $1,5 f_c'$.

dowel is taken to be 250 MPa. It must be noted that all the safe working loads refer to single dowels, which must be well grouted, have adequate cover (as specified in Chapter 5.1) and must comply with Hetényi's classification limits for long dowels given in Chapter 3.2 (which generally means the length should exceed the dowel diameter by more than 10). In addition note that the tables of safe working loads given in this chapter are all calculated assuming that the tension in the dowel is zero (even in the case of the angled dowel, where the tension which is set up as a result of the shear force at the joint is automatically taken account of in the program "DOWEL"). If, however, a reinforcing bar acts both as tensile reinforcement *and* is subjected to a dowel shear at some connection, joint or crack, the tensile stress in the bar *in the region of the crack face* must be calculated and it can then be shown using the PFB foundation model that the values in the tables must be adjusted by multiplying by the factor, t, given by:

$$t = 1 - \frac{\sigma_t^2}{\sigma_p^2}$$ (only accurate where steel stress controls)

where σ_t is the stress in the bar resulting from a tensile force in the region of the crack face, due to loads *other* than the dowel shear, and σ_p is the permissible stress in the bar (150 MPa for mild steel and approx. 250 MPa for the high tensile steel dowels tested).

A study of the tables of safe working loads makes it apparent that difficulties are encountered when attempt-ing to specify the best material or geometry of a particular joint, since variation of each parameter affects the performance characteristics of the joint associated with the remaining parameters. For example, mild steel appears to be a better dowel material for low strength concretes with joints of zero crack width, whereas high tensile steel is a better material for use in conjunction with higher strength concretes with larger crack widths and angled dowels. In addition, a number of small diameter dowels appears to be a better solution for low strength concrete joints of zero crack width than a single large diameter dowel giving the same steel area for the connection. On the other hand, large diameter dowels are more suited to higher strength concretes and joints of larger crack widths. The safe working loads generally increase with increase of concrete cube strength, and in addition the cover requirement decreases, thus allowing the construction of a more compact joint overall.

It can be seen that the PFB foundation model thus has very good overall application to the problem of the dowelled connection, and can be used for the accurate stress analysis of the connection in the elastic zone.

5.3 *THE ESTABLISHMENT OF AN APPROXIMATE RELATIONSHIP FOR THE DOWELLED CONNECTION YIELD LOAD*

In addition to the PFB foundation model predicting "yield" loads reasonably well (especially if account is taken of reduced moduli values) test results can be used to establish an approximate empirical relationship for the "yield" load of dowelled connections. Although the PFB foundation models the elastic zone of the dowelled joint load-deflection curves accurately, the analysis is tedious. For this reason, a tentative approximate relationship is given for the "yield" loads of the dowels tested, and a suitable factor of safety can be applied to the results.

Provided that the dowelled connection conforms with the requirements specified in the tables of Chapter 5.2, particularly regarding adequate cover, the experimentally determined yield load can be related to the parameters:

Concrete cube strength
Dowel yield stress
Dowel diameter
Joint crack width
Dowel angle

The simplified functions for each of these variables are given in Fig. 5.3.1. It must be noted that the functions for crack width and dowel angle can result in errors if extrapolated too far beyond the limits considered. Connections in practice would generally be within these limits, however. The number of tests performed was obviously insufficient to establish these functions with certainty, but the large number of parameters that had to be considered limited the number of tests that could be performed varying each parameter. In addition to the functions established by test, the PFB foundation model was again

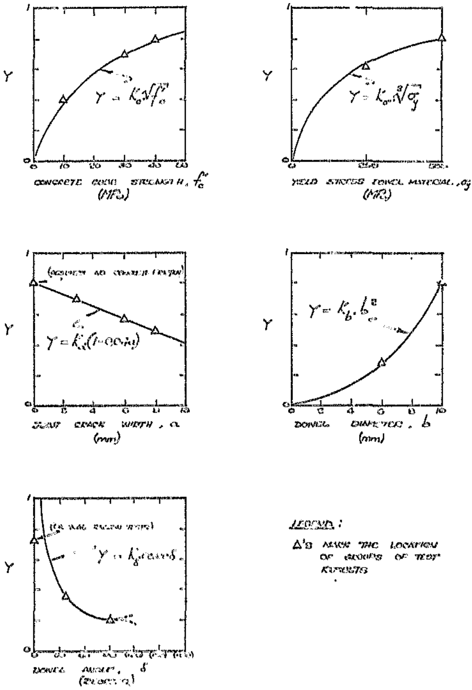

FIG. 5.3.1

APPROXIMATE FUNCTIONS RELATING THE DIMENSIONLESS YIELD FORCE Y TO THE PARAMETERS f'_c, σ_y, a, b AND δ.

used to establish the effects of tensile stress in the dowel (as in Chapter 5.2), no specimens being tested that had significant tensile stresses in the dowels. The empirical relationship established from the functions given in Fig. 5.3.1 was thus finally:

$$S_y \doteq \frac{\sqrt{f'_c} \cdot b^2 \cdot (\sigma_y)^{\frac{1}{3}} \, (1-0{,}04a)\left(1-\frac{\sigma_t^2}{\sigma_y^2}\right)}{430 . \sin\delta} \qquad 5.3.1$$

where S_y is the "yield" load of the dowel (in kN), f'_c is the cube strength of the concrete used in the connection (in MPa), σ_y is the yield stress of the dowel material (in MPa), σ_t is the tensile stress in the dowel due to tensile forces other than those associated with the shear transfer of the connection (in MPa), a is the crack width of the joint (in mm) and δ is the angle the dowel makes to the crack face of the joint (if not normal to the crack face, it must be angled such that it aids the shear transfer in tension).

If a factor of safety of about 2,5 is applied to equation 5.3.1, it is evident that the result gives reasonable overall correlation with those of the tables given in Chapter 5.2. The results in these tables can be considered to be more accurate in general, however.

5.4 *THE EFFECT OF DOWEL LENGTH*

Safe shear transfer loads given in both Chapters 5.2 and 5.3 depend on the fact that the dowel has adequate length. Hetényi's classification limits generally imply that this must be in excess of approximately 10 times the dowel diameter. Where the length of the dowel is less than this value (or near the specified limits) it is unlikely that the same safe working loads can be used. This applies particularly to the case of the *self-expanding type bolt* that are fitted into a hole drilled into an existing concrete structure. In addition to being shorter than Hetényi's limits in general, self-expanding bolts set into mass concrete exert approximately axi-symmetric compressive stresses on the surrounding concrete foundation even before the application of a shear load. The overall implication is that *additional safety factors* should be used in conjunction with the tables of Chapter 5.2 for short dowels or self-expanding type bolts set into existing concrete structures, and further research into this particular aspect of dowel action would be desirable.

5.5 A GENERAL EVALUATION OF THE PARAMETERS INVOLVED IN THE ANALYSIS OF DOWEL ACTION

The parameters involved in the analysis of dowel action in reinforced concrete connections were given in Chapter 1.2 as:

(a) *Crack width*
(b) *The transfer of shear by the concrete*
(c) *Dowel diameter*
(d) *Yield stress of the dowel material*
(e) *Tensile force in the dowel*
(f) *Dowel elastic modulus*
(g) *Concrete crushing strength*
(h) *Cover to dowels*
(i) *The number of dowels crossing the crack face*
(j) *Angle of dowels*
(k) *Length of dowel*
(l) *Effect of stirrups*
(m) *Type of loading*

Each of these parameters has been investigated within the scope of this dissertation and a summary of their effects (obtained from research associated with this work) is given below:

(a) *Crack width*

This variable is well modelled by the PFB foundation and its effect on safe working loads for dowelled connections is clearly indicated in the tables given in Chapter 5.2. In addition, an evaluation of test results gives an approximately linear relationship (within limits) between this parameter and the "yield" load of the dowelled joint.

(b) *The transfer of shear by the concrete*

This parameter was not studied intentionally in the experimental program of this dissertation. Experimental results nevertheless indicated friction effects were present in specimens of zero crack width although the concrete interfaces had been cast smoothly and were well oiled. Both the application of the PFB model and the approximate "yield" load expression assume no friction present at the crack face, however. Where the friction of the concrete is considered to be an important contributing factor in the design of a dowelled connection, Mast's theory can be applied (as in Chapter 2.2).

(c) *Dowel diameter*

The effect of this parameter is well modelled by the PFB foundation and it can also be related approximately to the "yield" load, as shown in Chapter 5.3. In addition the dowel diameter affects the minimum cover requirements to a reinforcing bar subjected to a dowel shear.

(d) *Yield stress of the dowel material*

Permissible stresses in the dowel used in the PFB foundation analysis in Chapter 5.2 depend on this parameter and it is also related approximately to the "yield" load of a dowelled connection (as in Chapter 5.3).

(e) *Tensile force in the dowel*

Results from the PFB foundation analysis indicate the approximate factor (discussed in Chapter 5.2) to be used in conjunction with the safe working load of a dowelled connection where a tensile force is present in the dowel due to forces other than those associated with the dowel shear. This result agrees well with the factor used in Dulacska's investigation (given in Chapter 2.2).

(f) *Dowel elastic modulus*

This parameter is taken into account in the elastic analysis of the dowelled connection using the PFB foundation model.

(g) *Concrete crushing strength*

The concrete cube strength affects the PFB foundation elastic analysis by affecting the value of the subgrade modulus of the concrete. In addition, the cube strength affects permissible sub-dowel pressures, the safe concrete cover to the dowel and is related approximately to the "yield" load (as shown in Chapter 5.3).

(h) *Cover to dowels*

This parameter (in conjunction with concrete cube strength and dowel diameter) affects the failure mode of the dowelled connection and this effect is indicated in Table 5.1.2.

(i) *The number of dowels crossing the crack face*

The tables of safe working loads for dowelled connections given in Chapter 5.2 indicate that the advantages to be gained by varying the number of dowels in a connection (but maintaining a constant steel area) depend on other parameters of the connection, particularly the concrete cube strength and joint crack width.

(j) *Angle of dowels*

This parameter increases the shear transfer capacity of a dowelled connection in general, but it can be seen from the tables of Chapter 5.2 that this increase depends on other joint parameters. The effect on the "yield" load is given by an approximate relationship.

(k) *Length of dowel*

The length of the dowel was not tested in the laboratory program and this is an avenue of further research. Shorter dowels are expected to result in decreased safe working loads in general as discussed in Chapter 5.4.

(l) *Effect of stirrups*

Stirrups have a pronounced effect on dowels having insufficient cover as specified in Chapter 5.1 but have little effect in general on dowels with adequate cover or where local spalling was not a problem.

(m) *Type of loading*

The position of the loading on the beam specimens affects the fracture characteristics relating to the spalling of the concrete cover. For multi-dowel joints the position of the loading also affects the tensile forces that are set up in steel bars which might act as both tensile reinforcement and dowels, and this effect can then be taken account of as in (c).

CHAPTER 6

CONCLUDING SUMMARY OF THE STUDY OF DOWEL ACTION

An investigation of dowel action in reinforced concrete connections was undertaken, using specimens substantially different to those used by previous researchers in the field. Results were nevertheless consistent with many of those of previous investigators. In addition, the specimen geometry made possible the study of the parameters of concrete cover and the effect of the position of the load on the performance of a dowelled connection. The validity of the beam on elastic foundation theory (particularly the PFB foundation model) was verified by test, but it was found that the utility of the theory depended on the establishment of a realistic value for the concrete subgrade modulus.

Test results indicated the existence of two principal ultimate modes, these being "yielding" of the connection prior to the fracture of the concrete cover to the dowels or cover failure prior to the "yield" load being attained. Permissible sub-dowel concrete pressures were found to be in excess of the concrete cube strength for connections having "yield" type ultimate modes. The occurrence of this type of ultimate mode depended on there being adequate cover to a dowel subjected to shear loading. This criterion, determined by test, depended on the specimen geometry and overall application is expected to be conservative. Tentative design criteria were thus established for dowelled connections and this enabled the prediction of safe working loads and the establishment of an approximate relationship for the "yield" load for such connections.

The test series, however, considered only static loadings and in addition the loading rate was fairly fast. The implication is that neither the effect of cyclic loading or prolonged loading were studied. Cyclic loading could lead to fatigue of the concrete surrounding the dowel and although concrete has no fatigue limit, the strength extrapolated to ten million cycles is about half the static strength. Thus dowels subjected to cyclic loading could be designed having an addition safety factor of about two in general. Prolonged loading (due to dead loads) could be taken into account by considering the effects of creep of the concrete, generally resulting in a reduction of the concrete elastic modulus, subgrade modulus and permissible sub-dowel pressures. Thus dowels subjected to prolonged loadings would be designed having an addition s fety factor.

Short, self-expanding type bolts subjected to a shear loading could be an avenue of further research, the indication being that safe working loads for these bolts would be lower than those obtained for the dowels investigated in this dissertation. Nevertheless, a general evaluation of the dowelled connection and a tentative prediction of the safe shear loading that can be transmitted by a variety of such connections have been presented in this work.

LIST OF REFERENCES

1. Acharya, D.N., and Kemp, K.O., "Significance of Dowel Forces on the Shear Failure of Rectangular Reinforced Concrete Beams Without Web Reinforcement", *ACI Journal*, V. 62, No. 10, Oct., 1965, pp. 1265-1278.

2. Anderson, A.R., "Composite Designs in Precast and Cast-in-Place Concrete", *Progressive Architecture*, V. 41, No. 9, Sept., 1960, pp. 172-179.

3. Baumann, T., "Tests to Study the Dowel Action of the Bending Tension Reinforcement of Reinforced Concrete Beams", Bericht Nr. 77, Munich Technischen Hochschule, 1968 (English Translation by Portland Cement Association).

4. Birkeland, P.W., and Birkeland, H.W., "Connections in Precast Concrete Construction", *ACI Journal, Proceedings*, V. 63, No. 3, March, 1966, pp. 345-368

5. [illegible]ecka, H., "Dowel Action of Reinforcement [illegible]ing Cracks in Concrete", *ACI Journal, Pro[illegible]ngs*, V. 69, No. 12, Dec., 1972, pp. 754-757.

6. Faber, J., and Mead, F., *"Oscar Ferber's Reinforced Concrete"*, E. and F.N. Spon, Ltd., London, 1967.

7. Friberg, B.F., "Design of Dowels in Transverse Joints of Concrete Pavements", *Transactions, ASCE*, V. 105, 1940, pp. 1076-1116.

8. Gerald, C.F., *"Applied Numerical Analysis"* Addison-Wesley Publishing Company, 1970.

9. Gergely, P., "Splitting Cracks Along the Main Reinforcement in Concrete Members", *Report to the Bureau of Public Roads*, U.S. Department of Transportation, Cornell University, Ithaca, N.Y., April 1969.

10. Hetényi, M., *"Beams on Elastic Foundation. (Theory with applications in the field of civil and mechanical engineering),"* Ann Arbor, University of Michigan Press, 1946

11. Hetényi, M., "Beams and Plates on Elastic Foundation and Related Problems", *Applied Mechanics Reviews*, V.19, No. 2, Feb., 1966, pp. 95-102.

12. Hofbeck, J.A., Ibrahim, I.A., and Mattock, A.H., "Shear Transfer in Reinforced Concrete", *ACI Journal, Proceedings*, V. 66, No. 2, Feb., 1969, pp 119-128.

13. Johnston, D.W., and Zia, P, "Analysis of Dowel Action", *Journal of the Structural Division, Proceedings ASCE*, V.97, No. ST5, May, 1971, pp. 1611-1630.

14. Jones, R., "The Ultimate Strength of Reinforced Concrete Beams in Shear", *Magazine of Concrete Research* (London), V.8, No. 23, Aug., 1956, pp. 69-84.

15. Kerr, A.D., "Elastic and Viscoelastic Foundation Models, "*Journal of Applied Mechanics, ASME, Transactions*, Sept., 1964, pp. 491-498.

16. Krefeld, W.J., and Thurston, C.W., "Contribution of Longitudinal Steel to Shear Resistance of Reinforced Concrete Beams", *ACI Journal, Proceedings*, V. 63, No. 3, March, 1966, pp. 325-344.

17. Mast, R.F., "Auxilliary Reinforcement in Concrete Connections", *Proceedings, ASCE Journal*, V. 94, No. ST6, June, 1968, pp. 1485-1504.

18. Newman, K., and Newman, J.B., "Failure Theories and Design Criteria for Plain Concrete", *Proceedings of the Southampton 1969 Civil Engineering Materials Conference*, John Wiley and Sons Ltd., 1971, pp. 963-995.

19. Ockleston, A.J., *Notes on the mathematical solution to the Winkler beam on elastic foundation.*

20. Parmelee, R.A., "A Study of the Ultimate Shear Strength of Reinforced Concrete Beams", *Structural Engineering and Structural Mechanics Report*, No. 61-11, University of California, Berkeley, Calif., Jan., 1961, 66pp.

21. Saemann, J.C., and Washa, G.W., "Horizontal Shear Connections Between Precast Beams and Cast-in-Place Slabs", *ACI Journal*, Detroit, Mich., V. 61, No. 11, Nov., 1964.

22. Terzaghi, K.,*"Theoretical Soil Mechanics"*, John Wiley and Sons, Inc., 1943.

23. Timoshenko, S., *"Strength of Materials, Part II"*, Second Edition, D. van Nostrand Co., Inc., New York, 1941.

24. Timoshenko, S., and Lessels, J.M., *"Applied Elasticity"*, Westinghouse Technical Night School Press, pp. 133-141.

25. Timoshenko, S., and Woinowski-Krieger, S., *"Theory of Plates and Shells"*, McGraw-Hill Book Company, Inc., 1959.

26. "The Shear Strength of Reinforced Concrete Members", by the Joint ASCE-ACI Task Committee 426 on Shear and Diagonal Tension of the Committee on Masonry and Reinforced Concrete of the Structural Division of the ASCE, June 1973.

27. Code of Practice for *The Structural Use of Concrete*, CP 110, Part I, British Standards Institution, London, Nov. 1972.

APPENDIX A

A.1 *THE WINKLER FOUNDATION MODEL AND ITS MATHEMATICAL SOLUTION*

The differential equation for the Winkler model is shown in Chapter 3.2 to be

$$\frac{d^4y}{dx^4} + \frac{k}{EI} \cdot y = \frac{q}{EI} \qquad \text{A.1}$$

This can be solved for using Laplace Transforms or D-operators. Using the latter, the complementary function is:

$$y = Ae^{-mx} \sin(mx+\alpha) + Be^{+mx} \sin(mx-\beta) \qquad \text{A.2}$$

and the particular integral is:

$$\left[\frac{4m^4}{D^4+4m^4}\right] \cdot \frac{q}{k} = \frac{q}{k} \qquad \text{A.3}$$

provided that q is not higher than a cubic function of x. The full solution to equation A.1 can thus be shown to be

$$y = Ae^{-mx} \sin(mx+\alpha) + Be^{+mx} \sin(mx+\beta) + \frac{q}{k} \qquad \text{A.4}$$

There are 4 arbitrary constants to be solved for in equation A.4 and these are obtained from known end conditions of deflection, slope, bending moment or shear. In order to solve for the constants, equation A.4 must be differentiated.

$$\frac{d}{dx}\left[e^{-mx}\sin(mx+\alpha)\right] = -me^{-mx}\sin(mx+\alpha)+me^{-mx}\cos(mx+\alpha)$$

$$= \sqrt{2}\,me^{-mx}\left[\sin(mx+\alpha)\,.\,-\frac{1}{\sqrt{2}}+\cos(mx+\alpha)\,.\frac{1}{\sqrt{2}}\right]$$

$$= \sqrt{2}\,me^{-mx}\sin(mx+\alpha+\frac{3\Pi}{4}) \qquad \text{A.5}$$

Similarly

$$\frac{d}{dx}\left[e^{+mx}\sin(mx+\beta)\right] = \sqrt{2}me^{+mx}\sin\ (mx+\beta+\frac{\Pi}{4}) \qquad \text{A.6}$$

Applying equations A.5 and A.6 to equation A.4 gives:

$$\frac{dy}{dx} = \sqrt{2}m\left[Ae^{-mx}\sin(mx+\alpha\frac{3\Pi}{4}) + Be^{+mx}\sin(mx+\beta+\frac{\Pi}{4})\right] + \frac{1}{k}.\frac{dq}{dx} \qquad \text{A.7}$$

$$\frac{d^2y}{dx^2} = 2m^2\left[Ae^{-mx}\sin(mx+\alpha\frac{3\Pi}{2})+Be^{+mx}\sin(mx+\beta+\frac{\Pi}{2})\right] +\frac{1}{k}.\frac{d^2q}{dx^2} \qquad \text{A.8}$$

$$\frac{d^3y}{dx^3} = 2\sqrt{2}m^3\left[Ae^{-mx}\sin(mx+\alpha+\frac{\Pi}{4})+Be^{+mx}\sin(mx+\beta+\frac{}{4})\right]+\frac{1}{k}.\frac{d^3q}{dx^3} \qquad \text{A.9}$$

where $m = \sqrt[4]{\frac{k}{4EI}}$

From equations A.4, A.7, A.8 and A.9, the arbitrary constants can be solved for, and thus deflection, slope, bending moment and shear are obtained for the beam (or dowel).

The same analysis can be applied in simplified form for the semi-infinite Winkler beam on elastic foundation and similar techniques are adopted for the solution of the PFB foundation model. (The full solution to the PFB foundation is given in the program "DOWEL" in Appendix B.1).

A.2 *THE EQUATIONS USED BY TERZAGHI FOR DEFORMATIONS UNDER UNIFORMLY LOADED BASES*

The following equations were used to determine the I_ρ factors used in Chapter 4.1.

For the case of infinite sub-base or sub-dowel depth:

$$I_\rho = \frac{1}{\pi}\left[\ell \log\left(\frac{1+\sqrt{\ell^2+1}}{\ell}\right) + \log\left(\ell + \sqrt{\ell^2+1}\right)\right]$$

$$\text{where } \ell = \frac{L}{B}$$

and L is the length of the base

B is the breadth of the base.

For the case of the finite sub-base or sub-dowel depth, supported by a rigid base:

$$F_1 = \frac{1}{\pi}\left[\ell \log\left\{\frac{(1+\sqrt{\ell^2+1})\cdot\sqrt{\ell^2+d^2}}{\ell(1+\sqrt{\ell^2+d^2+1})}\right\} + \log\left\{\frac{(\ell+\sqrt{\ell^2+1})\sqrt{1+d^2}}{\ell+\sqrt{\ell^2+d^2+1}}\right\}\right]$$

and

$$F_2 = \frac{d}{2\pi}\cdot\tan^{-1}\left[\frac{1}{d\sqrt{\ell^2+d^2+1}}\right]$$

where $\ell = \frac{L}{B}$

and $d = \frac{2D}{B}$

L is the length of the base

B is the breadth of the base

D is the depth of subgrade from the base to the rigid layer.

APPENDIX B

B.1 *THE COMPUTER PROGRAM DOWEL, INCORPORATING THE FULL SOLUTION TO THE PFB FOUNDATION MODEL*

The program "DOWEL" was compiled to give solutions to the PFB foundation model and results from this program were used to produce tables of safe working loads for dowelled connections in Chapter 5.2. In addition to the PFB solution, Winkler results are also obtainable from the program for the data given. A comparison of results indicates that the PFB solution gives a slightly "stiffer" solution in general, and in addition takes account of tensile forces in the reinforcement when considering permissible stresses in the dowel. The program, indicating the data required pertaining to the connection under study, is given overleaf.

```
c                    PROGRAM 'DOWEL'
c
c This program gives results for the Pasternak-Filonenko-Borodich (P-F-B)
c foundation model.
c The solution applies to a single dowel crossing a joint in reinforced
c concrete construction.
c
c The program requires the following data:
c
c Diameter of the steel dowel in mm. (=bd)
c Elastic Modulus of the dowel in GPa. (=est)
c Length in mm along dowel over which stresses
c are required. (=bl)
c Spacing in mm along dowel where stresses
c must be given. (=s)
c Angle in degrees dowel makes to face of joint. (=phi)
c Estimated tension (if any) in dowel in region
c of the crack face. (=thl) Usually =0 for most
c dowelled joints if moment at joint is small.
c Yield stress of steel dowel in MPa. (=fy)
c Shear force in N applied across joint. (=sf)
c Crack width of joint in mm. (=cw)
c Cube strength of the concrete in MPa. (=fc)
c Note: for PFB solutions write 1 at the end of
c the data,for an additional Winkler check, write
c the figure 2.
c
read (5,100) bd,est,bl,s,phi,thl,fy,sf,cw,fc,k
100 format (11f)
c
pi=3.141593
aib=(pi*bd**4.)/64.
ab=0.250*pi*bd**2.
es=est*1000.0
ei=4.*es*aib
ph=phi*pi/180.0
c
sh=sf*sin(ph)
th2=sf*cos(ph)
th=thl+th2
em=sh*cw/2.
c Note: This approximation is valid for small
c crack width to bar diameter ratios (1 or < to 1).
c It is always true for phi =90 degrees.
c
c Empirical calculation of concrete Elastic Modulus:
c (Using values given in CP 110)
ec=4900.*sqrt(fc)
ec=ec/1000.0
c Poisson's ratio is assumed to be 0.2 and constant
c for this elastic analysis.
ge=ec/2.40
c Empirical calculation of concrete subgrade modulus
c as obtained from tests:
akc=136.9*sqrt(fc)
ak=akc*bd
c
c Basic parameters of the PFB foundation model:
thet=(ak/ei)**0.250
thet2=thet**2.
gt=ge*th
if (thet2-gt/ei) 6,7,7
6 write (6,8)
8 format (//t20,'Bar tension too high for solution-mode given by "PDOWEL",(see Hetenyi p. 136)')
go to 200
7 continue
c Properties of the PFB foundation model:
alph=(thet2+gt/ei)**0.50
bet=(thet2-gt/ei)**0.50
c
alph2=alph**2.0
bet2=bet**2.0
c
g1=3.0*alph2-bet2
g2=alph2-bet2
g3=3.0*bet2-alph2
gh=alph2**2.0-6.0*alph2*bet2+bet2**2.0
c
z1=sh/(thet*ak)
z2=(2.0*alph*em)/z1
z3=em/(es*aib)
c
```

```
den=es*alb*bet*g1
t11=-1.0*sb/den
t21=-1.0*am/den
c
den=bet*g1
an11=-2.0*sh*thet2/den
an21=-1.0*am/den
c
qv11=-1.0*sh/den
qn21=-1.0 *am/den
c
delta3=sh*ew**3.0/(24.*es*alb)
gbar=2.*bd/(3.*pi)
fo=fy*ab*gbar
c Properties of the dowelled joint are given as follows:
write (6,101)
101 format (////t10,'PROPERTIES OF THE DOWELLED JOINT',/t10,32('*'))
write (6,102) fc
102 format (/t20,'CONCRETE PROPERTIES',//t20,'CUBE STRENGTH= ',f5.1,1x,'MPa')
write (6,103) ec,alc
103 format (t20,'ELASTIC MODULUS= ',f5.1,1x,'GPa',/t20,'SUBGRADE MODULUS= ',f5.1,1x,'MPa/mm')
write (6,104) bd
104 format (/t20,'DOWEL PROPERTIES',//t20,'DOWEL DIAMETER= ',f5.1,1x,'mm')
write (6,105) th1,ph
105 format (t20,'DOWEL TENSION= ',f7.1,1x,'N',/t20,'DOWEL ANGLE= ',f5.1,1x,'Degrees')
write (6,106) es,fy,fpm
106 format (t20,'ELASTIC MODULUS= ',f6.1,1x,'GPa',/t20,'YIELD STRESS= ',f6.1,1x,'MPa',/t20,'FU
LLY PLASTIC MOM OF RES= ',f8.1,1x,'N mm')
write (6,107) ew,sf
107 format (/t20,'CRACK WIDTH= ',f5.1,1x,'mm',/t20,'SHEAR FORCE ACROSS JOINT= ',f7.1,1x,'N')
if (k-1) 21,21,22
22 continue
write (6,108)
108 format (///t10,'WINKLER CHECK ON RESULTS',/t10,24('*'))
write (6,109)
write (6,110)
c Winkler results are now calculated:
n=bl/s
n=n+1
do 111 i=1,n
x=(i-1)*s
wdec=-1.*thet*x
wa=exp(wdec)*(cos(thet*x)+sin(thet*x))
wb=exp(wdec)*sin(thet*x)
wc=exp(wdec)*(cos(thet*x)-sin(thet*x))
wd=exp(wdec)*cos(thet*x)
c
wy1=2.*sh*thet*wd/alc
wth1=-2.*sh*thet2*wa/alc
wm1=-1.*sh*wb/thet
wq1=-1.*sh*wc
c
wy2=2.*am*thet2*wc/alc
wth2=-4.*am*thet**3.*wd/alc
wm2=-1.*am*wa
wq2=2.*am*thet*wb
c
wy=wy1+wy2
wth=wth1+wth2
wm=wm1+wm2
wq=wq1+wq2
c
wbs=wm*bd/(2.*alb)
wp=wy/...
wc=alc*wy
wt=wth/...
wth=abs(wbs)+abs(wt)
c
111 write (6,112) x,wy,wth,wm,wq,wbs,wp,wc,wth
112 format (t4,f4.1,...,f9.5,...,f9.5,4x,f5.1,3x,f9.1,4x,f9.1,5x,f7.1,6x,f7.1,5x,f7.1)
c Deflection at steel face for Winkler model
c is now calculated:
wd1=sh/(2.*es*...)
wd2=(1.+(1.+thet*ew)**2.)/thet**3.
wd3=ew**3./6.
wdelta=wd1*(wd2+wd3)*sin(ph)
c
wk=sf/wdelta
wal=...alc/1000.
c
write (6,113) sf,wdelta
write (6,114) wal
21 continue
c PFB foundation model results follow
c
```

```
 write (6,115)
 115 format (//t10,'FEM COMPUTATION RESULT',/t10,22('*'))
 write (6,109)
 109 format (/t3,'X',6x,'Y DEPL',7x,'TETA',7x,'MOMENT',7x,'SHEAR',6x,'ROC STRS',6x,'CH STRSS',6x,'LOAD STR',6x,'ADJUSTED STR')
 write (6,110)
 110 format (t3,'(mm)',5x,'(mm)',7x,'(rad)',7x,'(N mm)',3x,'(N)',9x,'(MPa)',7x,'(MPa)',7x,'(MPa)',7x,'(MPa)'//)
 c
 n=b1/s
 
 m=n+1
 c
 do 116 i=1,m
 x=(i-1)*s
 decr=-1.*alph*x
 bex=bet*x
 c
 y11=c1*c2*exp(decr)
 y12=2.*alph*bet*cos(bex)
 y13=q1*sin(bex)
 ya=y11*(y12+y13)
 c
 y21=(c3*exp(decr))/(bet*g1)
 y22=bet*cos(bex)
 y23=alph*sin(bex)
 yb=y21*(y22-y23)
 c
 y1=ya+yb
 c
 t12=bet*cos(bex)+alph*sin(bex)
 th1=t11*t12*exp(decr)
 t22=2.*alph*bet*cos(bex)
 t23=q2*sin(bex)
 t24=t22-t23
 th2=t21*t24*exp(decr)
 thi=th1+th2
 c
 am1=am11*exp(decr)*sin(bex)
 am22=q1*bet*cos(bex)
 am23=q1*alph*sin(bex)
 am24=am22+am23
 am2=am21*am24*exp(decr)
 am=am1+am2
 c
 qv12=q1*bet*cos(bex)
 qv13=q3*alph*sin(bex)
 qv14=qv12-qv13
 qv1=qv11*qv14*exp(decr)
 qn22=-4.*c3*alph*bet*cos(bex)
 qn23=q4*sin(bex)
 qn24=qn22+qn23
 qn2=qn21*qn24*exp(decr)
 c
 qv1=qv1-gt*thi
 qv2=-qn2-gt*thi
 qs1=qv1+qv2
 qu1=qn1+qn2
 c
 bs=am1*h/(2.*eith)
 ts=qn1/ah
 cs=ak*y1-qs1*gt*h./ei
 c This is in accordance with the PFR assumption.
 c
 ts=th/at
 ths=abs(ts)+abs(bs)
 c The tension in the bar is assumed to be
 c constant in the region of the joint.
 c
 116 write (6,117) x,y1,thi,am,qu1,bs,ts,cs,ths
 c Deflection of the crack face is now calculated
 dy11=c1*c2
 dy12=2.*alph*bet
 dya=dy11*dy12
 c
 dyb=c3/g1
 delta1=dya+dyb
 c
 dth1=t11*bet
 dth2=t21*2.*alph*bet
 dth=dth1+dth2
 delta2=0.5*dth
 c
 delta3,a=(delta1+delta2+delta3)
 delta=delta*sin(a)
 slo=sf/delta
 slop=slo/1000.0
 write (6,113) sf,delta
 113 format (//t10,'FOR A SHEAR FORCE OF ',f7.1,1x,'N, THE RELATIVE DEFLECTION OF THE CRACK FAC
 ES IS ',f6.4,1x,'mm')
 write (6,114) slop
 114 format (/t10,'THE SLOPE OF THE ELASTIC ZONE OF THE LOAD/DEFL CURVE IS ',f6.2,1x,'kN/mm')
 999 continue
 stop
```

B.2 LARGE FRAME COMPUTER PROGRAM SIMULATION OF THE BEAM ON ELASTIC FOUNDATION

The "STRUDL" simulation of the beam on elastic foundation concept appears overleaf. The program is derived from a diagrammatic representation of the beam elastic foundation shown below in Fig. B.2.1, in which the discontinuity of the foundation responce is clearly evident.

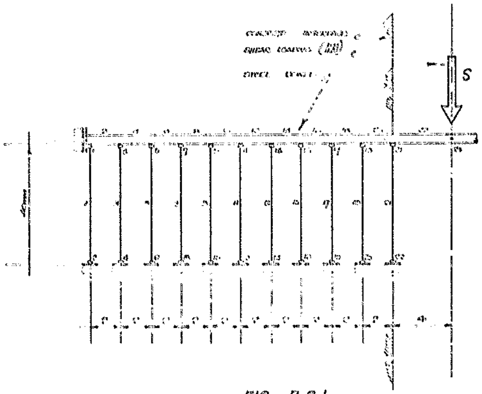

FIG. B.2.1

TYPICAL [illegible] OF THE BEAM ON ELASTIC FOUNDATION

```
STRUDL '[illegible]' SIMULATION OF BEAM ON ELASTIC FOUNDATION
          ***********************************************
          *                                             *
          *              ICES STRUDL-II                 *
          *       THE STRUCTURAL DESIGN LANGUAGE        *
          *                                             *
          *    CIVIL ENGINEERING SYSTEMS LABORATORY     *
          *   MASSACHUSETTS INSTITUTE OF TECHNOLOGY     *
          *         CAMBRIDGE, MASSACHUSETTS            *
          *          V2 M3    OCTOBER, 1970             *
          *          4:23:05       10/??/75             *
          *                                             *
          ***********************************************

TYPE PLANE FRAME XY

UNITS KG CMS DEGREES

JOINT COORDINATES

1 0.00 4.00 S

2 0.00 0.00 S

3 0.20 4.00

4 0.20 0.00 S

5 0.40 4.00

6 0.40 0.00 S

7 0.60 4.00

8 0.60 0.00 S

9 0.80 4.00

10 0.80 0.00 S

11 1.00 4.00

12 1.00 0.00 S

13 1.20 4.00

14 1.20 0.00 S

15 1.40 4.00

16 1.40 0.00 S

17 1.60 4.00

18 1.60 0.00 S

19 1.80 4.00

20 1.80 0.00 S

21 2.00 4.00

22 2.00 0.00 S

23 2.20 4.00

JOINT RELEASES

1 MOMENT Z

MEMBER INCIDENCES

1 1 2

2 1 3

3 3 4

4 3 5

5 5 6
```

```
6 5 7
7 7 8
8 7 9
9 9 10
10 9 11
11 11 12
12 11 13
13 13 14
14 13 15
15 15 16
16 15 17
17 17 18
18 17 19
19 19 20
20 19 21
21 21 22
22 21 23
MEMBER RELEASES
1,3,5,7,9,11,13,15,17,19,21 START MOM Z END MOM Z
CONSTANT E [illegible] 2,4,6,8,10,12,14,16,18,20,22
CONSTANT E [illegible] 1,3,5,7,9,11,13,15,17,19,21
CONSTANT BETA 0.0 ALL
MEMBER PROPERTIES PRISMATIC
$ CONSIDERING A [illegible]
2,4,6,8,10,12,14,16,18,20,22 AX [illegible] IZ [illegible] SZ [illegible]
1,3,5,7,9,11,13,15,17,19,21 AX [illegible] IZ [illegible] SZ [illegible]
LOADING 1 [illegible] 101.[illegible]
JOINT LOADS
23 FORCE Y -101.[illegible]
STIFFNESS ANALYSIS
OUTPUT DECIMAL 4
OUTPUT BY MEMBER
LIST LOADS DISPLACEMENTS [illegible] ALL
```

($E_{[illegible]}$ = 210 GPa)

($E_{[illegible]}$ = [illegible] GPa)

([illegible])

([illegible])

([illegible])

[illegible] }

JOINT DISPLACEMENTS - FREE JOINTS

JOINT		LOADING	X DISP	Y DISP	Y ROT	Z ROT
3	GLOBAL	1	0.0[illegible]	-0.1103		-0.0[illegible]7
5	GLOBAL	1	0.0300	-0.3[illegible]		-0.017[illegible]
7	GLOBAL	1	0.0[illegible]	[illegible]		-0.03[illegible]
9	GLOBAL	1	0.0[illegible]	[illegible]		-0.0576
11	GLOBAL	1	[illegible]	[illegible]		[illegible]
13	GLOBAL	1	[illegible]	[illegible]		[illegible]
15	GLOBAL	1	[illegible]	[illegible]		-0.1416
17	GLOBAL	1	[illegible]	[illegible]		-0.17[illegible]
19	GLOBAL	1	[illegible]	[illegible]		[illegible]
21	GLOBAL	1	[illegible]	[illegible]		[illegible]
23	GLOBAL	1	[illegible]	[illegible]		[illegible]

APPENDIX C

MIX DESIGN OF THE CONCRETE USED IN THE CRACKED-BEAM AND CUBE SPECIMENS

The concrete used in the laboratory test program made use of stone of maximum nominal size 13 mm (½") principally because of the limited dimensions of the test specimens. The materials of the laboratory mix were:

Water	Potable and free from contamination
Cement	Rapid Hardening Portland Cement
Sand	Washed sand from a residual granite pit (in the Halfway-House granite zone).
	(Fineness Modulus = 3,3)
	(Relative Density = 2,65)
Stone	Granite chips of maximum nominal size 13 mm
	(Relative Density = 2,65)

No admixtures were used.

The concrete mix was designed according to the Portland Cement Institute method, and it was intended that it should have adequate workability for use in the laboratory moulds, considering the various reinforcing schemes, and that it should also have a 7 day strength of approximately

30 MPa. Although slight adjustments were made for various reasons, the basic mix proportions (with a sand moisture content of 5%) were as follows per cubic metre of concrete:

	Water	240 ℓ
R.H.P.	Cement	384 kg
	Stone	880 kg
	Sand	811 kg

Cement/Water Ratio = 1,6.

Mixing and Casting Techniques:

The concrete was mixed in a rotary pan mixer, for about 5 minutes, and the volume of a single mix never exceeded 30ℓ. Steel moulds were made of channel sections bolted together to form moulds of nominal dimensions 101mmx101mmx720mm. Specimens were compacted on the V.B. consistometer and reinforcing dowels were held in position by the crack-formers during casting. Special care was thus taken to ensure that the reinforcement was not disturbed when pouring the concrete into the moulds. Cubes were cast concurrently for control cube tests and these were also compacted using the V.B. machine. The specimens were generally stripped after 24 hours and cured in a water bath (temperature not controlled) until the time of testing. There was no problem with workability, bleeding or segregation of the concrete used in the test program.

APPENDIX D

DETAILS OF APPARATUS USED IN THE LABORATORY TEST PROGRAM

Beam Specimens End Clamps

The clamps holding the ends of the crack-beam specimens acastré were made up of mild steel ½" (12 mm) plate and 3½" x 1½" x 4,5 lb/ft (76x38x6,69 kg/m) channels, welded together as shown in Fig. D.1. Studs were welded onto the channels so that the clamps fitted into the groove of the lower loading platen of the Macklow-Smith hydraulic testing machine. The ½" (12 mm) diameter black bolts (length 150mm) which held the upper mild steel plate in position, were tightened sufficiently to hold to ends of the concrete specimens in position and direction, but not to such an extent that the compression they created in the concrete would become an important factor.

Loading Rig

The loading rig shown in Fig. 4.2.1 was made up of ½" (12 mm) mild steel plate and the 2 point loading was applied through this rig to the upper surface of the concrete beam specimens by bright steel ½" (12 mm) round rod.

Electronic Testing Apparatus

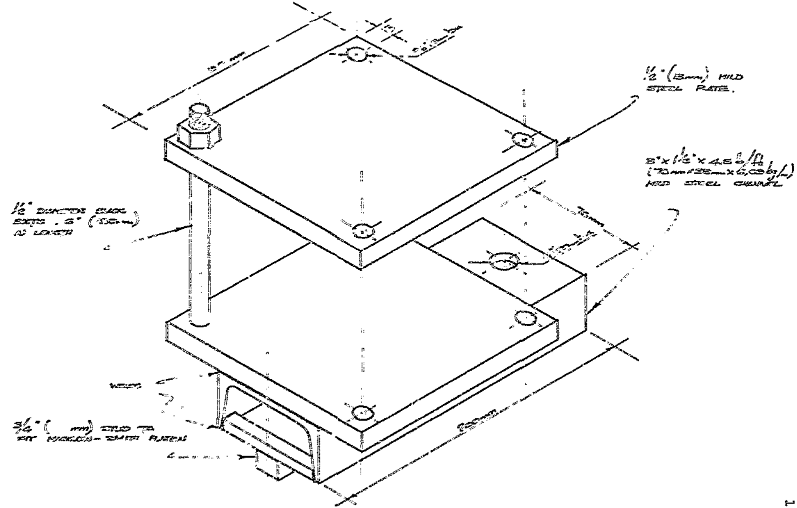

FIG D.1

DETAILS OF END CLAMPS FOR CRACKED SLAB SPECIMENS

Electronic Load Cell

This was made by the Kyowa Electronic Instruments Co. Ltd., Tokyo, Japan, and was a compression/tension strain gauge type load cell. The bridge voltage input was 10,0V D.C., output sensitivity 2mV/V (±0,2%) and the capacity was 20 kN. In cases where it was felt that this load would be exceeded, the load cell was removed and the load recorded mechanically through the Macklow-Smith hydraulic testing machine.

Linear Variable Differential Transformers (LVDT's)

One LVDT was used to record the deflection at each crack face, the average deflection being plotted for most consistent results. The specifications of the LVDT's, made by G.L. Collins Corp., Long Beach, Calif., were:

Length	20 mm
Diameter	10 mm
Linear range	± 1 mm

(where deflections exceeded this value, they were recorded by mechanical Mitutoyo deflection gauges). The two LVDT's used had serial numbers 18472 and 18473, with calibration constants of $8{,}8616\times10^{-4}$ mm/mV and $8{,}539\times10^{-4}$ mm/mV respectively. The average reading of the two LVDT's recorded on the X-Y plotter thus had a calibration factor of $8{,}678\times10^{-4}$ mm/mV.

Watanabe X-Y Autographic Recorder

The autographic X-Y plotter, shown in Fig. 4.2.5, was made by Watanabe Instruments Corp., Tokyo, Japan. The specifications of this machine were:

Model WX 411, Floating Differential Output
Response of Recorder:
Band Width = 1,0 H_z for the X axis
Bar Width = 1,25 Hz for the Y axis
(at 70% maximum amplitude)

Power Supply Modules

Separate power supplies were used for the load cell and LVDT's. The respective types used were:

Operational Amplifier (OA2) Module for the Load Cell
Type IC 100/6 for the LVDT's.

Both types were made by Contant Electronics Ltd., Reading, England and were powered by 220V A.C. mains voltage.